Rarefied Gas Dynamics: Theory and Applications to Vacuum

Lecture 2: Direct Simulation Monte Carlo

Felix Sharipov
Departamento de Física, Universidade Federal do Paraná
http://fisica.ufpr.br/sharipov

XLIV CBrAVIC, Short Course

São Paulo, November 25, 2023

Outline

- Direct simulation Monte Carlo method.
- Intermolecular collisions
- Hard sphere vs. ab initio potential
- Orifice flow
- Modelling of vacuum pumps
- 3D flows
- Transient flows

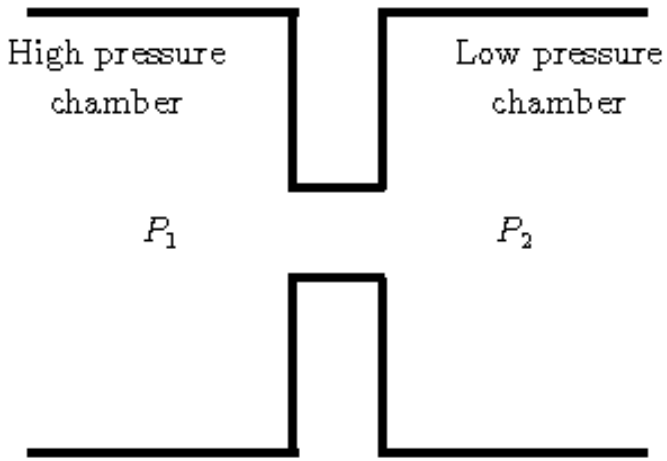

Example: Gas flow through a short tube.

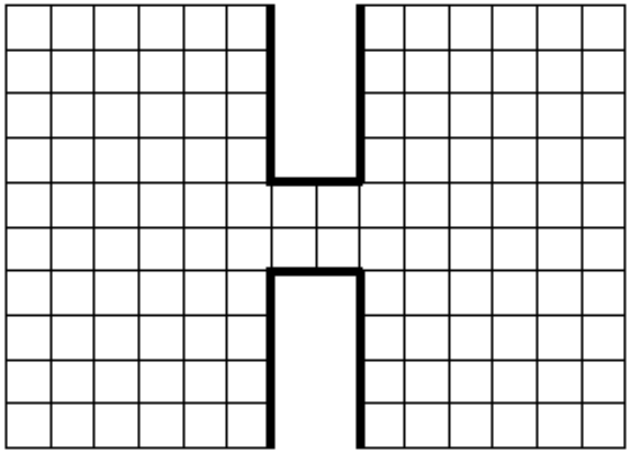

Flow region is divided into cells

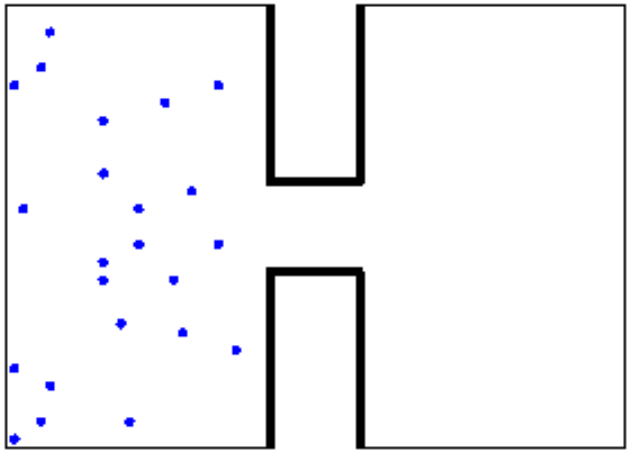

M model particles are considered.
Their positions $\boldsymbol{r}_i$ and velocities $\boldsymbol{v}_i$ are stored.

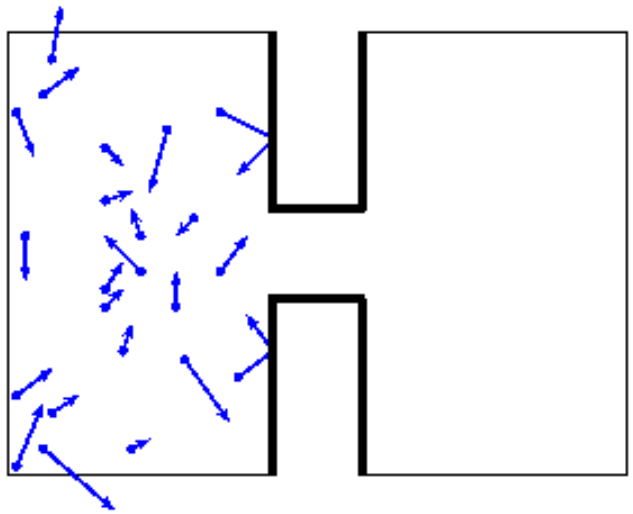

Time is advanced in steps Δt.
Free motion without collisions. New positions are calculated

$$\boldsymbol{r}_{i,new} = \boldsymbol{r}_{i,old} + \boldsymbol{v}_i \Delta t \tag{1}$$

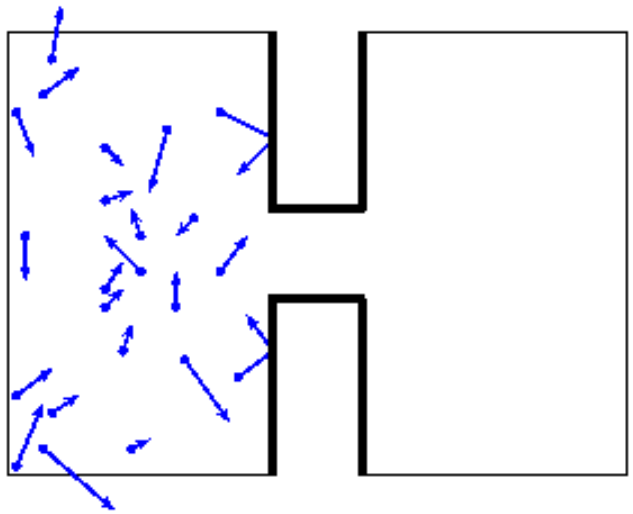

Gas-surface interaction is simulated.
Some particles are removed.

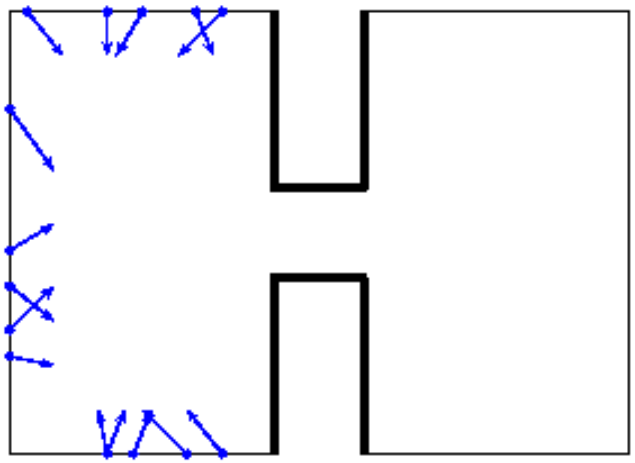

New particles are generated.

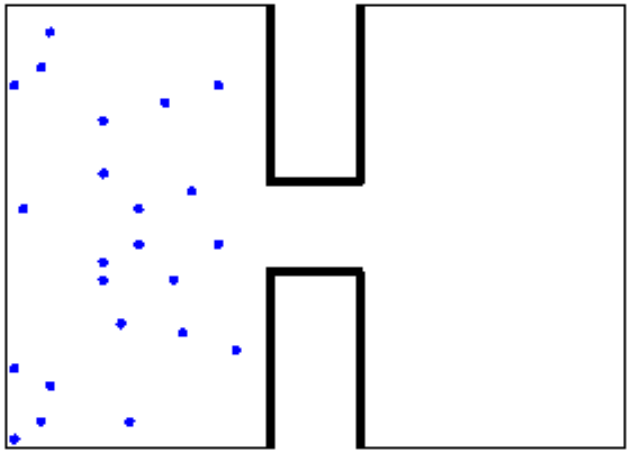

Intermolecular collisions are simulated. New velocities $\boldsymbol{v}_i$ are calculated
Macroscopic quantities are calculated.

All steps are repeated many times in order to reduce the statistical noise.

Diffuse scattering on solid surface

Normal component of velocity

$$f(v_n) = 2\frac{v_n}{v_w^2}\exp\left(-\frac{v_n^2}{v_w^2}\right), \quad v_w = \sqrt{\frac{2k_\mathrm{B}T_w}{m}} \quad 0 \le v_n < \infty \tag{2}$$

Diffuse scattering on solid surface

Normal component of velocity

$$f(v_n) = 2\frac{v_n}{v_w^2}\exp\left(-\frac{v_n^2}{v_w^2}\right), \quad v_w = \sqrt{\frac{2k_\mathrm{B}T_w}{m}} \quad 0 \le v_n < \infty \tag{2}$$

$$v_n = v_w\sqrt{-\ln R_f}, \quad R_f \text{ - random fraction of 1} \tag{3}$$

Diffuse scattering on solid surface

Normal component of velocity

$$f(v_n) = 2\frac{v_n}{v_w^2}\exp\left(-\frac{v_n^2}{v_w^2}\right), \quad v_w = \sqrt{\frac{2k_\mathrm{B}T_w}{m}} \quad 0 \le v_n < \infty \tag{2}$$

$$v_n = v_w\sqrt{-\ln R_f}, \quad R_f \text{ - random fraction of 1} \tag{3}$$

Tangential component

$$f(v_t) = 2\frac{v_t}{v_w^2}\exp\left(-\frac{v_t^2}{v_w^2}\right), \quad 0 \le v_t < \infty \tag{4}$$

Diffuse scattering on solid surface

Normal component of velocity

$$f(v_n) = 2\frac{v_n}{v_w^2}\exp\left(-\frac{v_n^2}{v_w^2}\right), \quad v_w = \sqrt{\frac{2k_\mathrm{B}T_w}{m}} \quad 0 \le v_n < \infty \tag{2}$$

$$v_n = v_w\sqrt{-\ln R_f}, \quad R_f \text{ - random fraction of 1} \tag{3}$$

Tangential component

$$f(v_t) = 2\frac{v_t}{v_w^2}\exp\left(-\frac{v_t^2}{v_w^2}\right), \quad 0 \le v_t < \infty \tag{4}$$

$$v_t = v_w\sqrt{-\ln R_f},$$

Diffuse scattering on solid surface

Normal component of velocity

$$f(v_n) = 2\frac{v_n}{v_w^2}\exp\left(-\frac{v_n^2}{v_w^2}\right), \quad v_w = \sqrt{\frac{2k_\mathrm{B}T_w}{m}} \quad 0 \le v_n < \infty \tag{2}$$

$$v_n = v_w\sqrt{-\ln R_f}, \quad R_f \text{ - random fraction of 1} \tag{3}$$

Tangential component

$$f(v_t) = 2\frac{v_t}{v_w^2}\exp\left(-\frac{v_t^2}{v_w^2}\right), \quad 0 \le v_t < \infty \tag{4}$$

$$v_t = v_w\sqrt{-\ln R_f}, \quad \phi = 2\pi R_f \tag{5}$$

Diffuse scattering on solid surface

Normal component of velocity

$$f(v_n) = 2\frac{v_n}{v_w^2}\exp\left(-\frac{v_n^2}{v_w^2}\right), \quad v_w = \sqrt{\frac{2k_\mathrm{B}T_w}{m}} \quad 0 \le v_n < \infty \tag{2}$$

$$v_n = v_w\sqrt{-\ln R_f}, \quad R_f \text{ - random fraction of 1} \tag{3}$$

Tangential component

$$f(v_t) = 2\frac{v_t}{v_w^2}\exp\left(-\frac{v_t^2}{v_w^2}\right), \quad 0 \le v_t < \infty \tag{4}$$

$$v_t = v_w\sqrt{-\ln R_f}, \quad \phi = 2\pi R_f \tag{5}$$

$$v_{t1} = v_t\cos\phi, \quad v_{t2} = v_t\sin\phi \tag{6}$$

Diffuse scattering on solid surface

Normal component of velocity

$$f(v_n) = 2\frac{v_n}{v_w^2}\exp\left(-\frac{v_n^2}{v_w^2}\right), \quad v_w = \sqrt{\frac{2k_\mathrm{B}T_w}{m}} \quad 0 \le v_n < \infty \tag{2}$$

$$v_n = v_w\sqrt{-\ln R_f}, \quad R_f \text{ - random fraction of 1} \tag{3}$$

Tangential component

$$f(v_t) = 2\frac{v_t}{v_w^2}\exp\left(-\frac{v_t^2}{v_w^2}\right), \quad 0 \le v_t < \infty \tag{4}$$

$$v_t = v_w\sqrt{-\ln R_f}, \quad \phi = 2\pi R_f \tag{5}$$

$$v_{t1} = v_t\cos\phi, \quad v_{t2} = v_t\sin\phi \tag{6}$$

each R_f is used once

Number of pairs to be tested

$$N_{coll} = \frac{N_p^2 F_N}{2V_C}(\sigma_t g_r)_{max}\Delta t \tag{7}$$

N_p number of model particles in cell

F_N is representation, number of real particles represented by a model one.

V_C is volume of cell

g_r relative speed of interacting particles

σ_t total cross section. function of g_r

Number of pairs to be tested

$$N_{coll} = \frac{N_p^2 F_N}{2V_C}(\sigma_t g_r)_{max}\Delta t \tag{7}$$

N_p number of model particles in cell

F_N is representation, number of real particles represented by a model one.

V_C is volume of cell

g_r relative speed of interacting particles

σ_t total cross section. function of g_r

a randomly chosen pair is accepted if $$\frac{\sigma_t g_r}{(\sigma_t g_r)_{max}} > R_f \tag{8}$$

faster particles collide more frequently

Once a pair is accepted

velocities $\boldsymbol{v}_1, \boldsymbol{v}_2$ are recalculated according to binary collision dynamics

Once a pair is accepted

velocities $\boldsymbol{v}_1, \boldsymbol{v}_2$ are recalculated according to binary collision dynamics

Scheme of binary collision

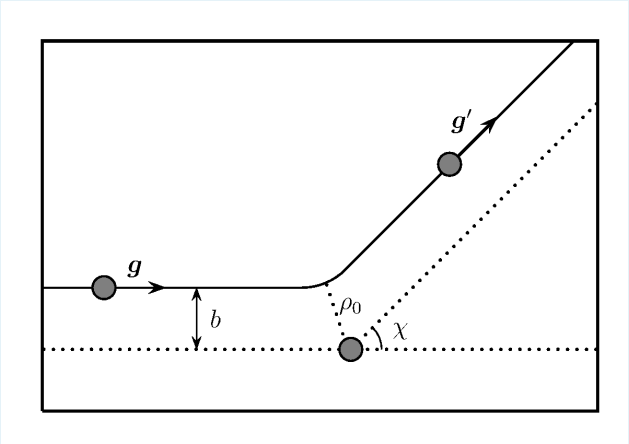

$g = g'$ relative speed does not change its magnitude

Once a pair is accepted

velocities $\boldsymbol{v}_1, \boldsymbol{v}_2$ are recalculated according to binary collision dynamics

Scheme of binary collision

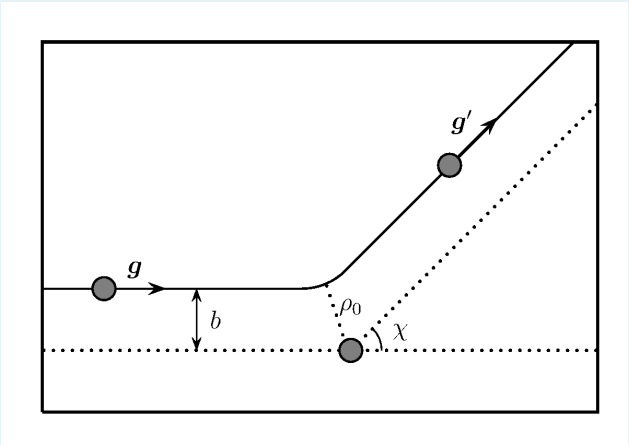

$g = g'$ relative speed does not change its magnitude

deflection angle $0 \leq \chi \leq \pi$

Once a pair is accepted

velocities $\boldsymbol{v}_1, \boldsymbol{v}_2$ are recalculated according to binary collision dynamics

Scheme of binary collision

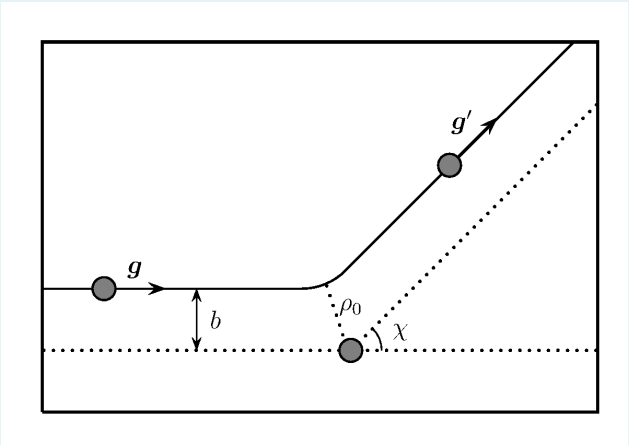

$g = g'$ relative speed does not change its magnitude

deflection angle $0 \leq \chi \leq \pi$ depends on potential

Once a pair is accepted

velocities $\boldsymbol{v}_1, \boldsymbol{v}_2$ are recalculated according to binary collision dynamics

Scheme of binary collision

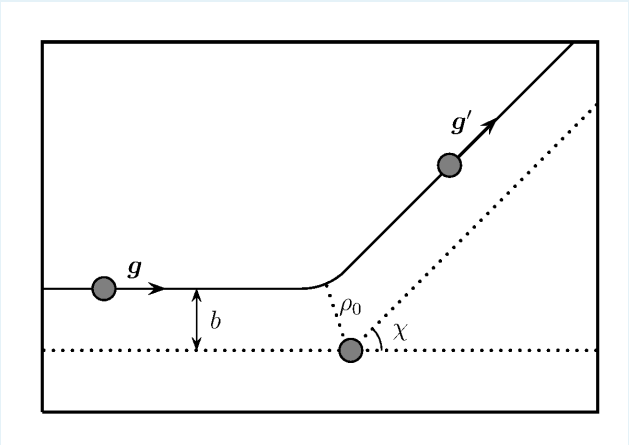

$g = g'$ relative speed does not change its magnitude

deflection angle $0 \leq \chi \leq \pi$ depends on potential

azimuthal impact angle $0 \leq \varepsilon \leq 2\pi$ determines the collision plane

$$\boldsymbol{v}, \boldsymbol{v}_* \Rightarrow \chi, \varepsilon \Rightarrow \boldsymbol{v}', \boldsymbol{v}'_*, \tag{9}$$

Hard sphere potential

Total cross section $\sigma_t = \pi d^2$ is constant.

Hard sphere potential

Total cross section $\sigma_t = \pi d^2$ is constant.

All directions of $\boldsymbol{g}'$ are equiprobable

$$\cos\chi = 2R_f - 1, \quad \varepsilon = 2\pi R_f \tag{10}$$

each R_f is used once

Hard sphere potential

Total cross section $\sigma_t = \pi d^2$ is constant.

All directions of $\boldsymbol{g}'$ are equiprobable

$$\cos\chi = 2R_f - 1, \quad \varepsilon = 2\pi R_f \tag{10}$$

each R_f is used once It is simple, but it leads to a wrong viscosity

$$\mu \propto T^{1/2} \tag{11}$$

Critics of variable hard sphere

All directions of $\boldsymbol{g}'$ are equiprobable.

Critics of variable hard sphere

All directions of $\boldsymbol{g}'$ are equiprobable.

Total cross section $\sigma_t = \pi d^2$ depends on g.

Diameter d is calculated assuming

$$\mu = \mu_{ref} \left(\frac{T}{T_{ref}} \right)^{\omega} \tag{12}$$

index ω is constant

Critics of Variable hard sphere

ω is not constant

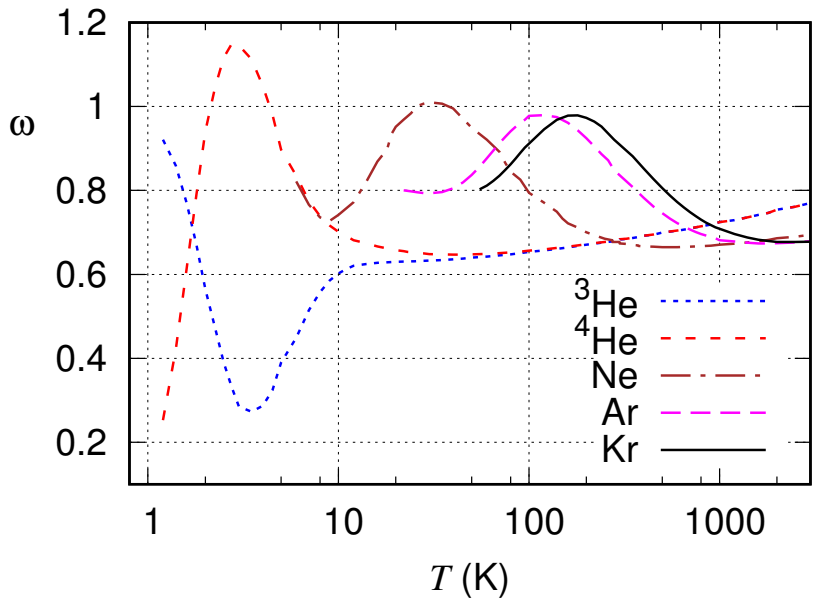

Critics of Variable hard sphere

ω is not constant

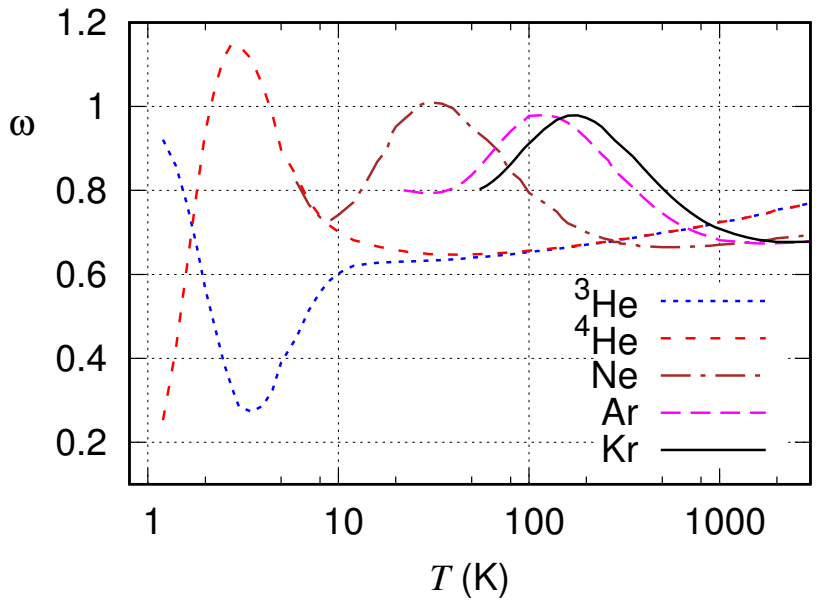

Parameters d and ω are still fitting

Critics of Variable hard sphere

ω is not constant

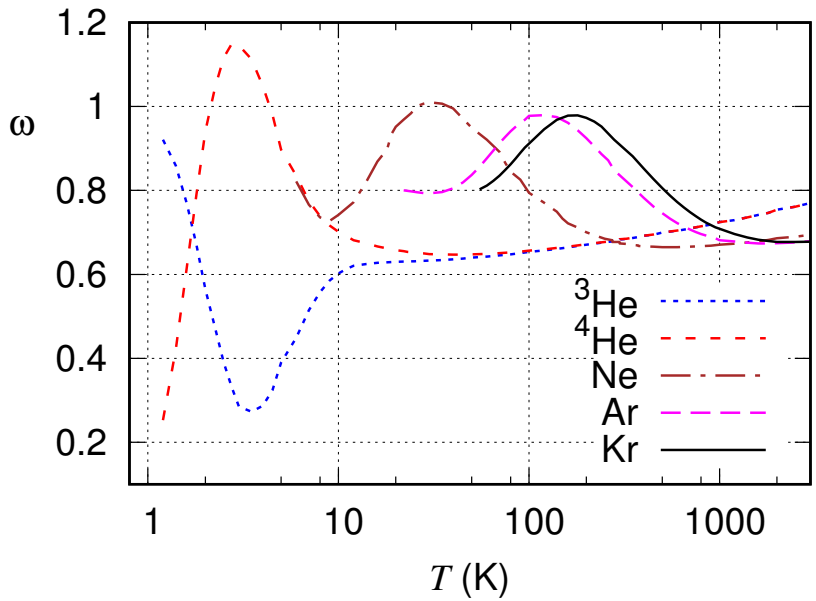

Parameters d and ω are still fitting

It is not clear ω for collisions between different species.

Arbitrary potential. Classical approach (Newton's laws)

$\chi = \chi(b, g)$

Arbitrary potential. Classical approach (Newton's laws)

$\chi = \chi(b, g)$

Deflection angle vs. impact parameter. Lennard-Jones potential.

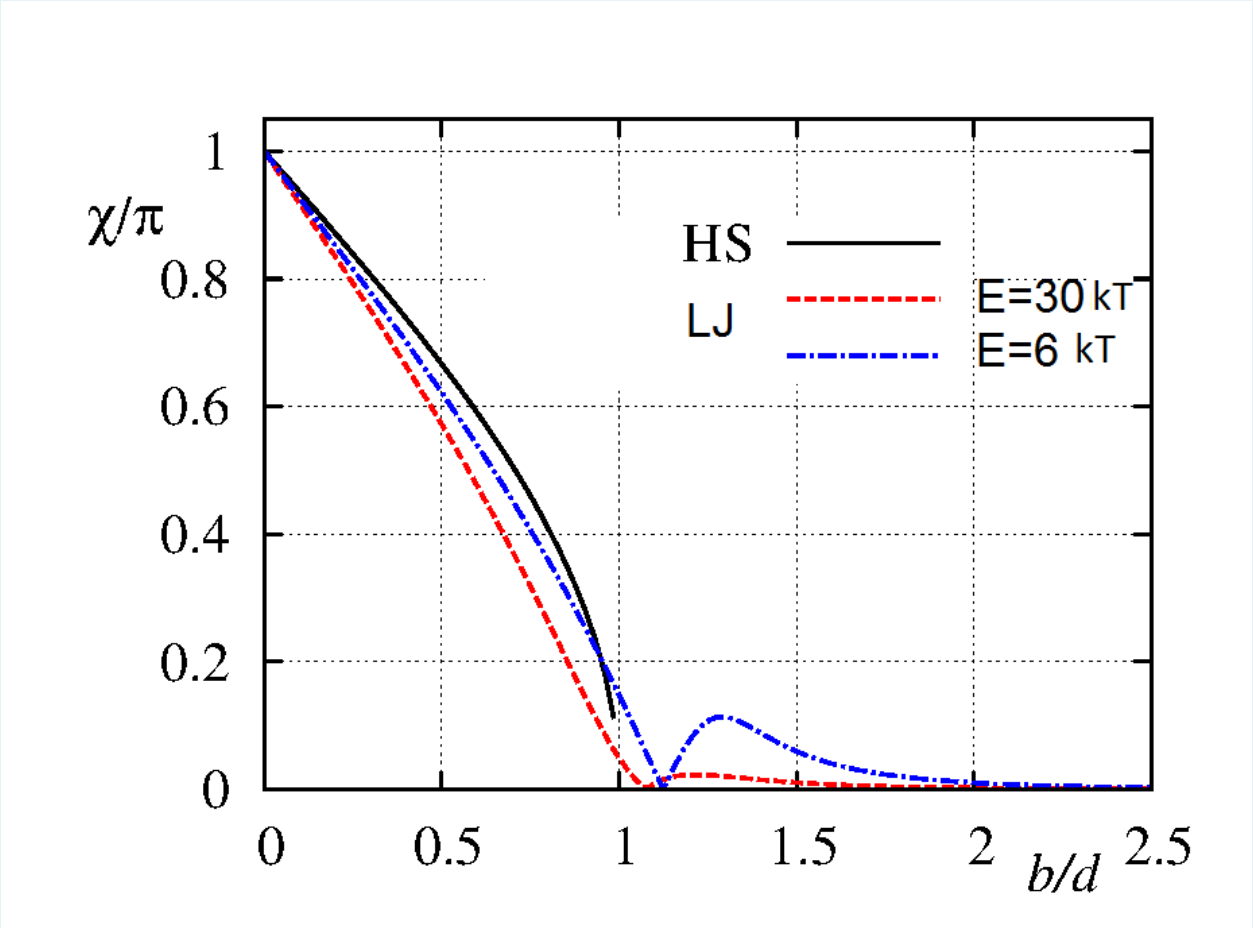

Deflection angle vs. impact parameter. Lennard-Jones potential.

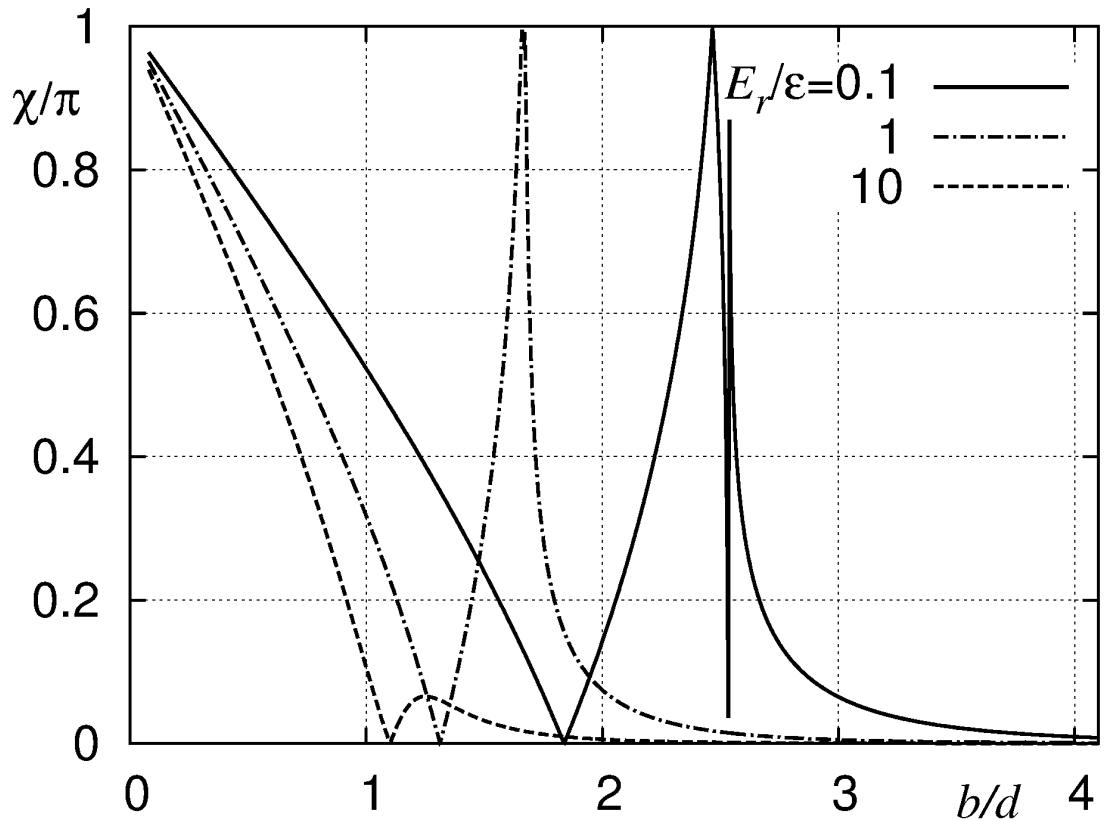

Arbitrary potential. Quantum approach

Schrödinger equation is applied

$\chi(g)$ is determined by differential cross section $\sigma(\chi, g)$

Arbitrary potential. Quantum approach

Schrödinger equation is applied

$\chi(g)$ is determined by differential cross section $\sigma(\chi, g)$

Arbitrary potential

Calculation of deflection angle χ in each collision takes a long time by both classical and quantum approaches.

Arbitrary potential. Quantum approach

Schrödinger equation is applied

$\chi(g)$ is determined by differential cross section $\sigma(\chi, g)$

Arbitrary potential

Calculation of deflection angle χ in each collision takes a long time by both classical and quantum approaches.

χ are calculated for many values of g and stored in lookup tables.

Sharipov & Strapasson, *Phys. Fluids* **24** (2012)

Arbitrary potential. Lookup tables.

Matrix χ_{ij} is precalculated for discrete values of g_j.

Arbitrary potential. Lookup tables.

Matrix χ_{ij} is precalculated for discrete values of g_j.

If g is a real relative speed, then j is the closets nodes g_j to g.

Arbitrary potential. Lookup tables.

Matrix χ_{ij} is precalculated for discrete values of g_j.

If g is a real relative speed, then j is the closets nodes g_j to g.

For a fixed j, all χ_{ij} are distributed so that all of them are

equiprobable so that

Arbitrary potential. Lookup tables.

Matrix χ_{ij} is precalculated for discrete values of g_j.

If g is a real relative speed, then j is the closets nodes g_j to g.

For a fixed j, all χ_{ij} are distributed so that all of them are

equiprobable so that i is chosen randomly

Arbitrary potential. Lookup tables.

Matrix χ_{ij} is precalculated for discrete values of g_j.

If g is a real relative speed, then j is the closets nodes g_j to g.

For a fixed j, all χ_{ij} are distributed so that all of them are

equiprobable so that i is chosen randomly

Once χ_{ij} are calculated, they can be used for ANY flow.

Arbitrary potential. Lookup tables.

Matrix χ_{ij} is precalculated for discrete values of g_j.

If g is a real relative speed, then j is the closets nodes g_j to g.

For a fixed j, all χ_{ij} are distributed so that all of them are

equiprobable so that i is chosen randomly

Once χ_{ij} are calculated, they can be used for ANY flow.

χ_{ij} are given in Supplementary material of several papers.

Arbitrary potential. Lookup tables.

Matrix χ_{ij} is precalculated for discrete values of g_j.

If g is a real relative speed, then j is the closets nodes g_j to g.

For a fixed j, all χ_{ij} are distributed so that all of them are

equiprobable so that i is chosen randomly

Once χ_{ij} are calculated, they can be used for ANY flow.

χ_{ij} are given in Supplementary material of several papers.

Computational effort with lookup tables is the same as for HS.

Hard sphere vs. *ab initio* potential

Classical approach vs. Quantum approach

Couette flow. Sharipov & Strapasson, *Phys. Fluids* **25** 027101 (2013)

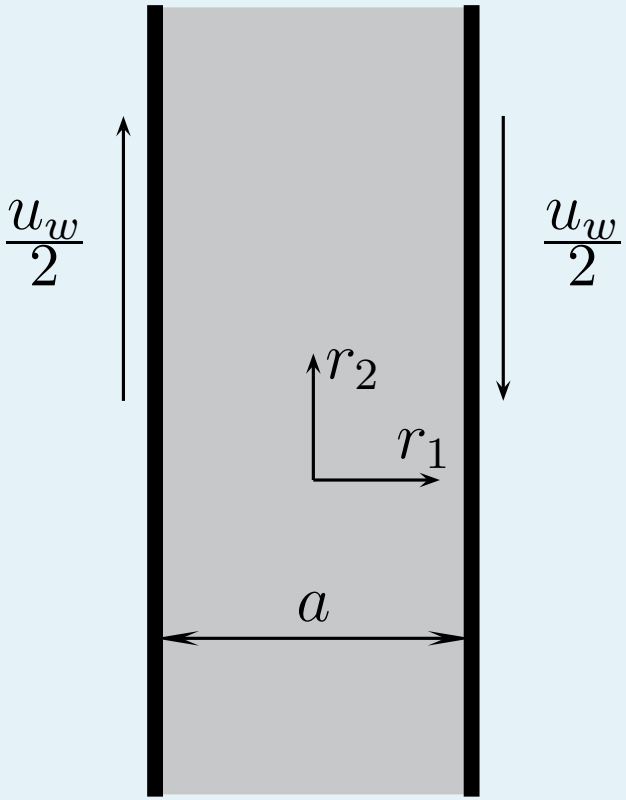

Couette flow. Sharipov & Strapasson, *Phys. Fluids* **25** 027101 (2013)

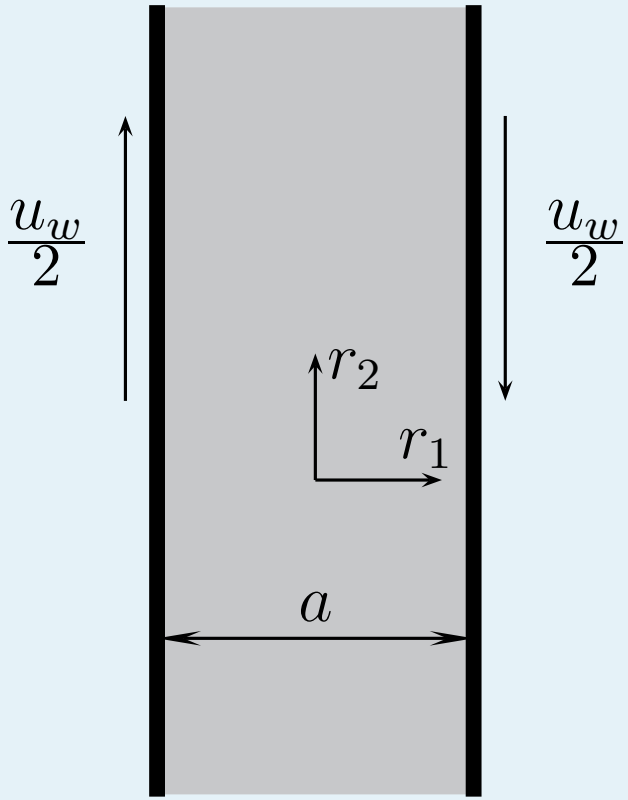

Shear stress P_{12} is calculated.

$$\Pi = -\frac{P_{12}}{p_0}\frac{v_0}{u_w}$$

Couette flow. Sharipov & Strapasson, *Phys. Fluids* **25** 027101 (2013)

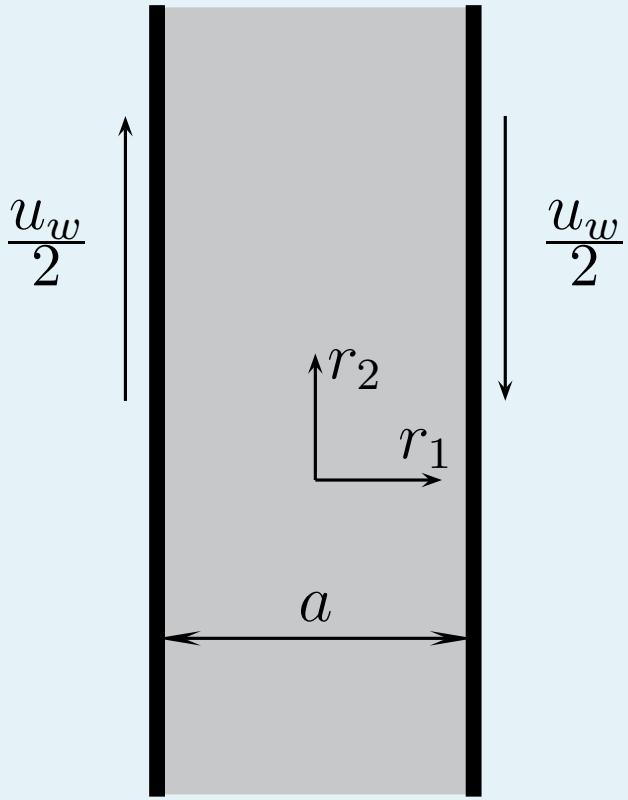

Shear stress P_{12} is calculated.

$$\Pi = -\frac{P_{12}}{p_0}\frac{v_0}{u_w} \tag{13}$$

as a function of mole fraction and rarefaction parameter

$$C = \frac{n_1}{n_1 + n_2}, \quad \delta = \frac{a\, p_0}{\mu v_0} \tag{14}$$

$$v_0 = \sqrt{\frac{2kT_0}{m}}, \quad m = Cm_1 + (1 - C_1)m_2 \tag{15}$$

Couette flow. Sharipov & Strapasson, *Phys. Fluids* **25** 027101 (2013)

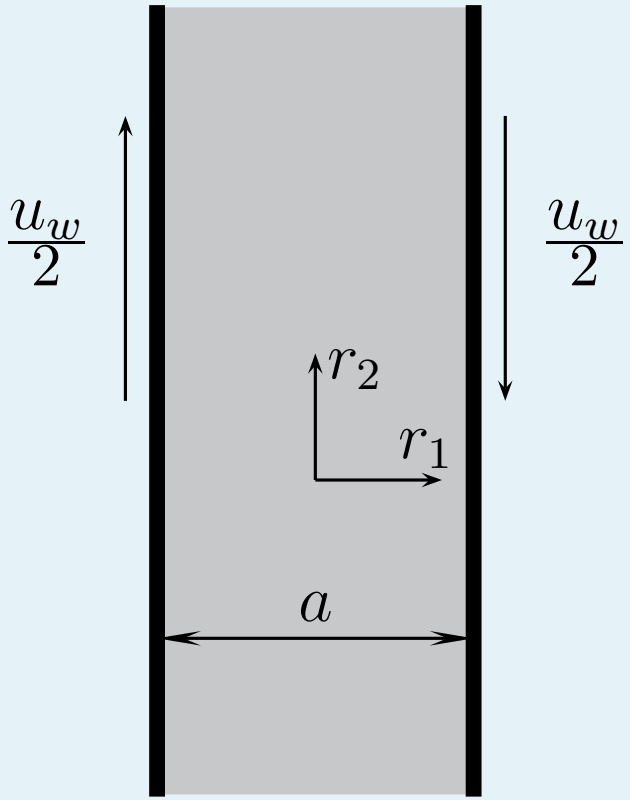

Numerical error 0.5%

Number of cells 400

Number of particles 40 000

Time step $0.002a/v_0$

Number of steps 10^6 for $u_w/v_0 = 2$

Number of steps 10^7 for $u_w/v_0 = 0.2$

Couette flow, Comparison with Discrete velocity method applied to BGK, $u_w = 0.2v_0$

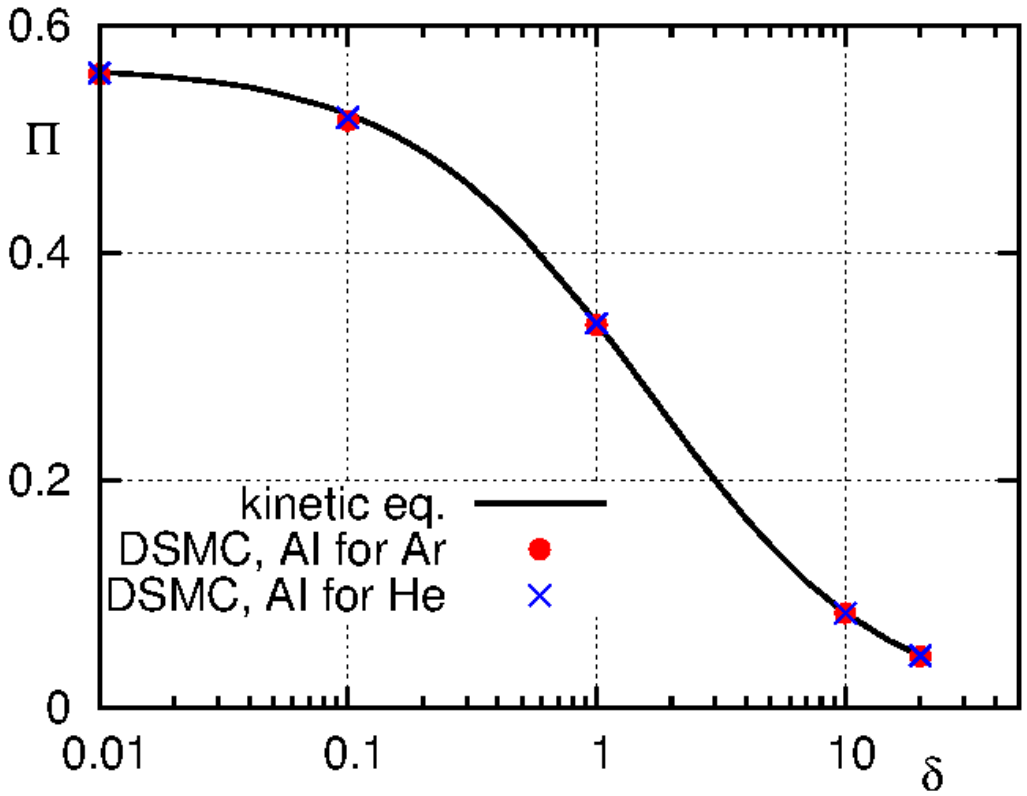

Numerical results based on AI potential, He-Ar, $u_w/v_0 = 0.2$. Sharipov & Strapasson, *Phys. Fluids* **25** 027101 (2013)

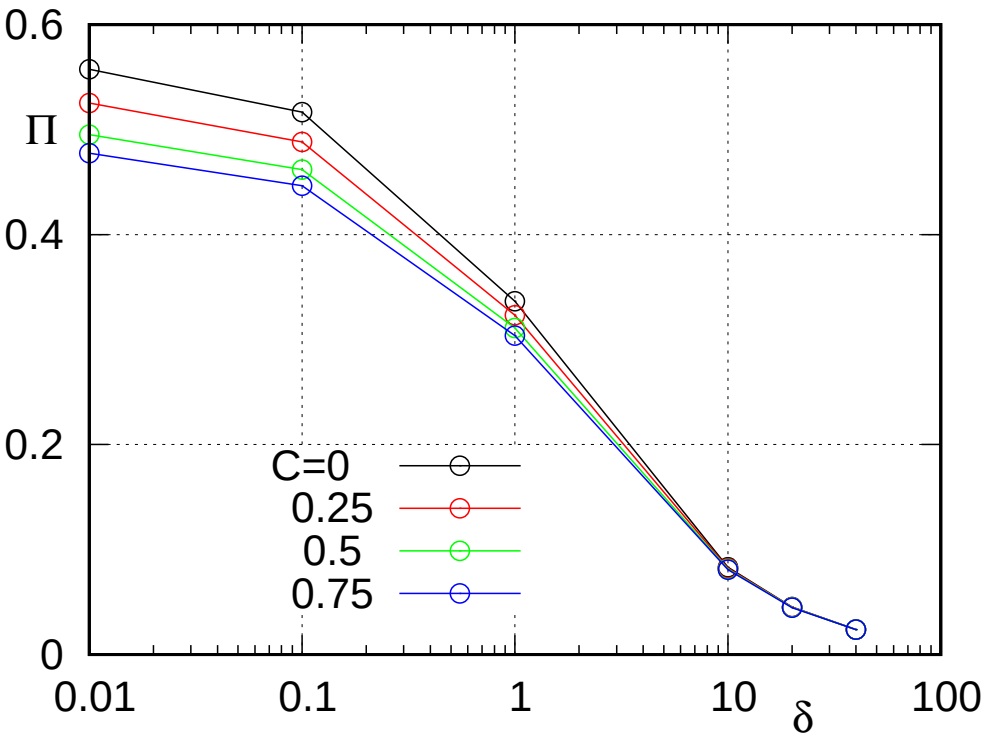

Relative difference between results based on AI and HS, $u_w/v_0 = 0.2$

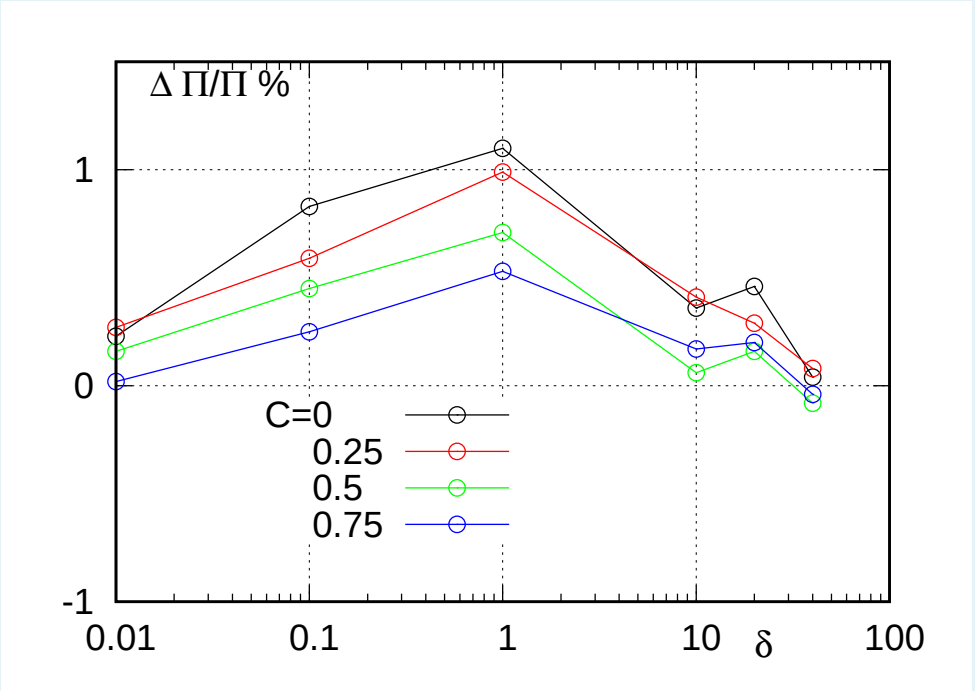

$$\frac{\Delta\Pi}{\Pi} = \frac{\Pi^{(HS)} - \Pi^{(AI)}}{\Pi^{(AI)}} \times 100\% \qquad (16)$$

Numerical results based on AI potential, He-Ar, $u_w/v_0 = 2$. Sharipov & Strapasson, *Phys. Fluids* **25** 027101 (2013)

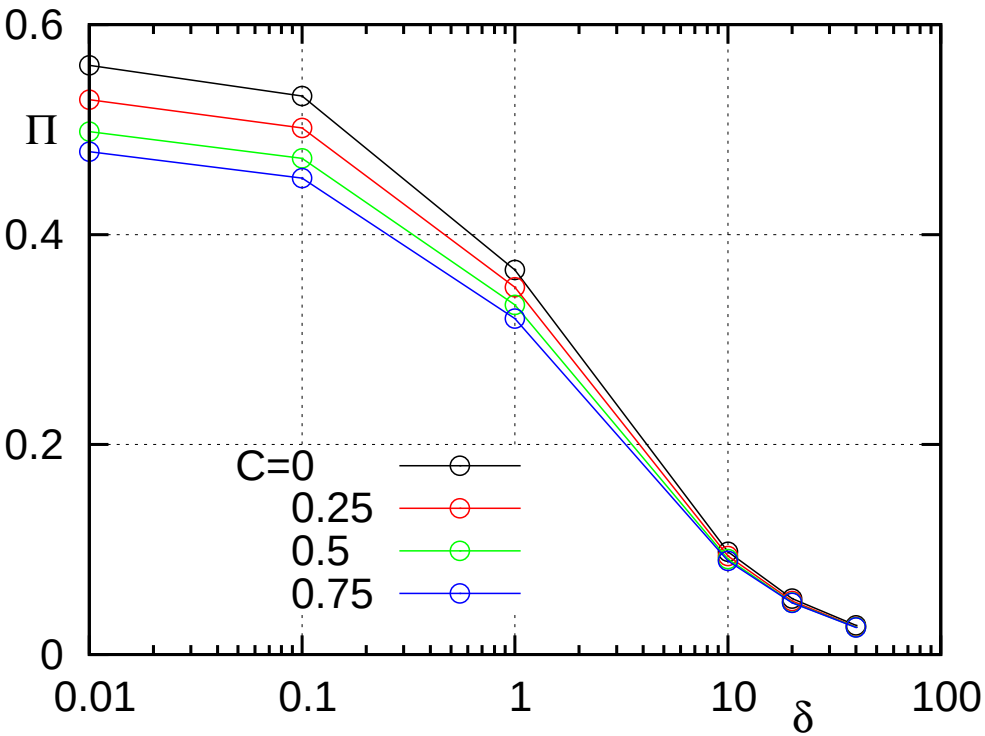

Relative difference between results based on AI and HS, $u_w/v_0 = 2$

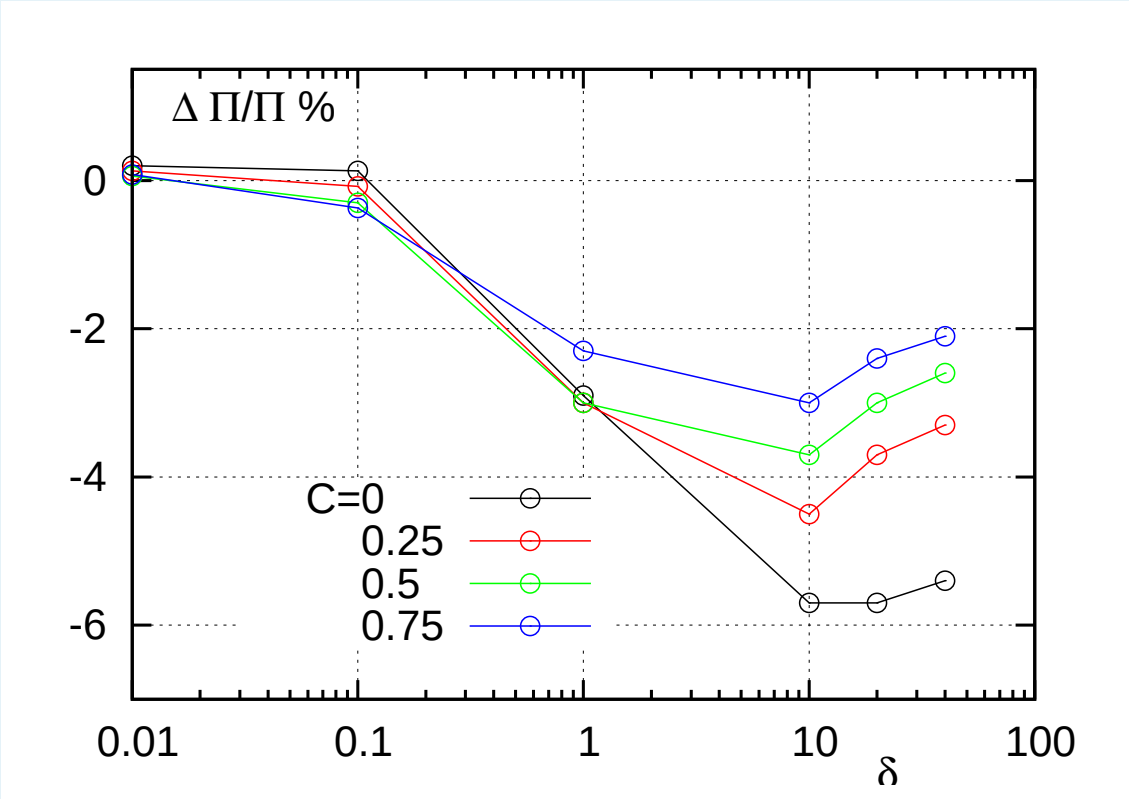

$$\frac{\Delta\Pi}{\Pi} = \frac{\Pi^{(HS)} - \Pi^{(AI)}}{\Pi^{(AI)}} \times 100\% \qquad (17)$$

Classical and quantum approaches, $u_w/v_0 = 2$. Sharipov, *Physica A* **508**, 797-805 (2018)

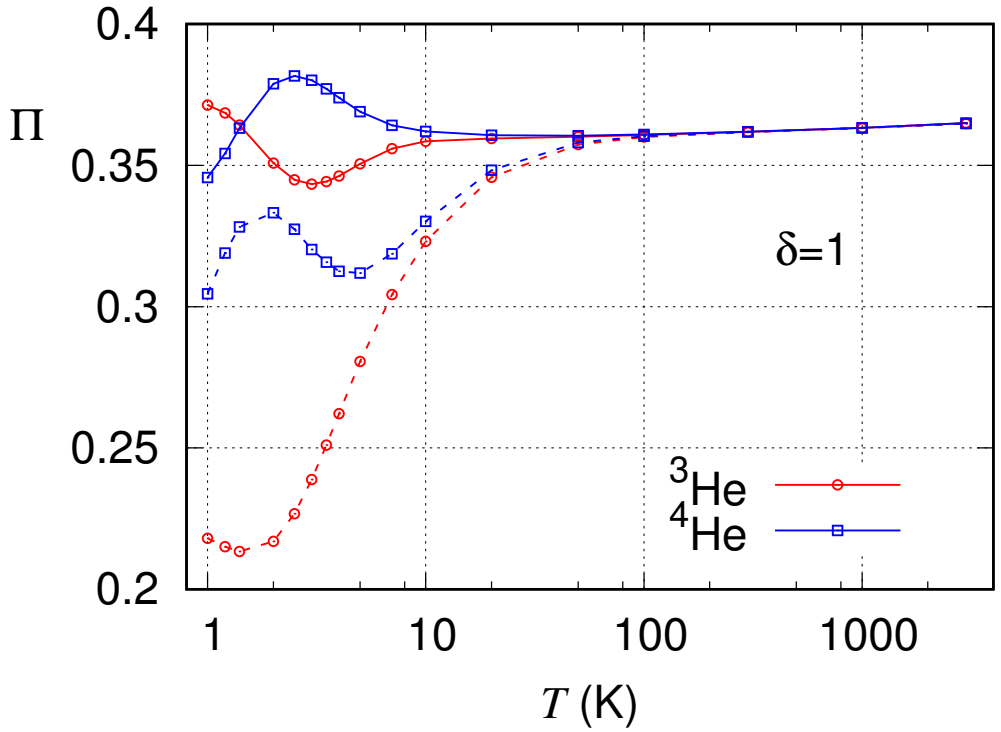

Solid line - quantum approach

dashed line -classical approach

Heat transfer between two plates.
Sharipov & Strapasson, *Int. J. Heat Mass Transfer* **71**, 91-97 (2014)

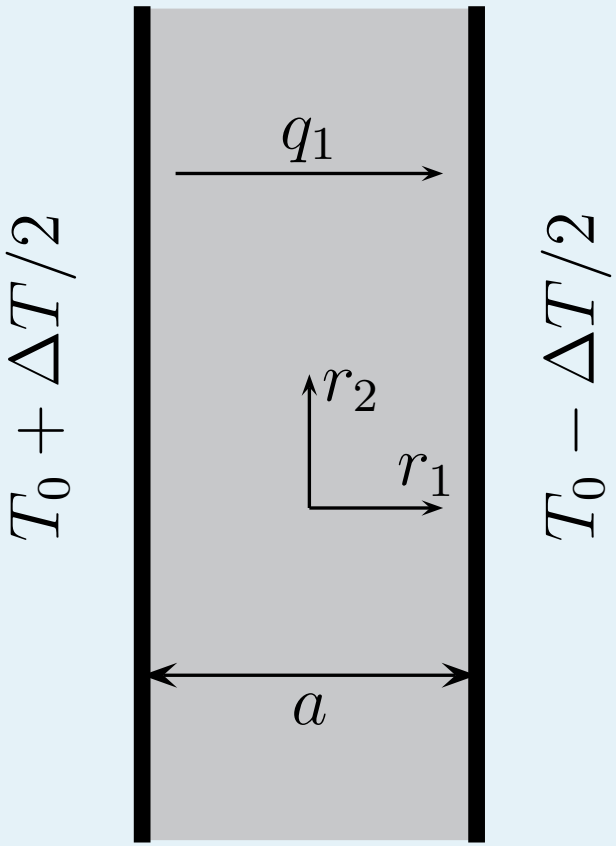

Heat q_x flow is calculated

$$Q = -\frac{q_x}{p_0 v_0}\frac{T_0}{\Delta T} \qquad (18)$$

as function of C and δ

Heat transfer.
Sharipov & Strapasson, *Int. J. Heat Mass Transfer* **71**, 91-97 (2014)

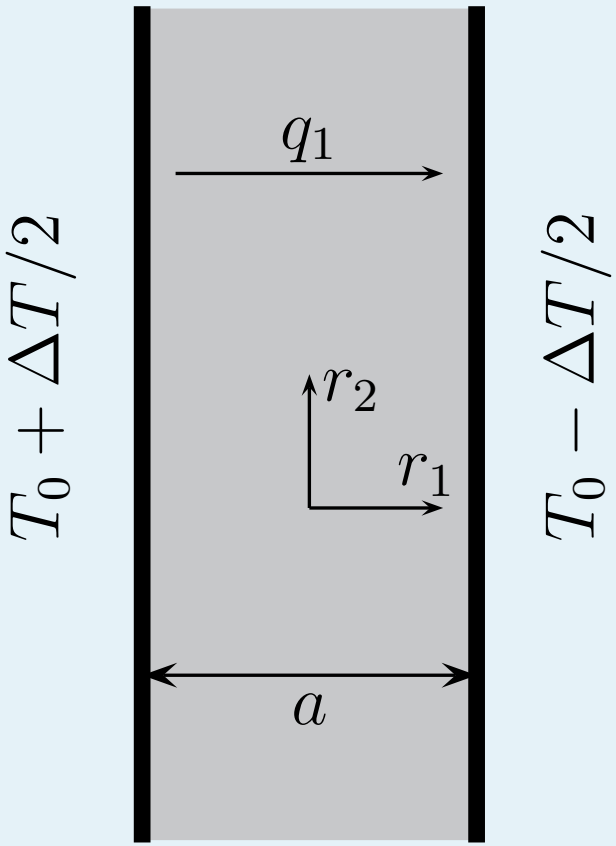

Numerical error 0.5%

Number of cells 400

Number of particles 40 000

Time step $0.002a/v_0$

Number of steps 5×10^6 for $\Delta T/T_0 = 1.5$

Number of steps 10^7 for $\Delta T/T_0 = 0.2$

Numerical results based on AI potential, He-Ar, $\Delta T/T_0 = 0.2$. Sharipov & Strapasson, *Int. J. Heat Mass Transfer* **71**, 91-97 (2014)

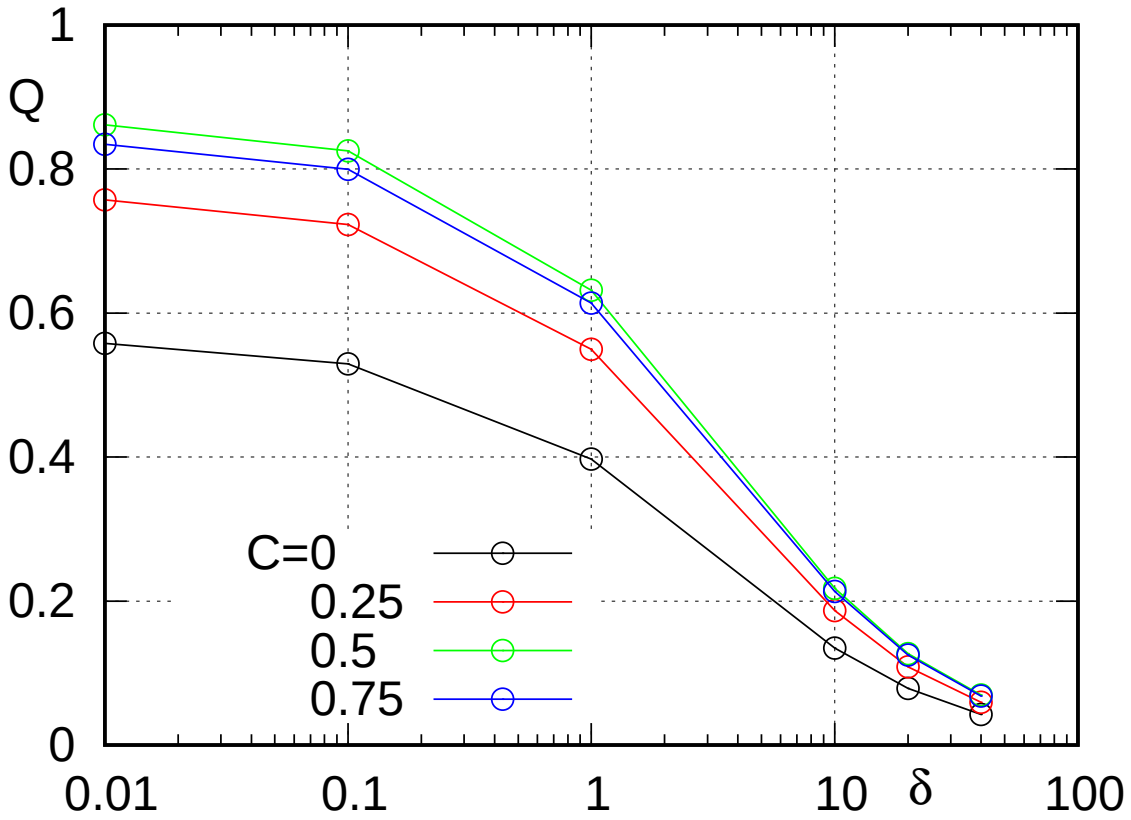

Relative difference between results based on AI and HS, $\Delta T/T_0 = 0.2$

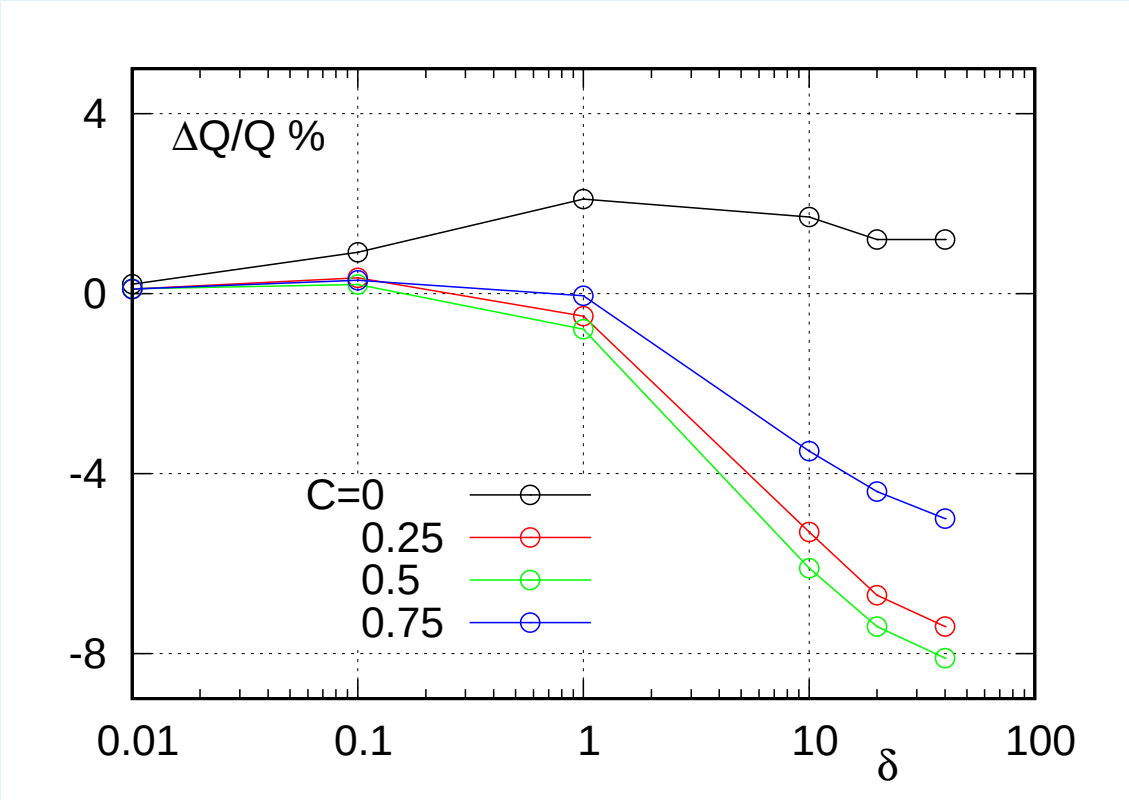

$$\frac{\Delta Q}{Q} = \frac{Q^{(AI)} - Q^{(HS)}}{Q^{(AI)}} \times 100\% \qquad (19)$$

Numerical results based on AI potential, He-Ar, $\Delta T/T_0 = 1.5$. Sharipov & Strapasson, *Int. J. Heat Mass Transfer* **71**, 91-97 (2014)

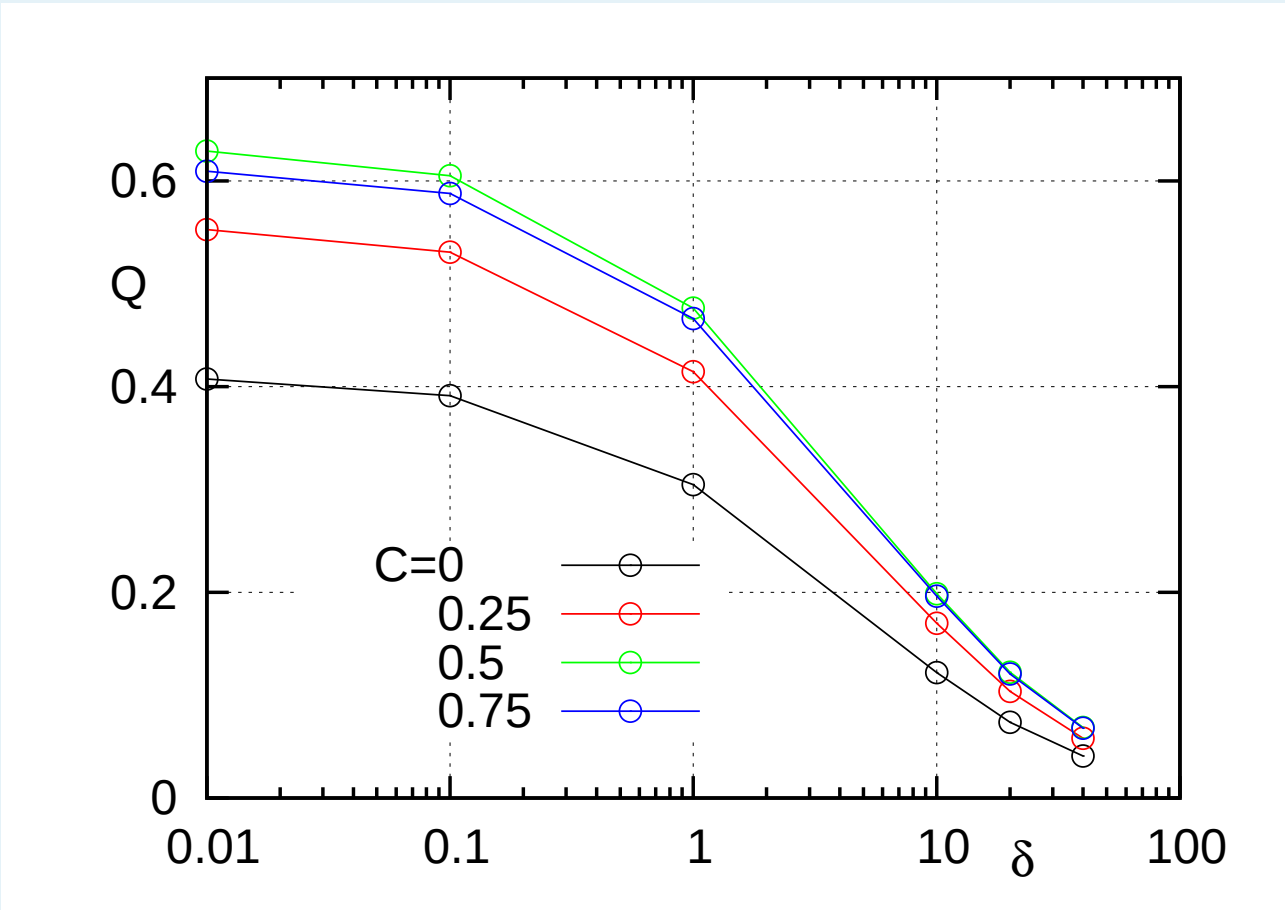

Relative difference between results based on AI and HS, $\Delta T/T_0 = 1.5$

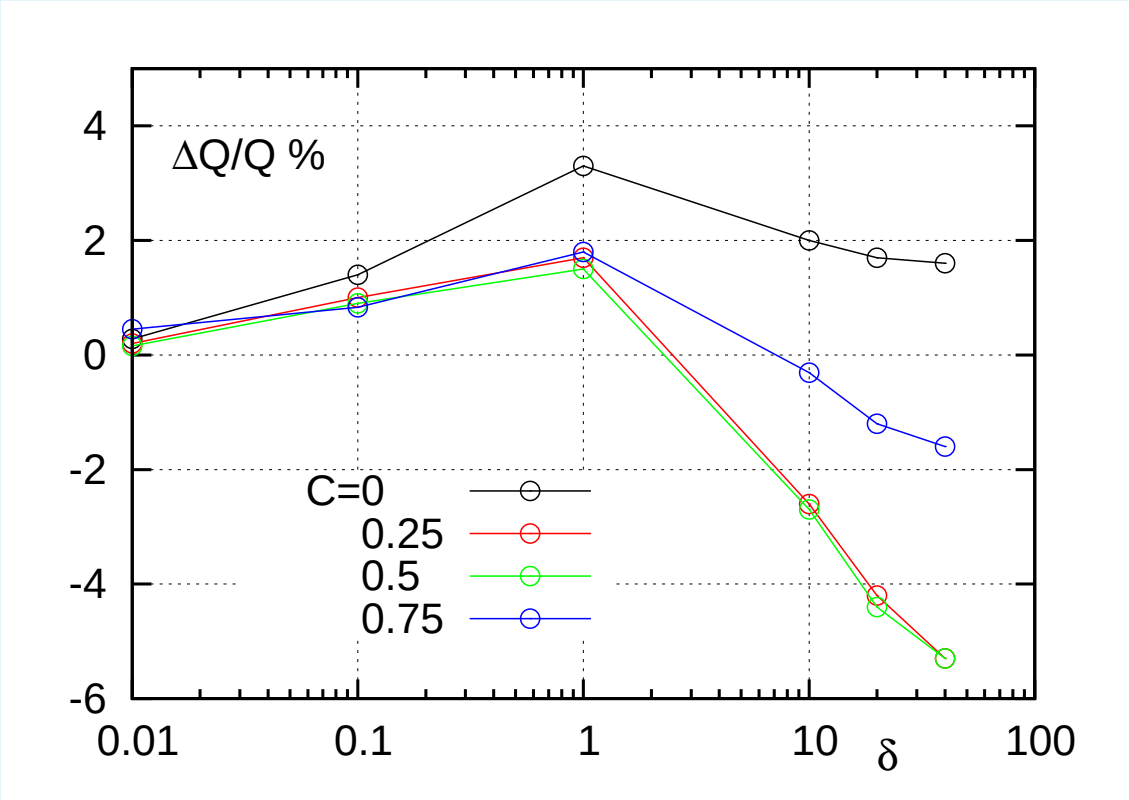

$$\frac{\Delta Q}{Q} = \frac{Q^{(AI)} - Q^{(HS)}}{Q^{(AI)}} \times 100\% \qquad (20)$$

Classical and quantum approaches, $\Delta T/T_0 = 1.5$. Sharipov, *Physica A* **508**, 797-805 (2018)

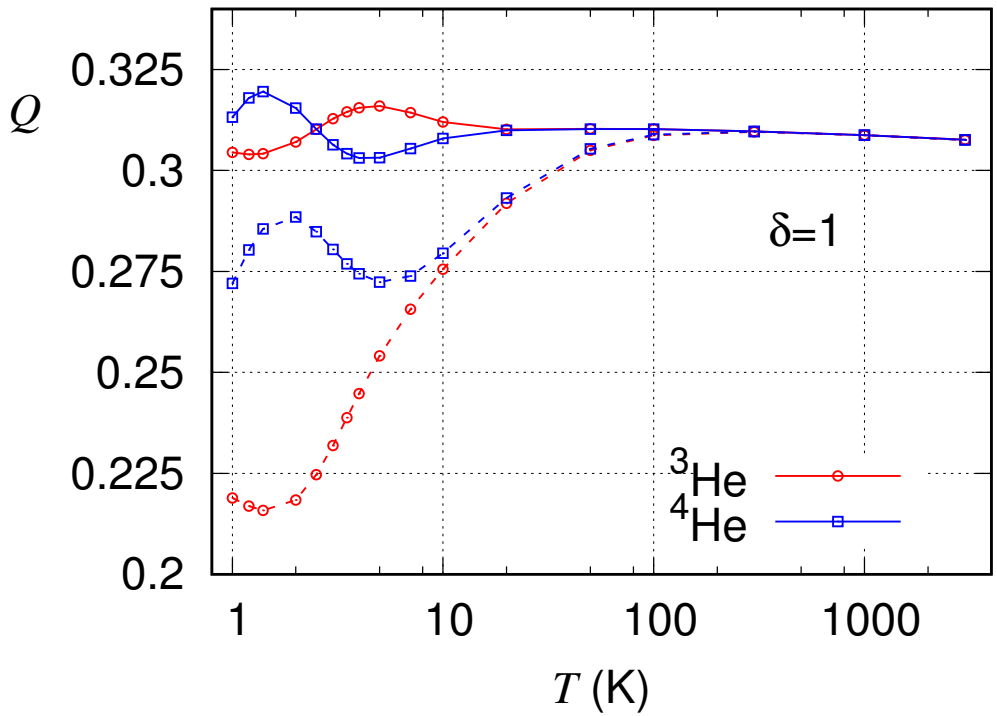

Solid line - quantum approach
dashed line -classical approach

Orifice flow. Sharipov & Strapasson, *Vacuum* **109**, 246-252 (2014)

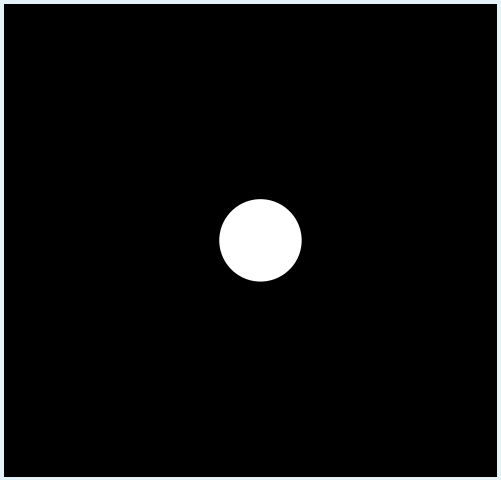

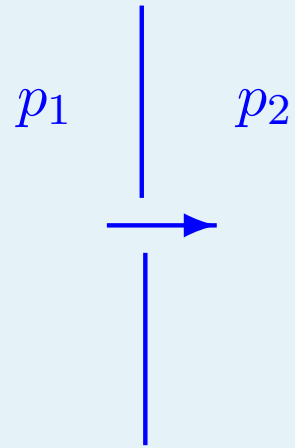

Orifice flow. Sharipov & Strapasson, *Vacuum* **109**, 246-252 (2014)

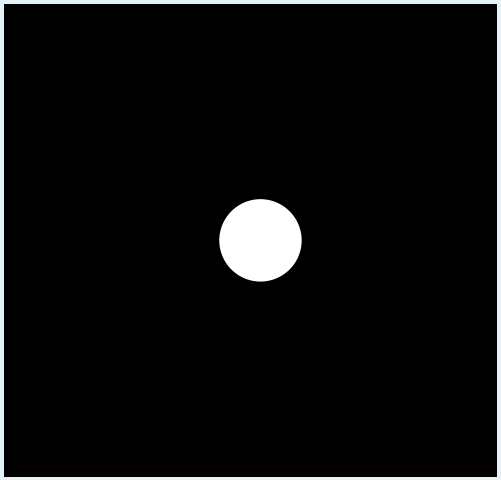

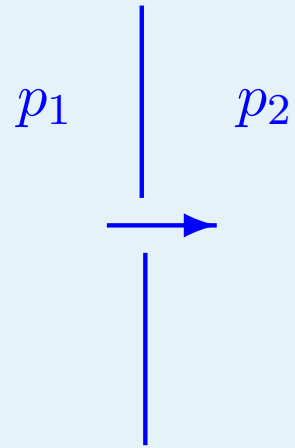

Reduced flow rate

$$W = \frac{\dot{M}}{\dot{M}_0}$$

$\dot{M}_0 = \sqrt{\pi} a^2 p_1 / v_m$ free-molecular flow into vacuum

Orifice flow. Sharipov & Strapasson, *Vacuum* **109**, 246-252 (2014)

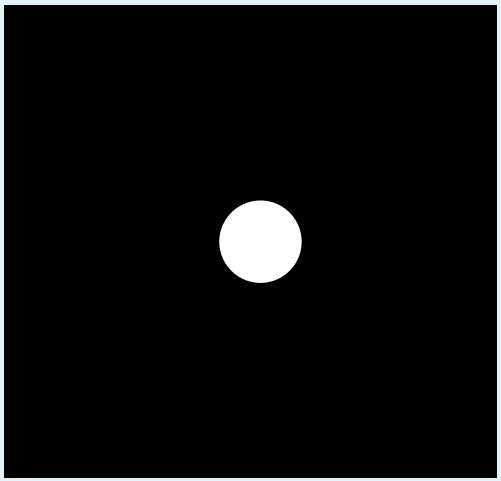

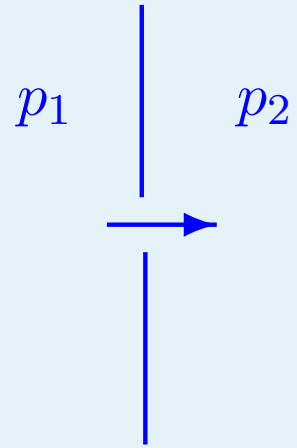

Determining parameters

- Rarefaction parameter

$$\delta = \frac{a p_1}{\mu \, v_m}$$

Orifice flow. Sharipov & Strapasson, *Vacuum* **109**, 246-252 (2014)

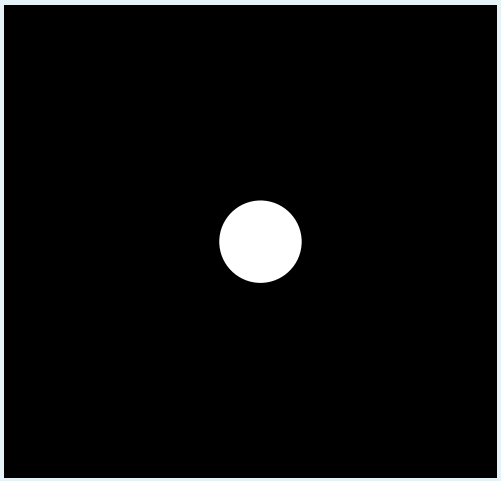

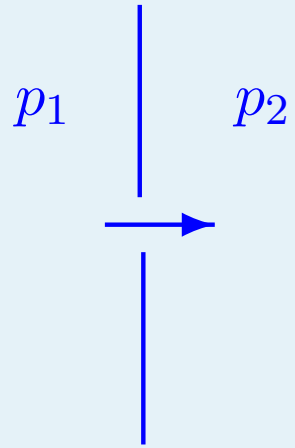

Determining parameters

- Rarefaction parameter

$$\delta = \frac{a p_1}{\mu \, v_m}$$

- Pressure ratio p_2/p_1

DSMC scheme

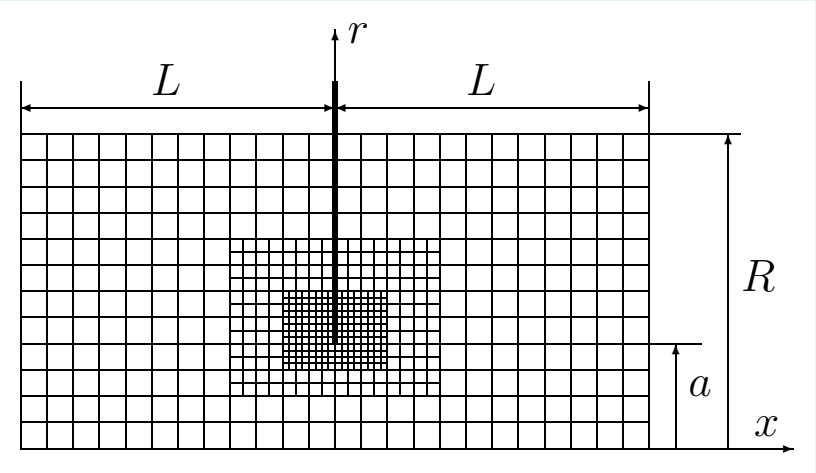

Sharipov & Strapasson, *Vacuum* **109** (2014)

AI potential for He, Ar, Kr

Number of model particles - 3×10^7

Time step - $0.005R/v_m$

Number of sample - 10^6

Numerical results based on AI potential, Ar.

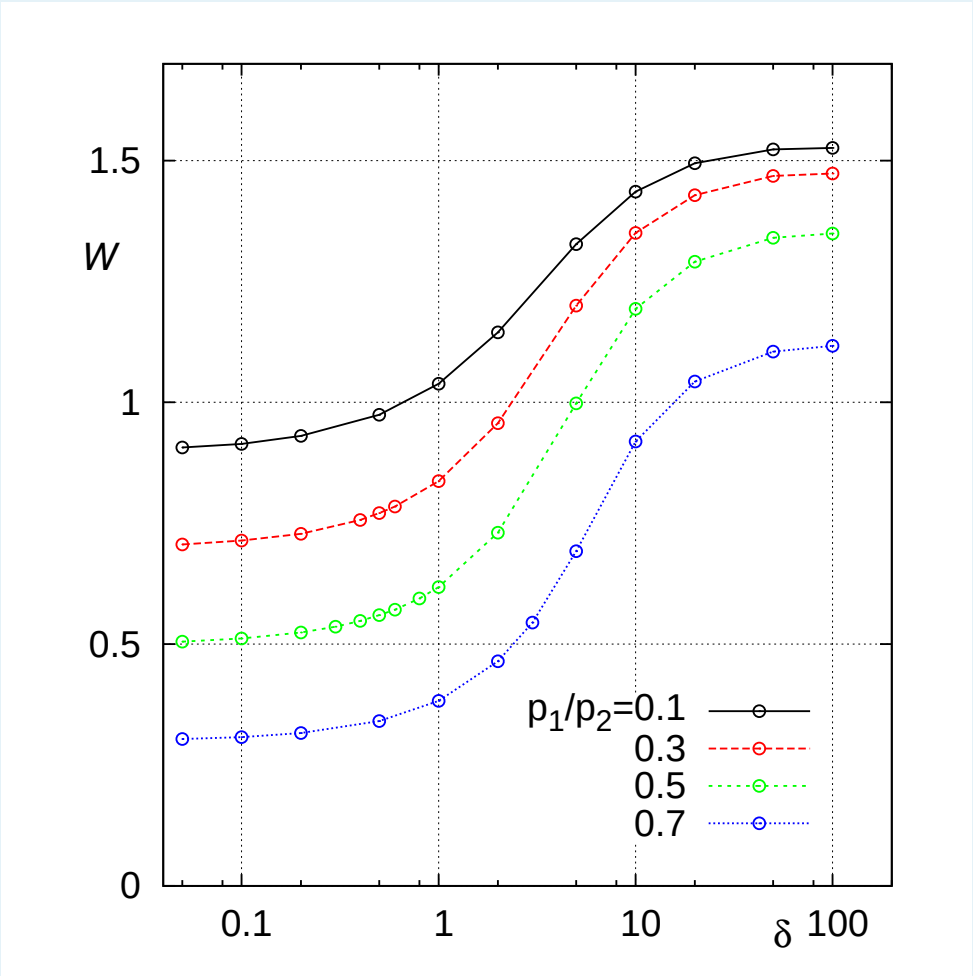

Sharipov & Strapasson, *Vacuum* **109** (2014)

Relative difference of flow rate between AI and HS, $p_1/p_0 = 0.7$

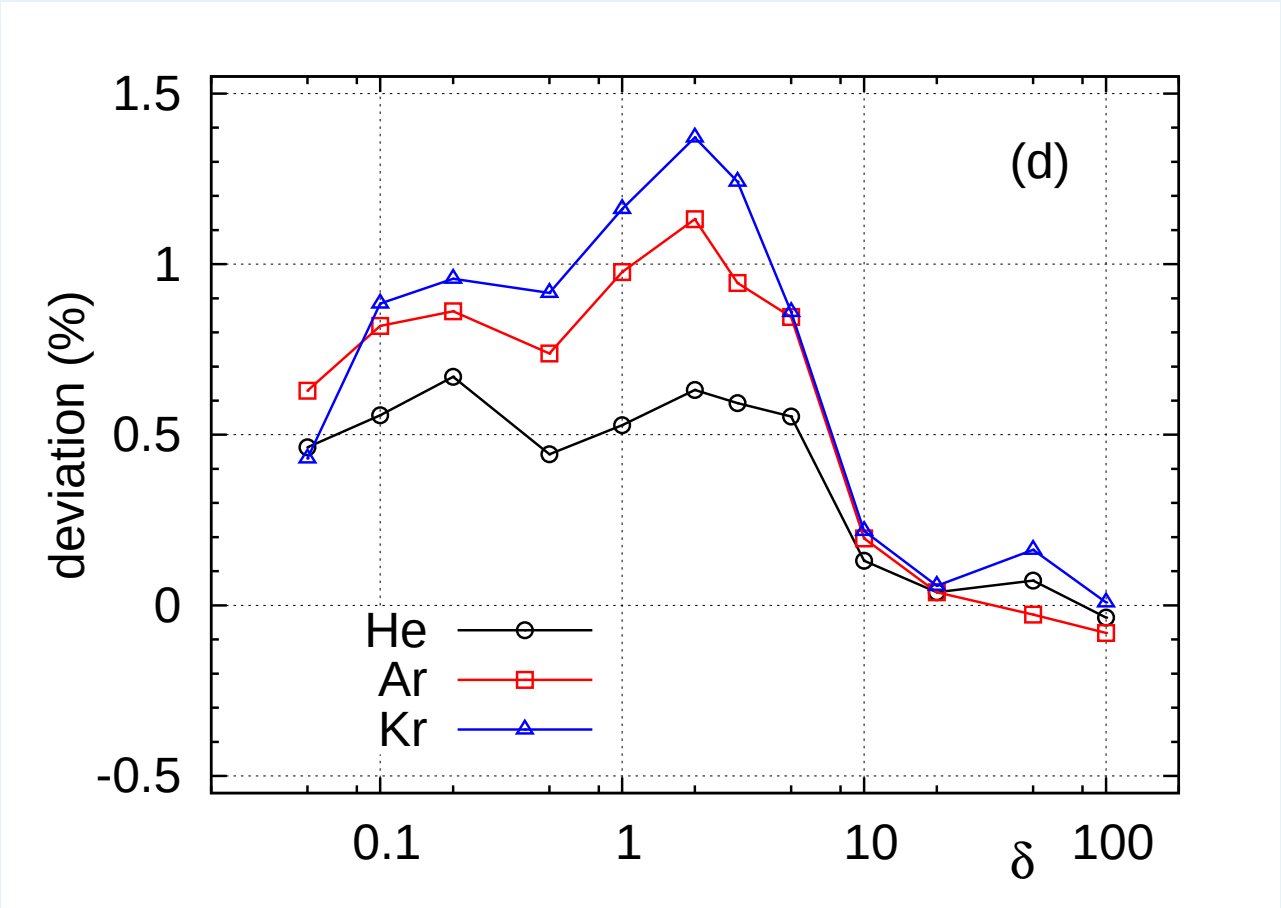

Relative difference of flow rate between AI and HS, $p_1/p_0 = 0.1$

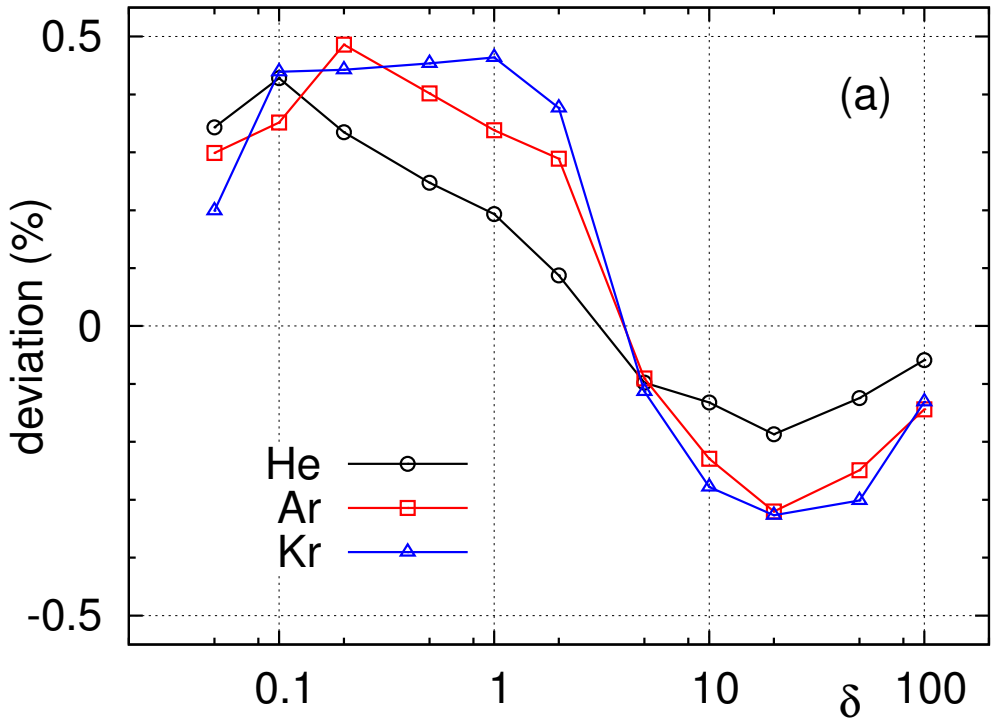

Sharipov & Strapasson, *Vacuum* **109** (2014)

Flow-field at $p_1/p_0 = 0.01$ and $\delta = 1000$

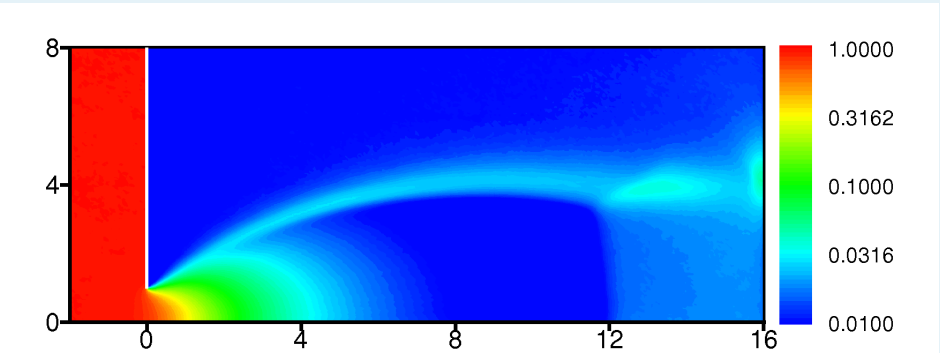

ϱ/ϱ_0 density

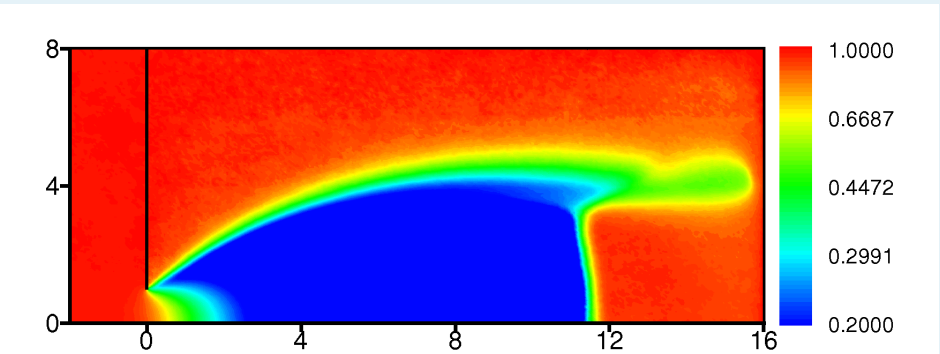

T/T_0 temperature

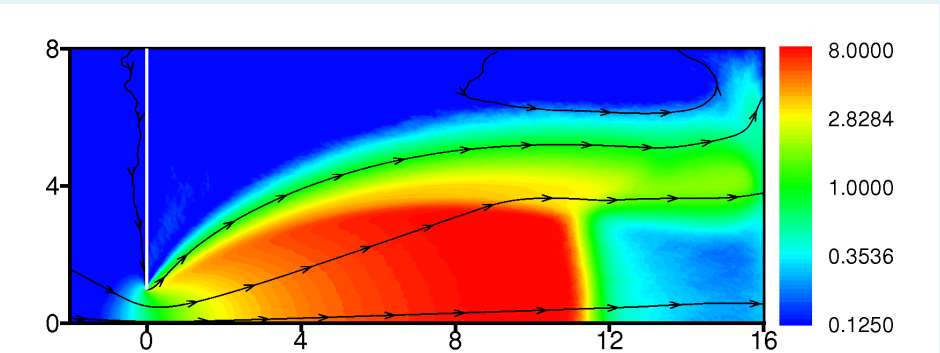

Local Mach number

Flow-field at $p_1/p_0 = 0.1$ and $\delta = 1000$

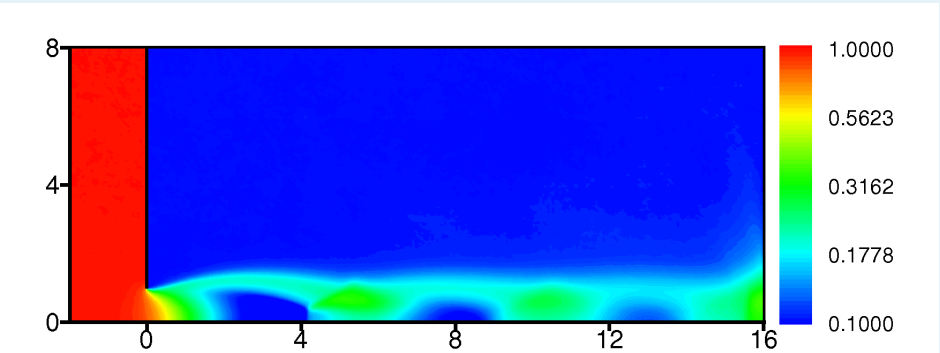

ϱ/ϱ_0 density

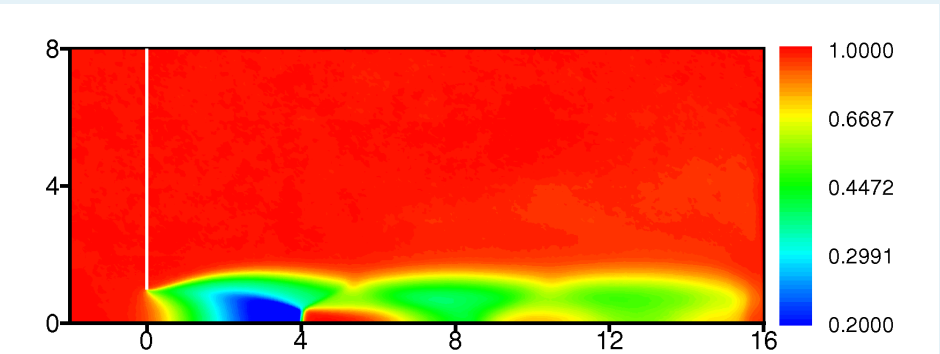

T/T_0 temperature

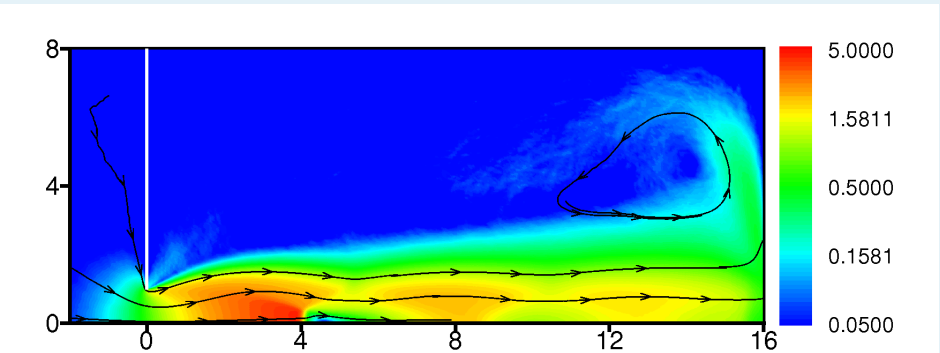

Mach number

Flow-field at $p_1/p_0 = 0.5$ and $\delta = 1000$

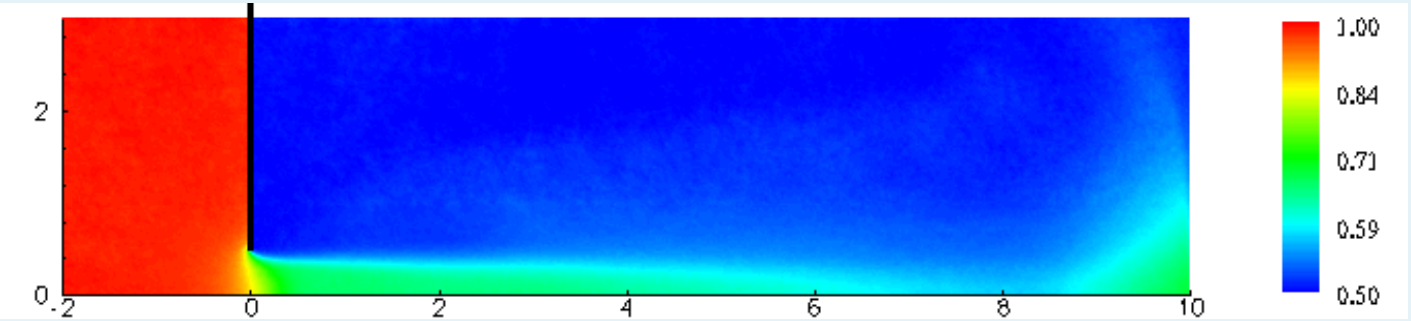

ϱ/ϱ_0 density

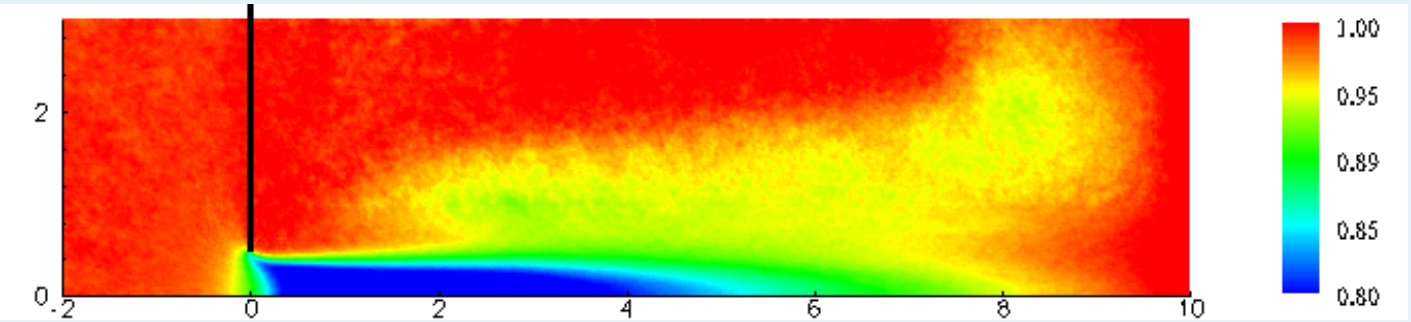

T/T_0

temperature

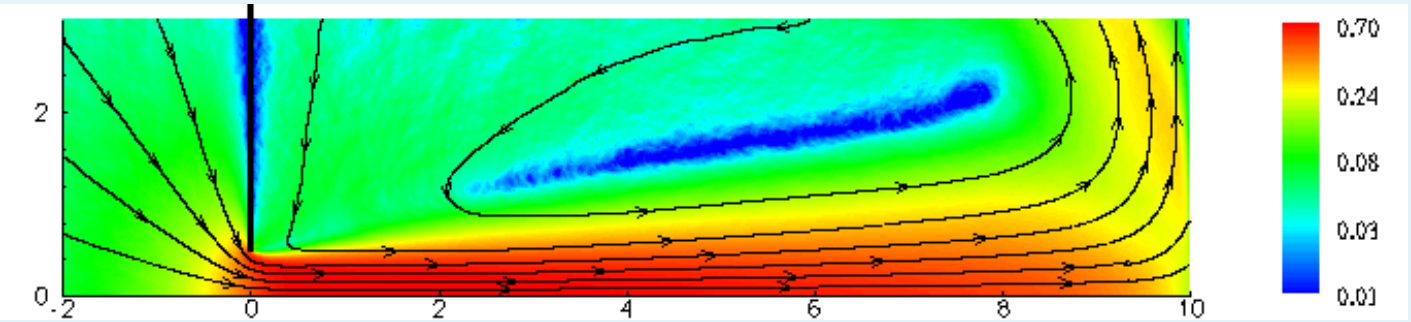

Mach number

AI potential, quantum effects.

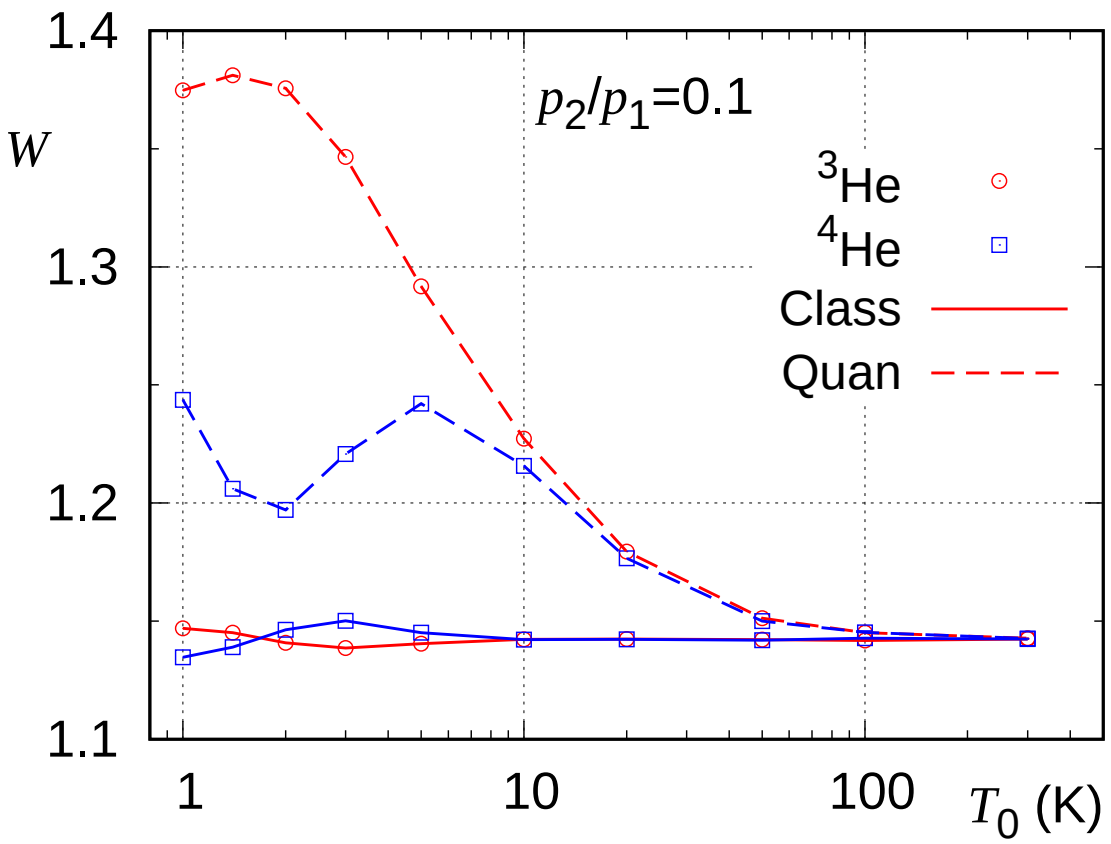

$\delta = 2$

solid - quantum,

dashed - classical

.

Sharipov, *Vacuum* **156**. 146 (2018)

Al potential, quantum effects.

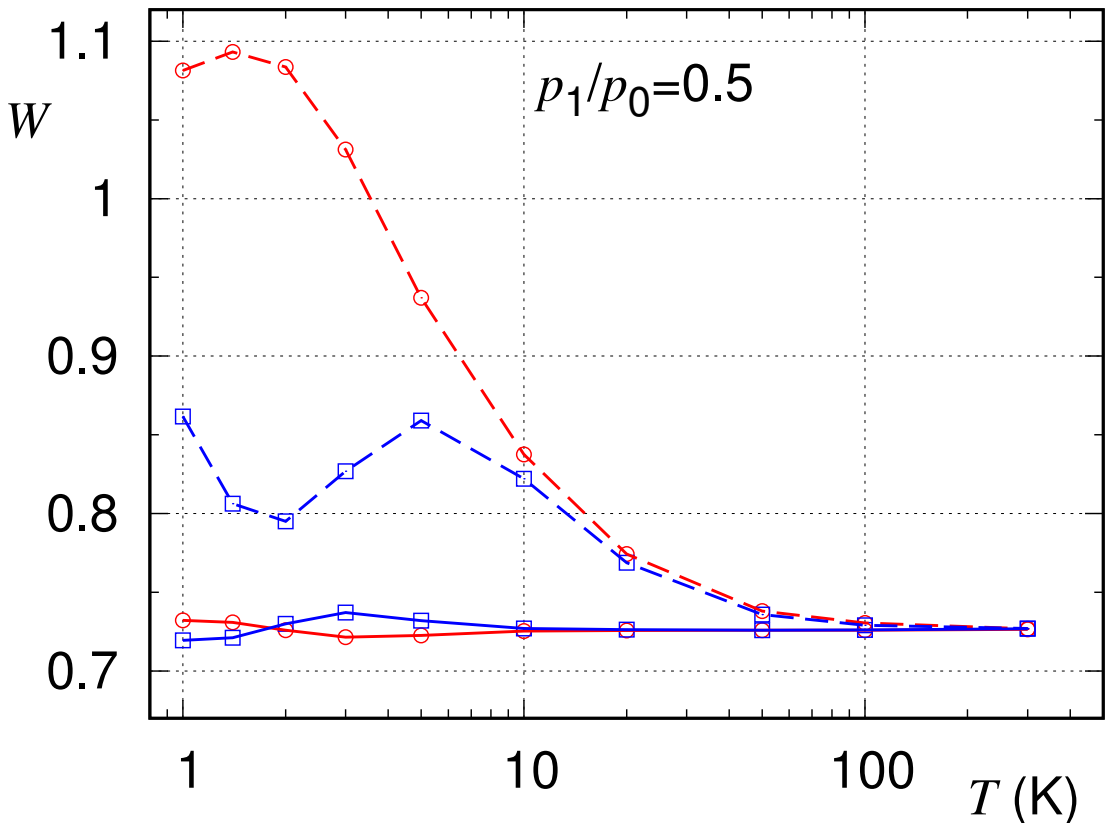

$\delta = 2$

solid - quantum,

dashed - classical

.

Sharipov, *Vacuum* **156**. 146 (2018)

AI potential, quantum effects.

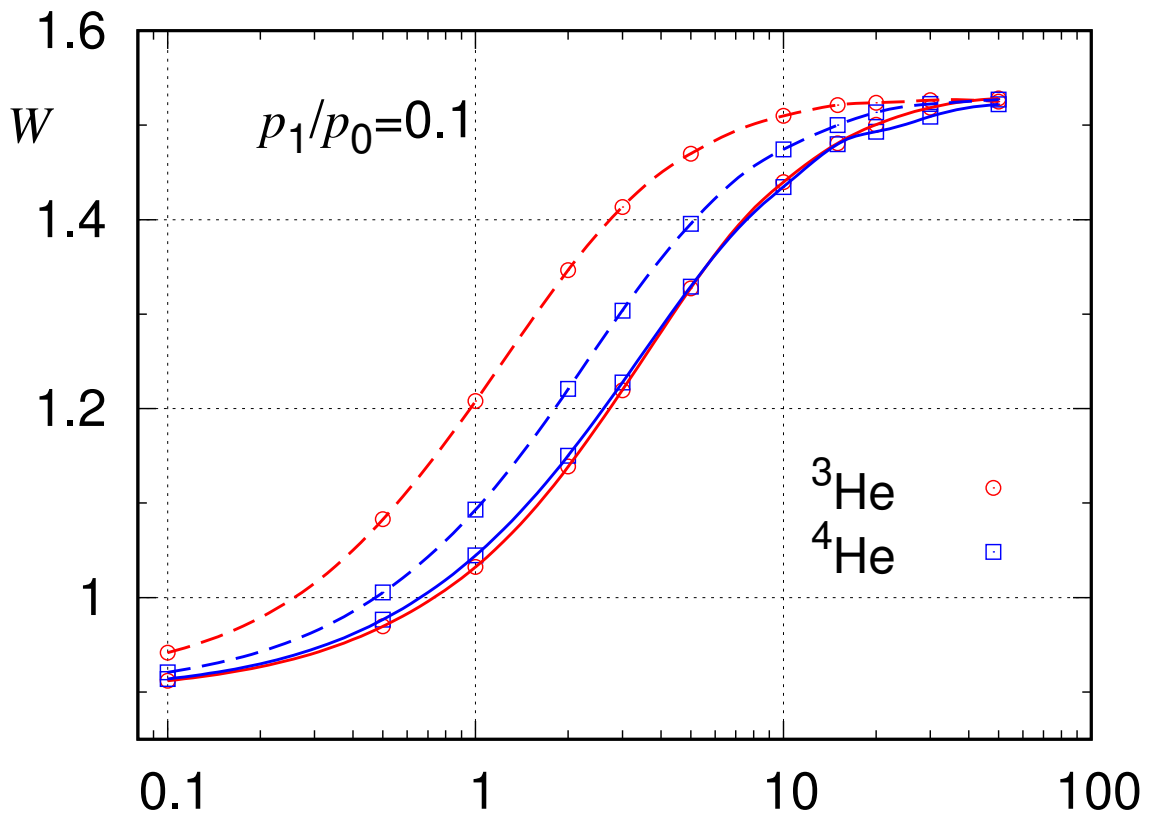

$T = 3$ K

solid - quantum,

dashed - classical

.

Sharipov, *Vacuum* **156**. 146 (2018)

Al potential, quantum effects

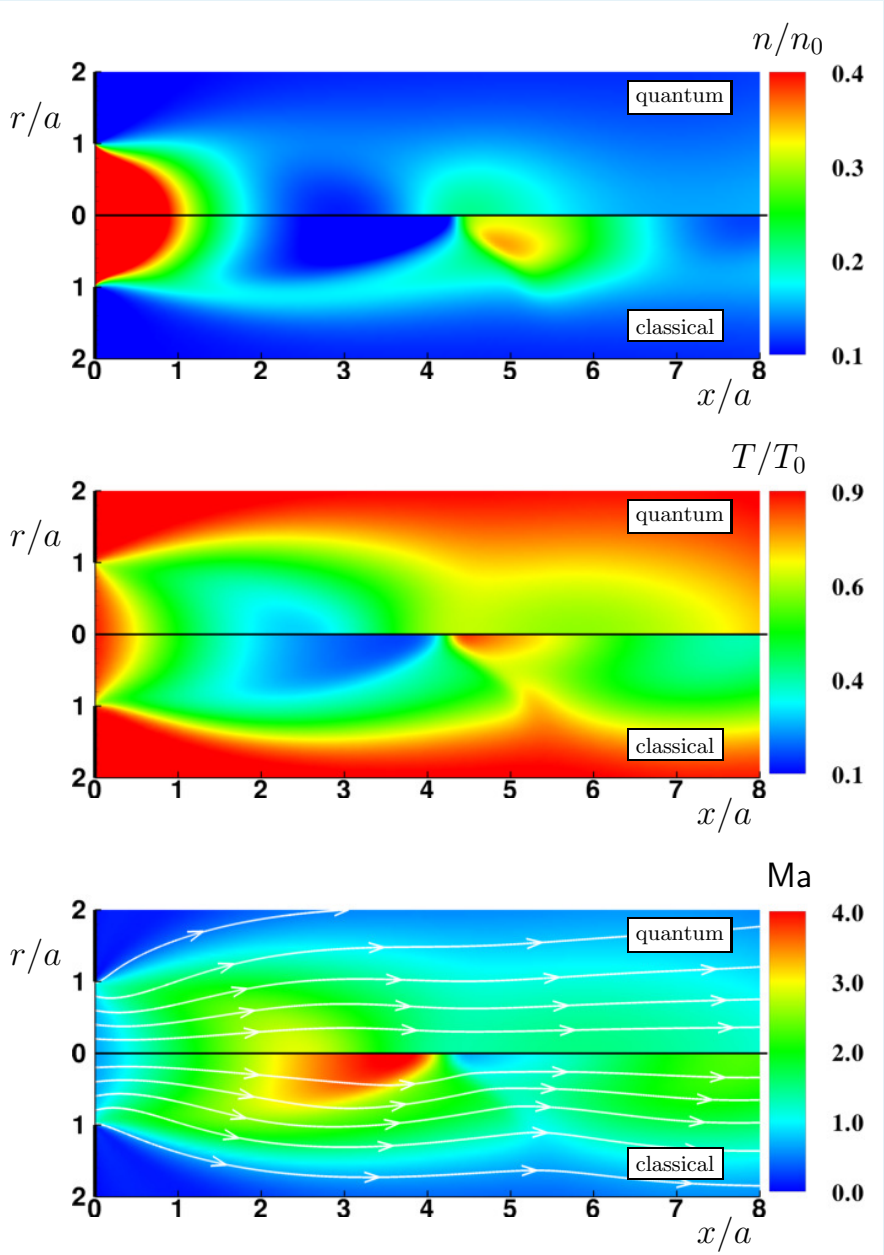

$p_1/p_0 = 0.1,$

$\delta = 50$

$T = 3$ K

cl. CPU time $= 4\times$

quan. CPU time

Al potential, quantum effects

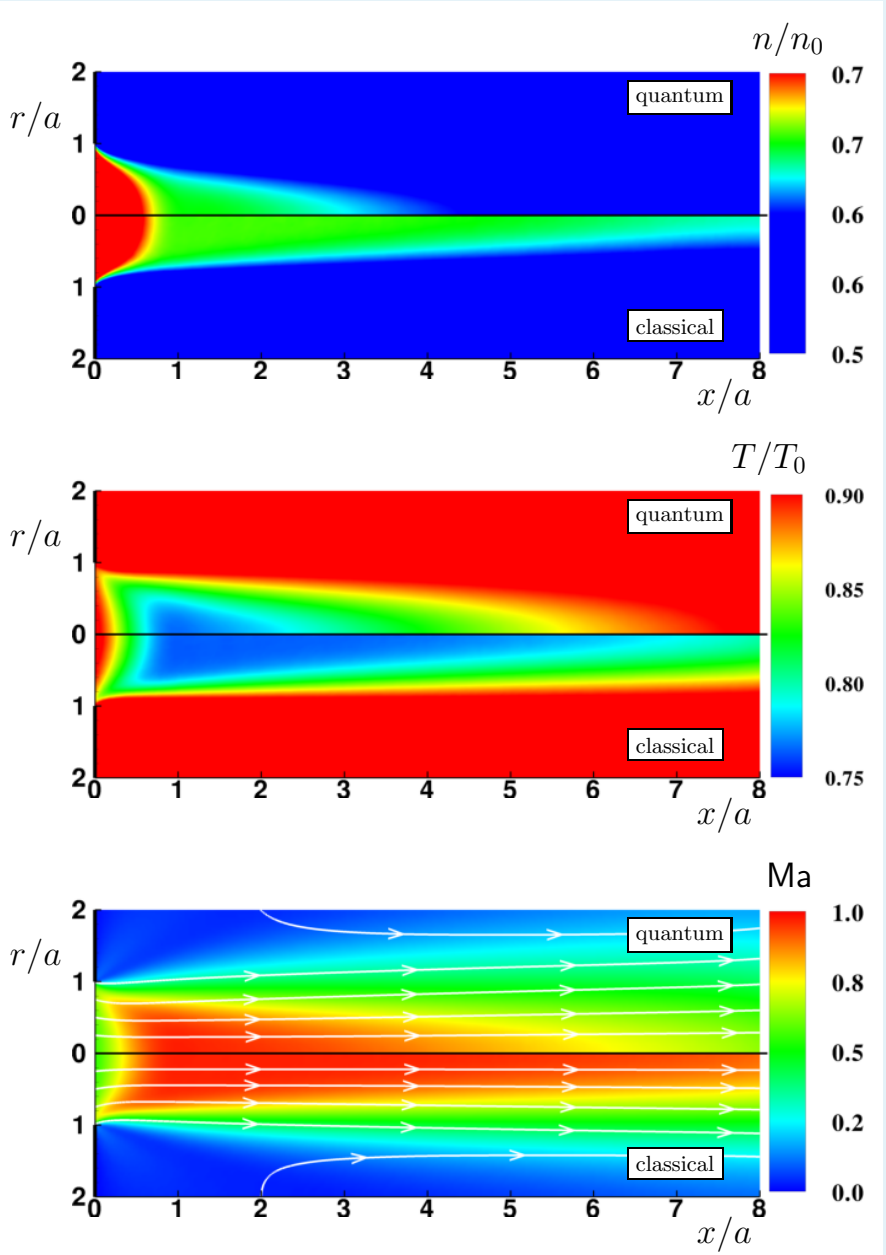

$p_1/p_0 = 0.5,$

$\delta = 50$

$T = 3$ K

cl. CPU time $= 4\times$

quan. CPU time

Reduced flow rate W vs δ at $p_1/p_0 = 0$, mixture of He-Ar. Sharipov, *Vacuum* **143** (2017)

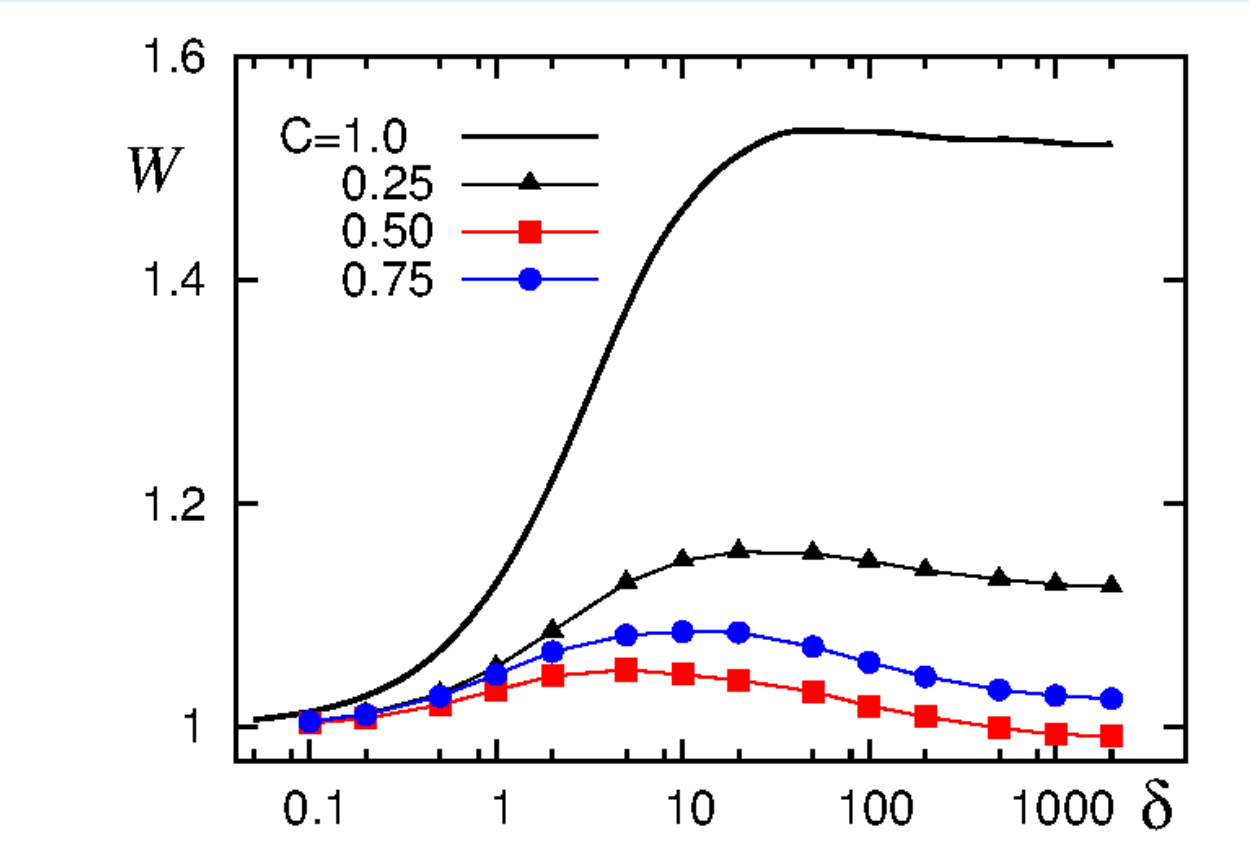

Reduced flow rate W vs δ at $p_1/p_0 = 0.5$, mixture of He-Ar. Sharipov, *Vacuum* **143** (2017)

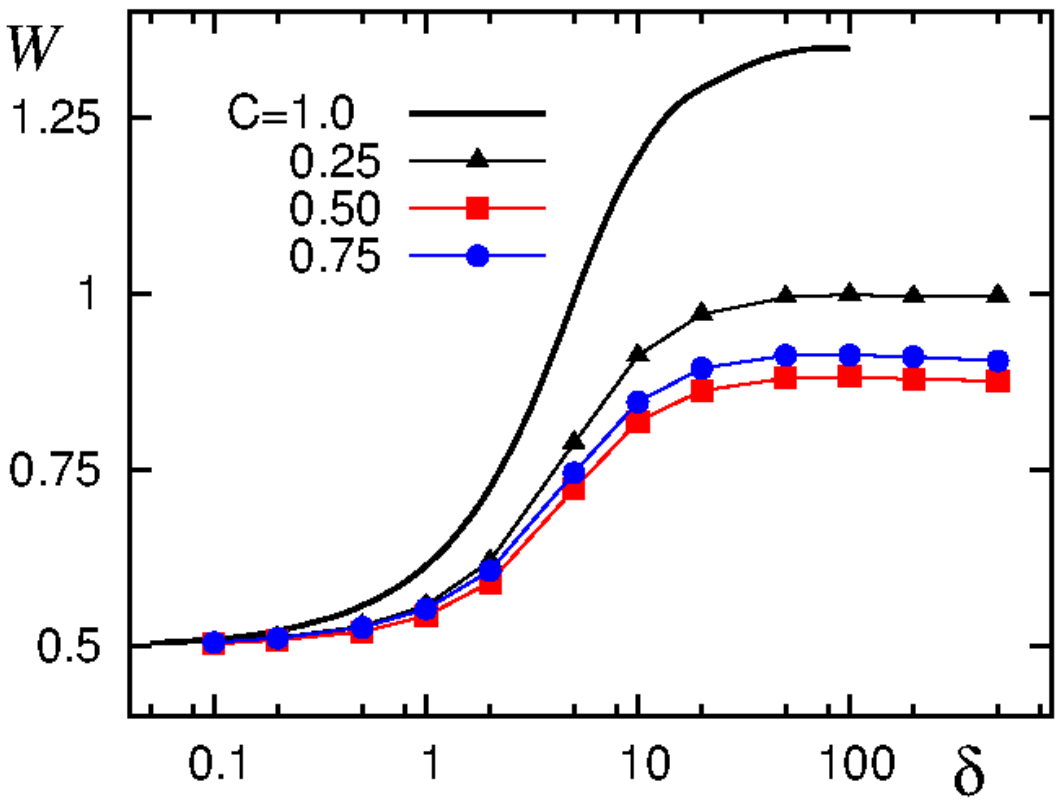

Flow-field of equimolar mixture He-Ar at $p_1/p_0 = 0.1$ and $\delta = 1000$, Sharipov, *Vacuum* **143** (2017)

,

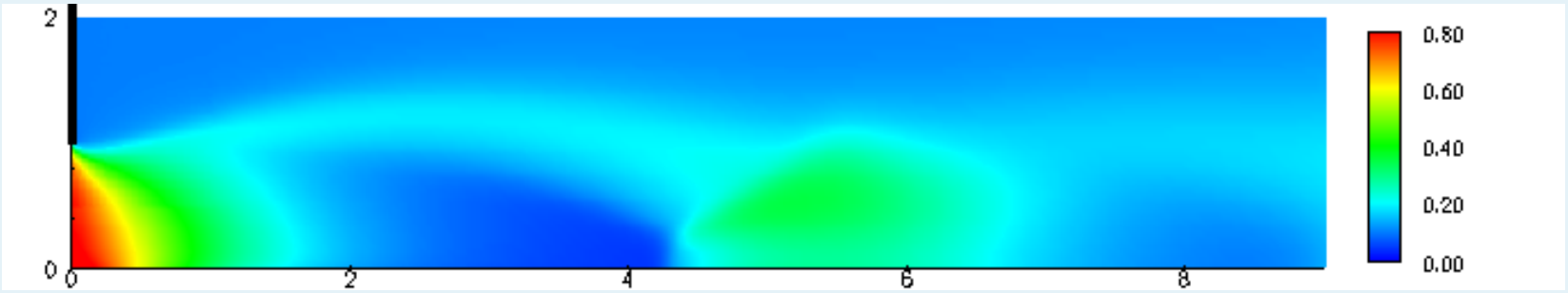

ϱ/ϱ_0

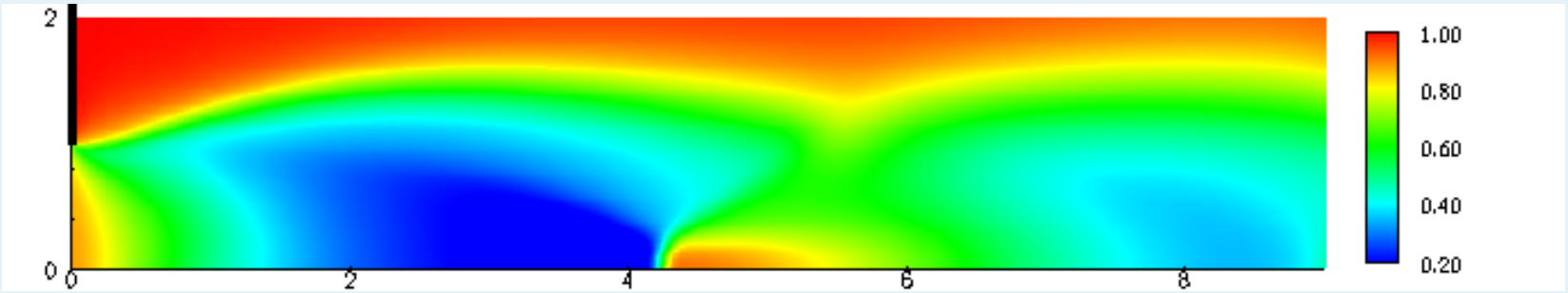

T/T_0

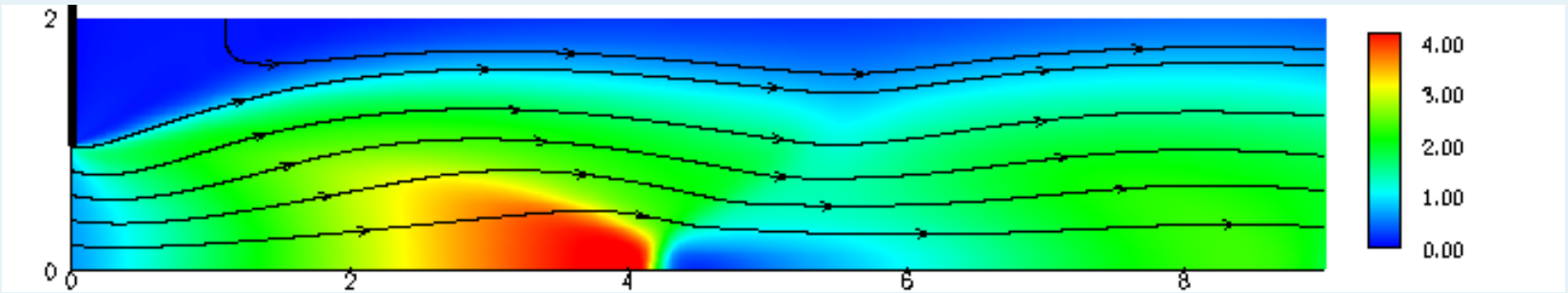

Ma

Axial distribution of equimolar mixture at $p_1/p_0 = 0.1$, Sharipov, *Vacuum* **143** (2017)

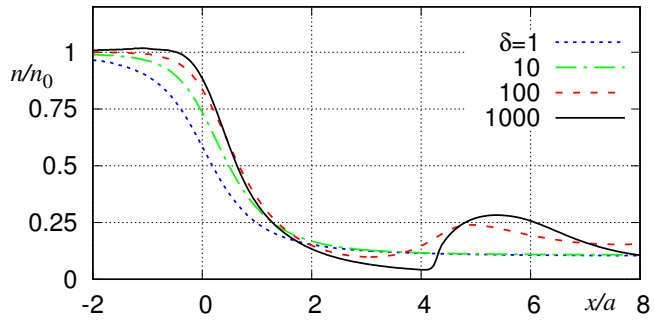

density

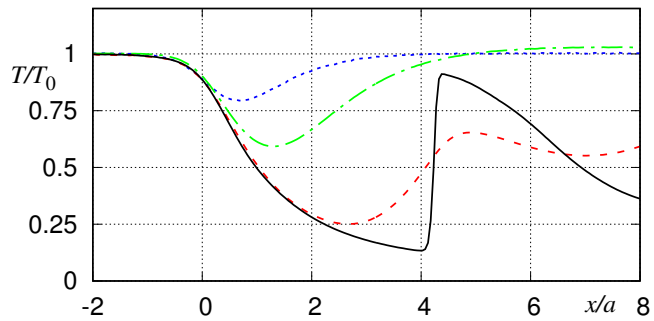

temperature

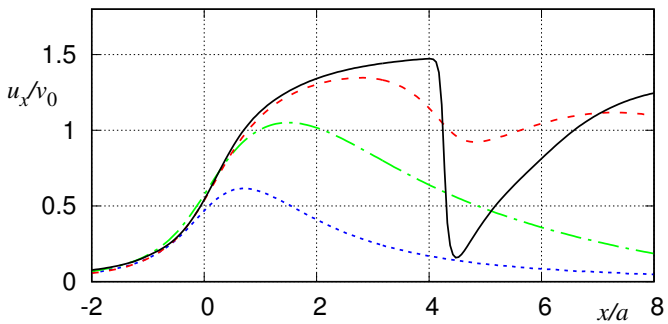

bulk velocity

Scheme of slit flow

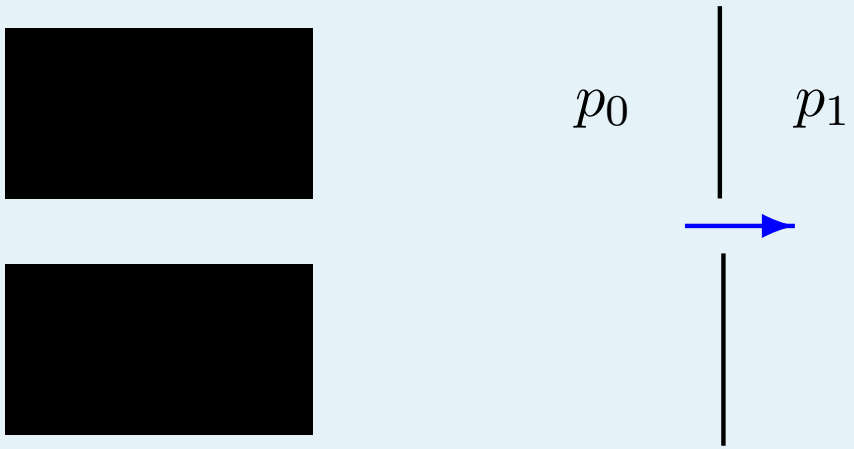

Scheme of slit flow

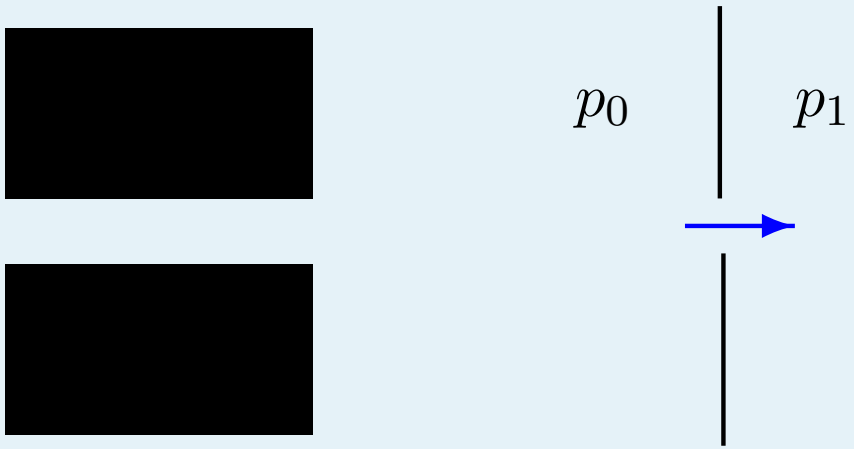

Reduced flow rate

$$W = \dot{M}/\dot{M}_0, \qquad \dot{M}_0 = p_0 H/\sqrt{\pi} v_m, \quad v_m = \sqrt{2kT/m} \tag{21}$$

Scheme of slit flow

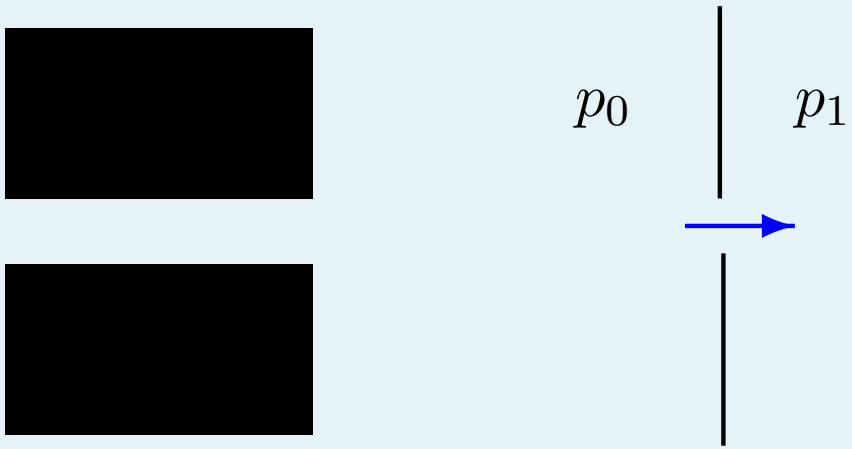

Reduced flow rate

$$W = \dot{M}/\dot{M}_0, \qquad \dot{M}_0 = p_0 H/\sqrt{\pi} v_m, \quad v_m = \sqrt{2kT/m} \tag{21}$$

Rarefaction parameter

$$\delta = p_0 H/\mu v_m \propto 1/\mathrm{Kn} \tag{22}$$

Flow rate through a slit. BGK vs. DSMC

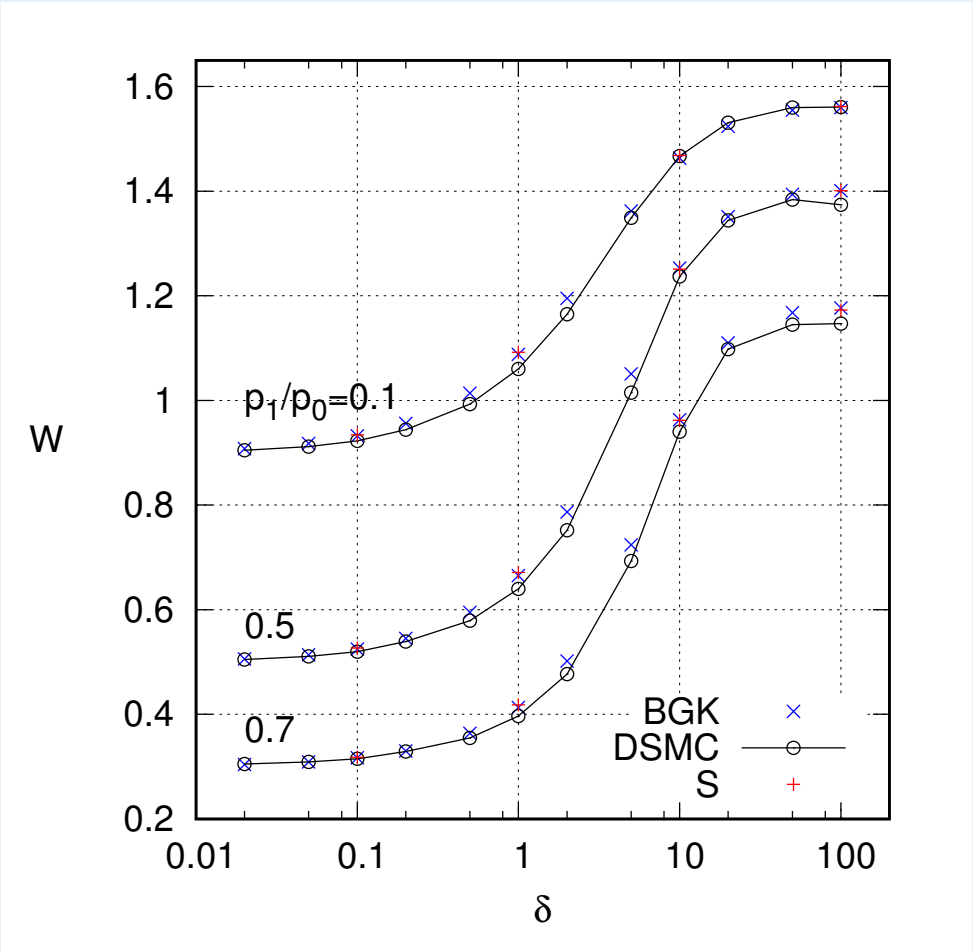

$\Delta W/W < 4\%$

DSMC: Sharipov & Kozak, *Eur. J. Mech. B/Fluids* **30**(5), (2011)

BGK and S: Graur, Polikarpov & Sharipov, *ZAMP* **63**, 503-50 (2012)

Axial distribution of flowfield past a slit at $p_1/p_0 = 0.1$. BGK vs. DSMC

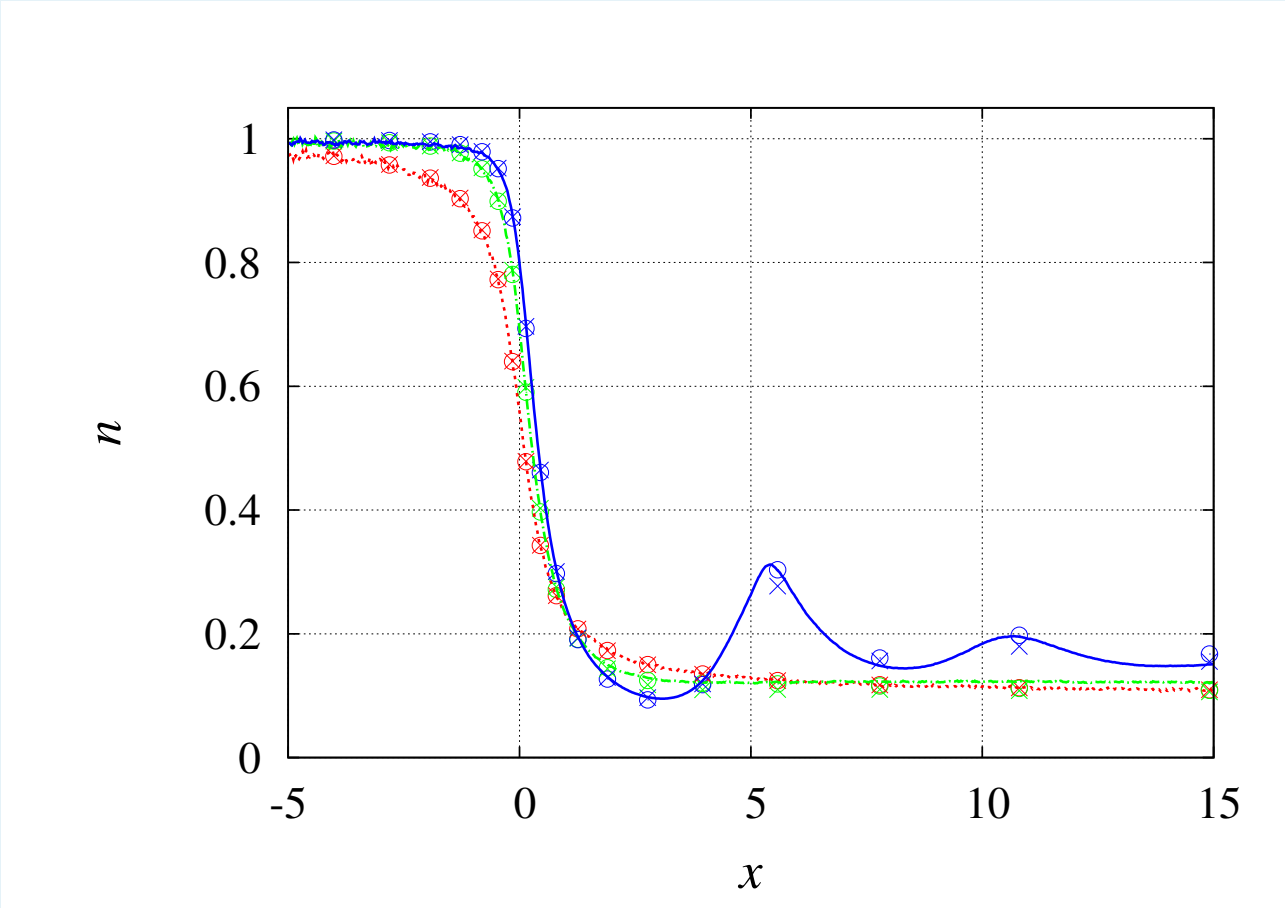

Density, Lines - DSMC, circles - BGK, crosses - S-model;

red - $\delta = 0.1$, green - $\delta = 10$, blue - $\delta = 100$

Axial distribution of flowfield past a slit at $p_1/p_0 = 0.1$. BGK vs. DSMC

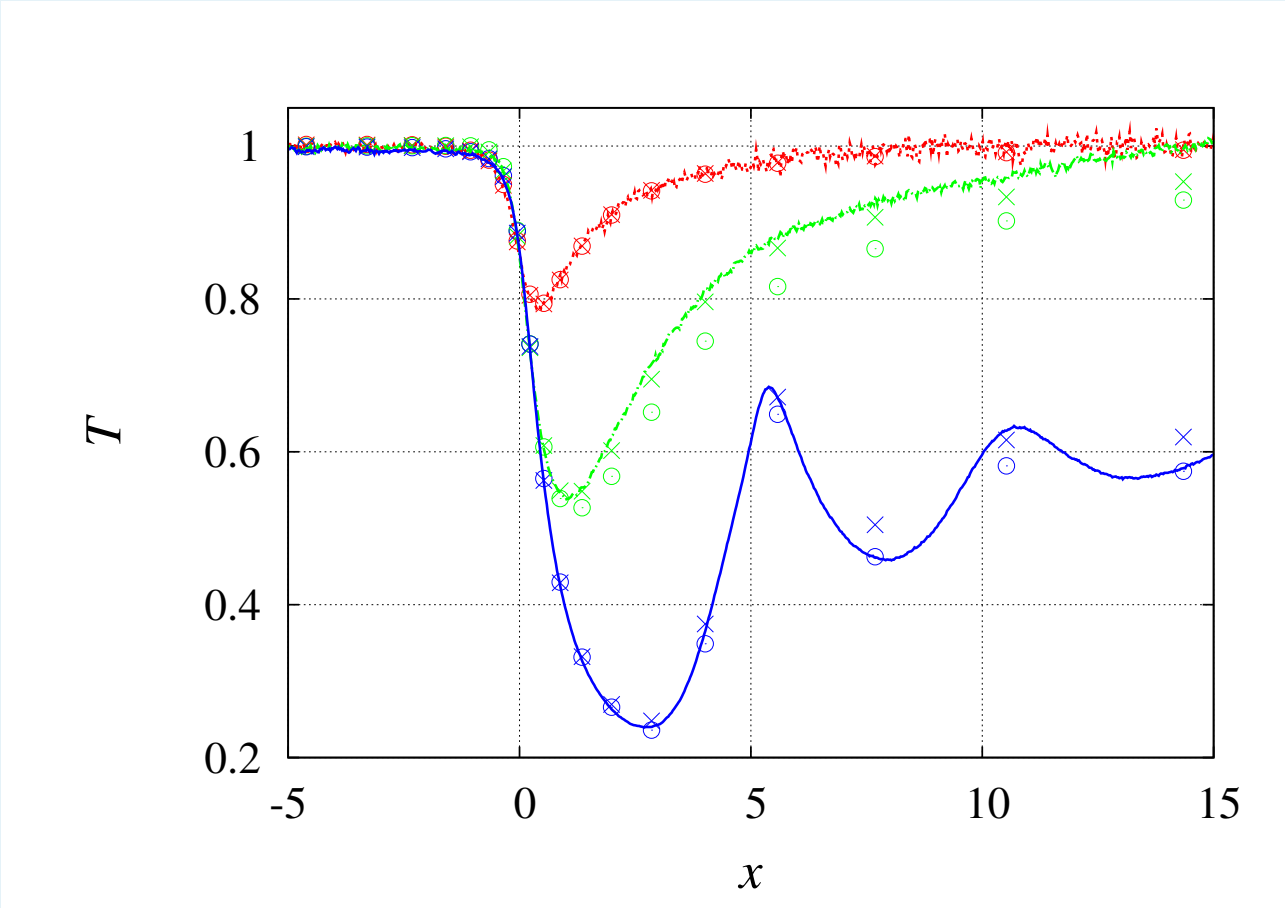

Temperature, Lines - DSMC, circles - BGK, crosses - S-model;

red - $\delta = 0.1$, green - $\delta = 10$, blue - $\delta = 100$

Axial distribution of flowfield past a slit at $p_1/p_0 = 0.1$. BGK vs. DSMC

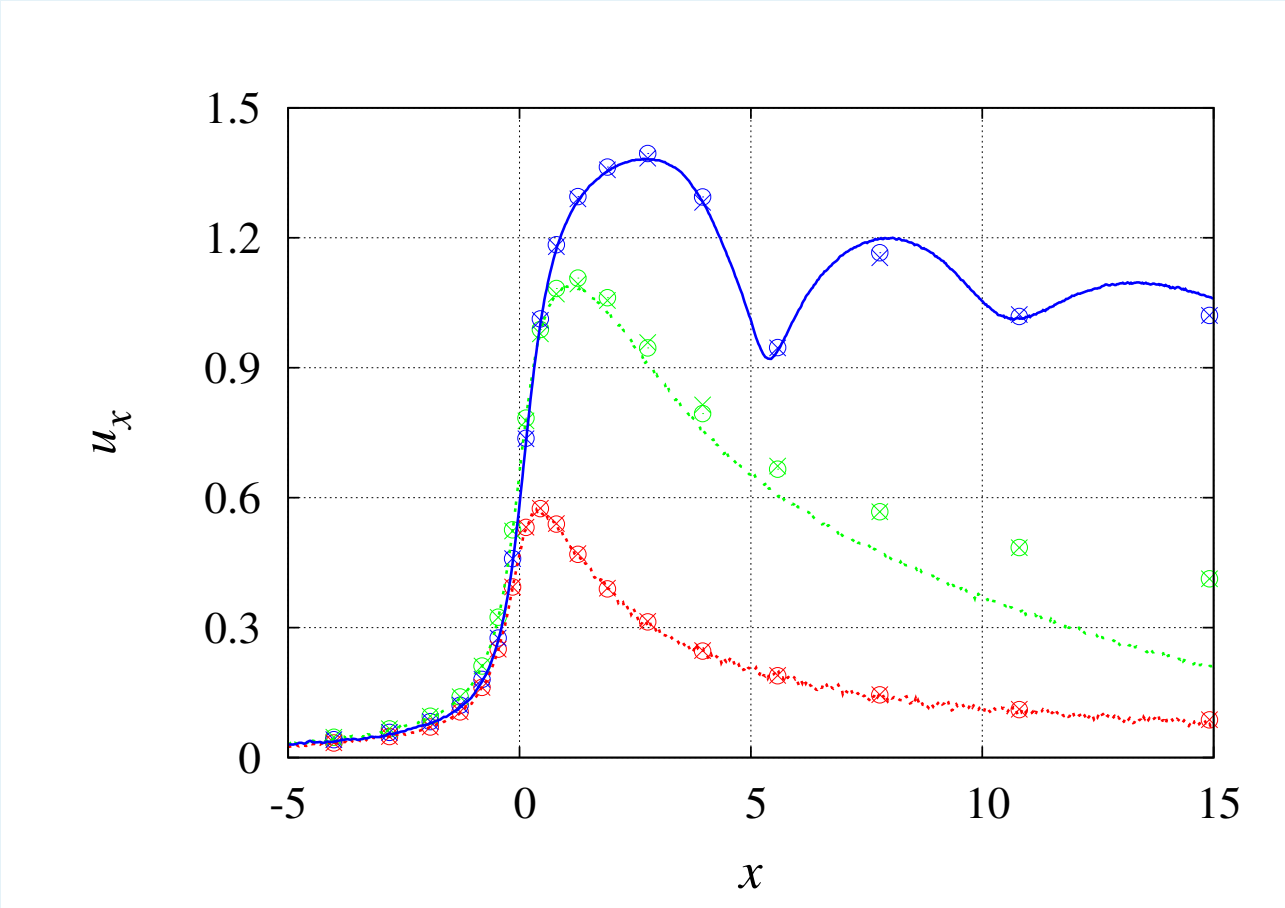

Bulk velocity, Lines - DSMC, circles - BGK, crosses - S-model;

red - $\delta = 0.1$, green - $\delta = 10$, blue - $\delta = 100$

Modelling of vacuum pumps

Scheme of pump

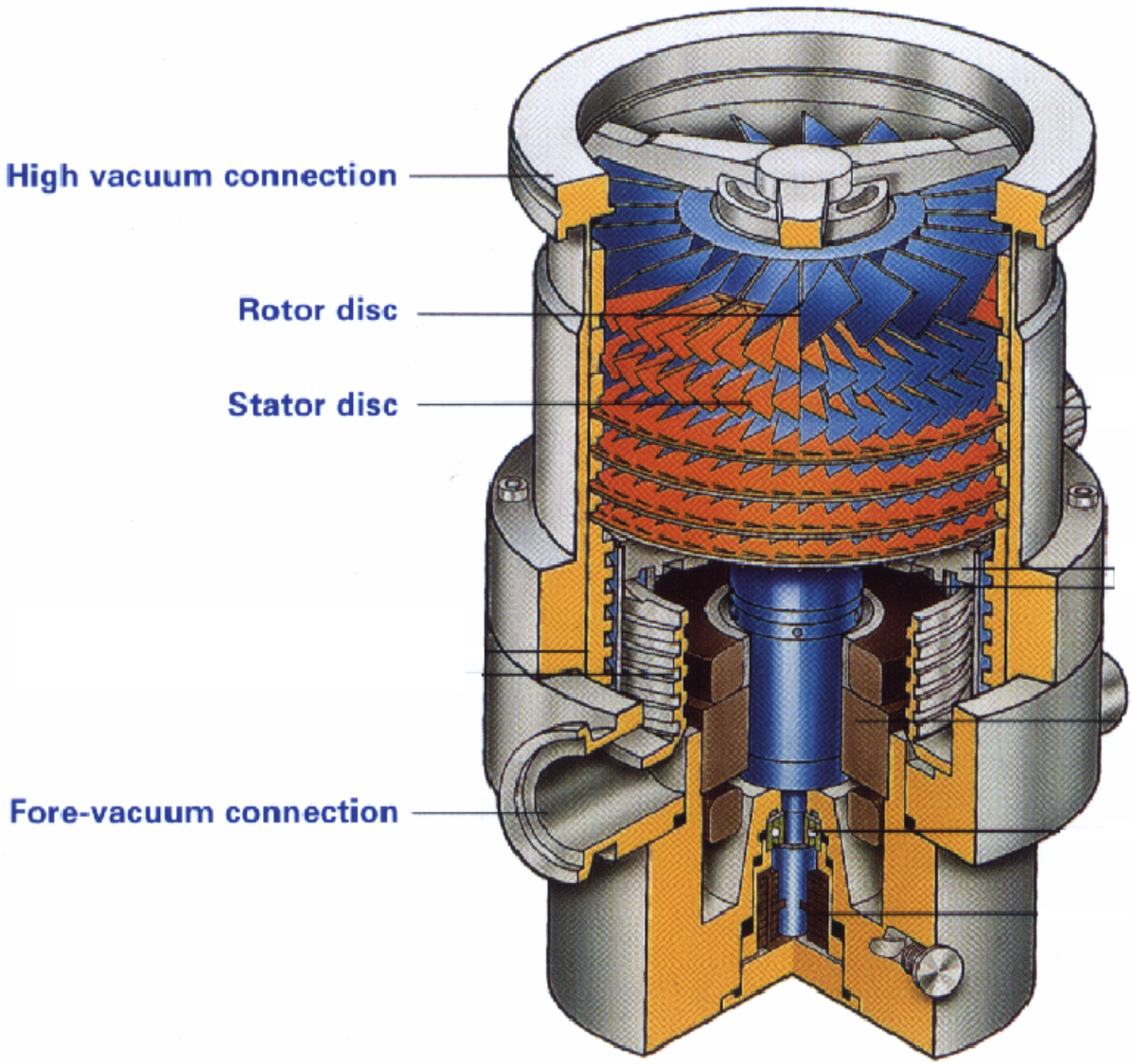

Scheme of pump, Sharipov, *J. Vac. Sci. Technol. A* **28**, 1312 (2010)

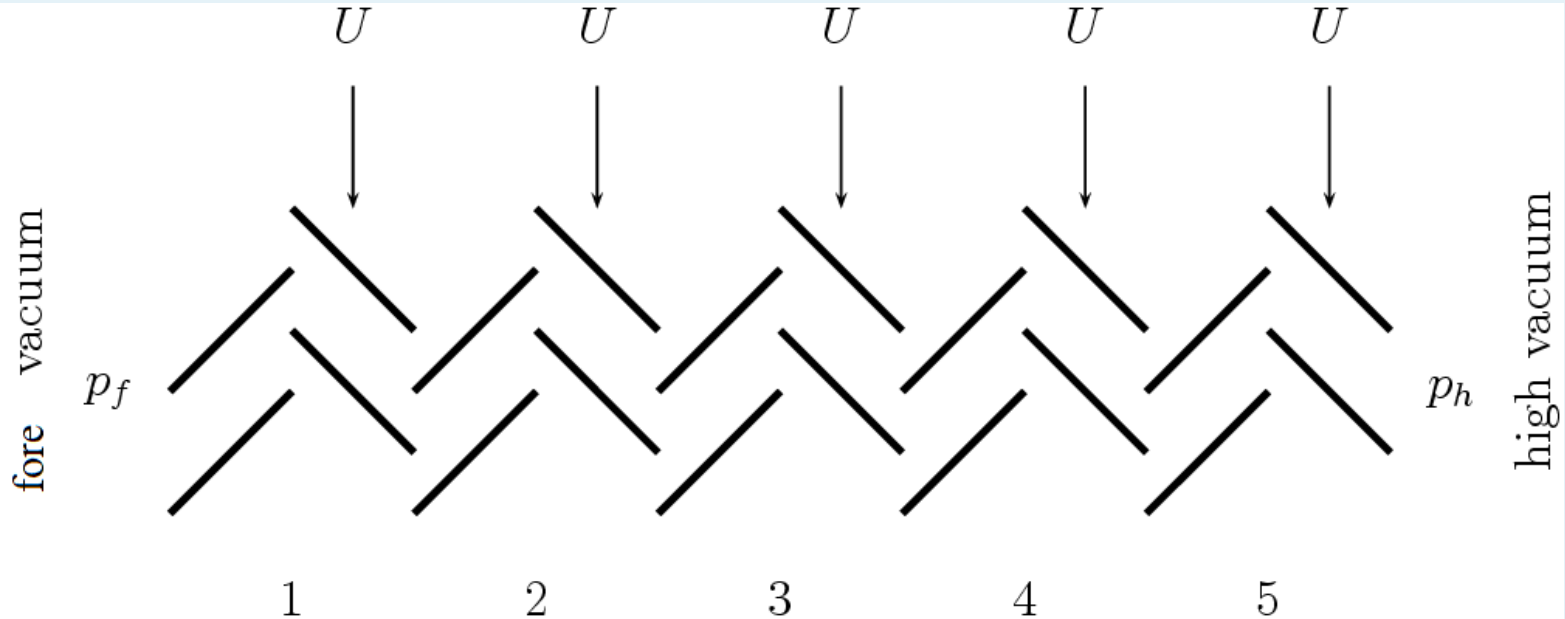

Pumping speed

$$S = \frac{2\sqrt{\pi}}{v_m A} \frac{q}{p_f} \tag{23}$$

Pumping speed

$$S = \frac{2\sqrt{\pi}}{v_m A}\frac{q}{p_f} \tag{23}$$

A - working area of TMP

v_m - the most probable speed of molecules

q - throughput [Pa m^3/s]

p_f - fore vacuum pressure

Compression ratio

$$k = \frac{\text{fore vacuum pressure}}{\text{high vacuum pressure}} \tag{24}$$

Main determining parameters

- $$U = \frac{\text{blade speed}}{\text{most probable molecular speed}} \tag{25}$$

Main determining parameters

- $$U = \frac{\text{blade speed}}{\text{most probable molecular speed}} \tag{25}$$

- Rarefaction parameter

$$\delta = \frac{hp_f}{\mu v_m} \tag{26}$$

h space between blades
μ gas viscosity

Numerical scheme, DSMC

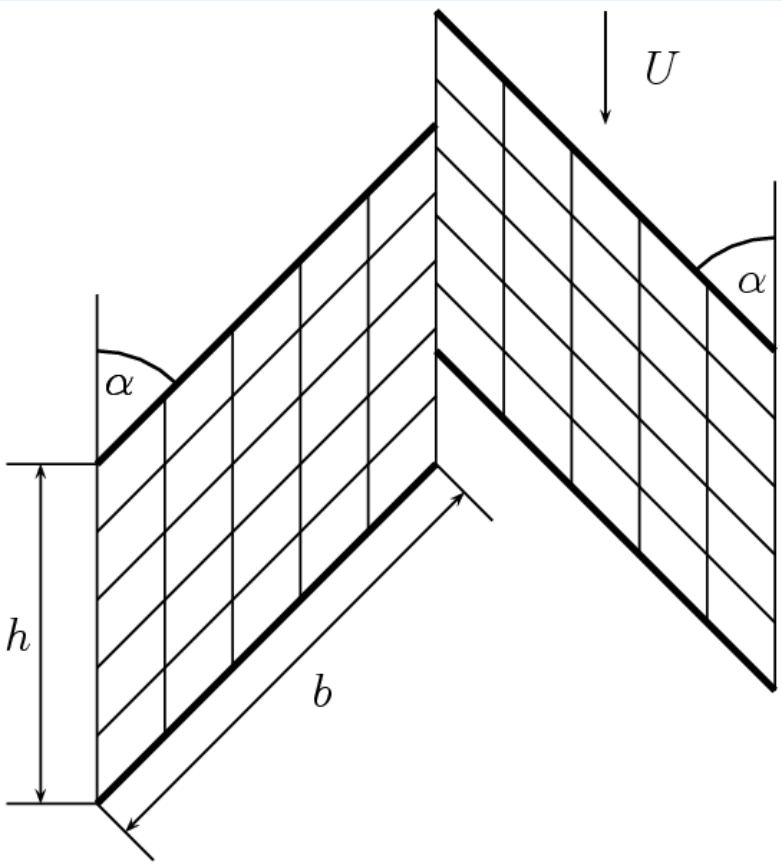

Results, Maximum pumping speed, $p_h = p_f$

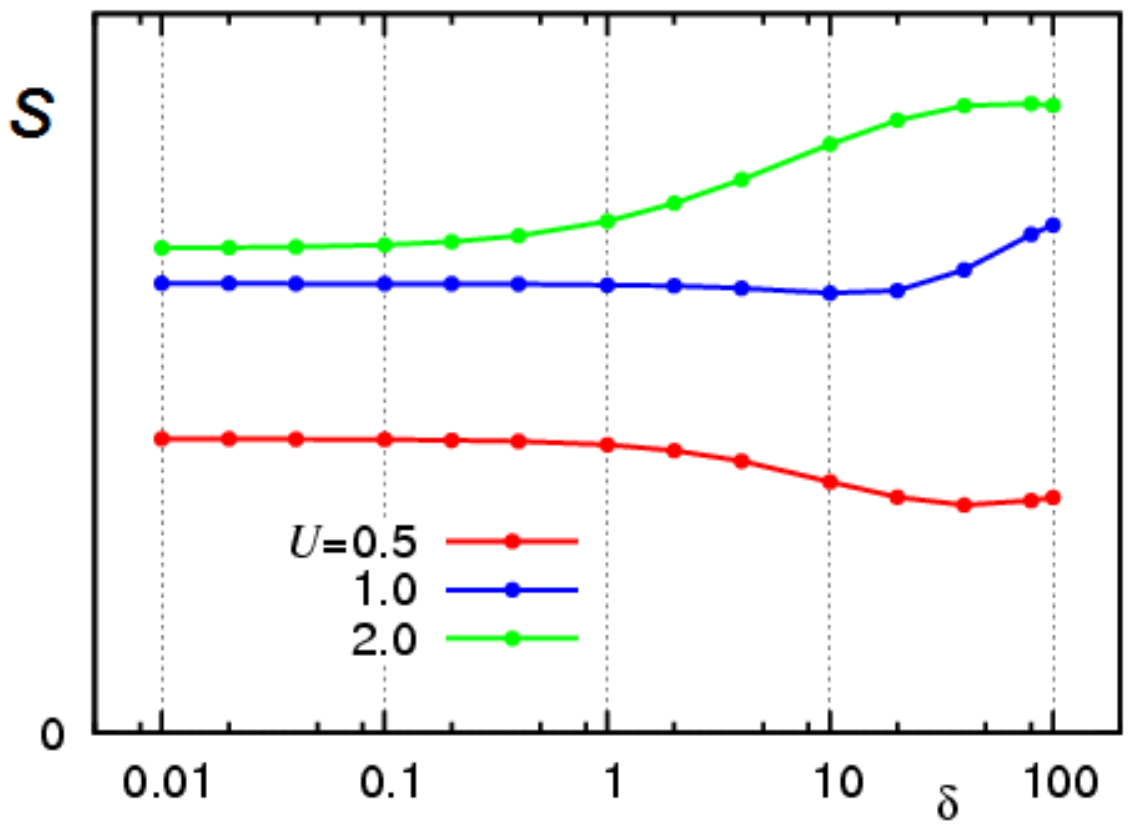

Results, Limit compression ratio, $S = 0$

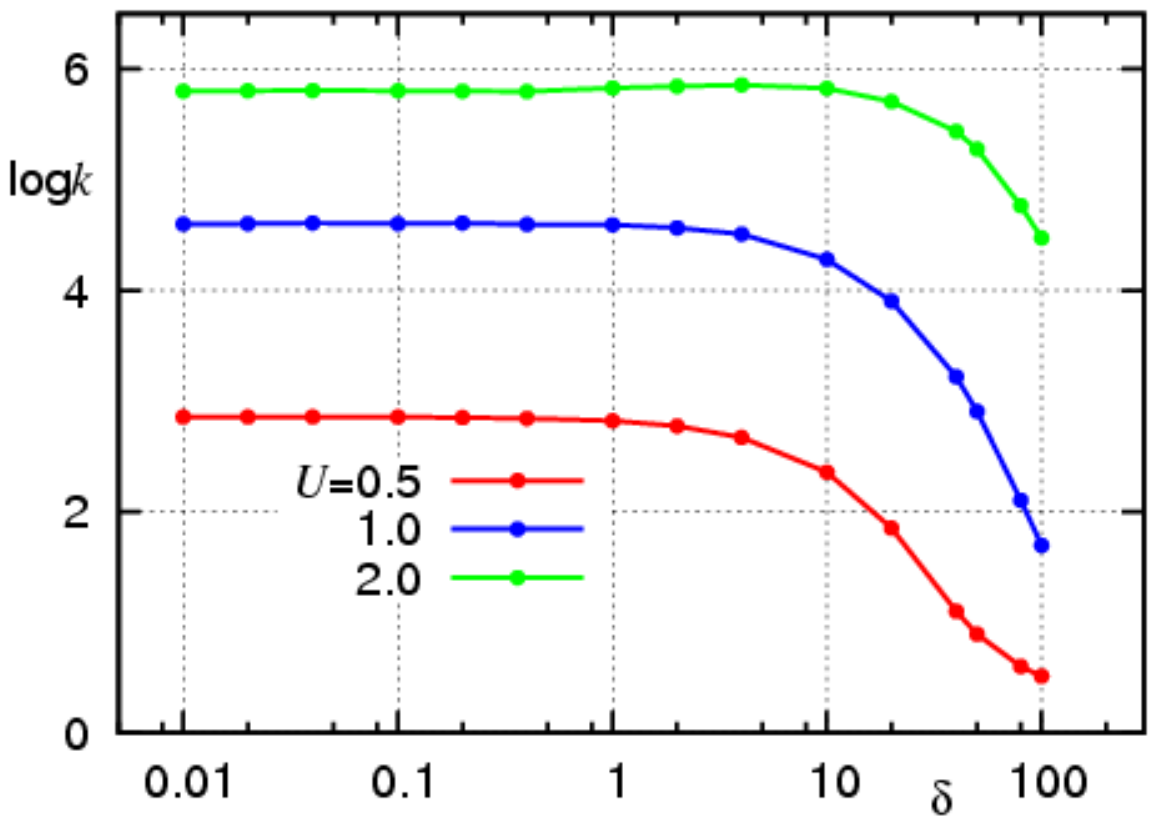

Measurement of neutrino mass (KATRIN)

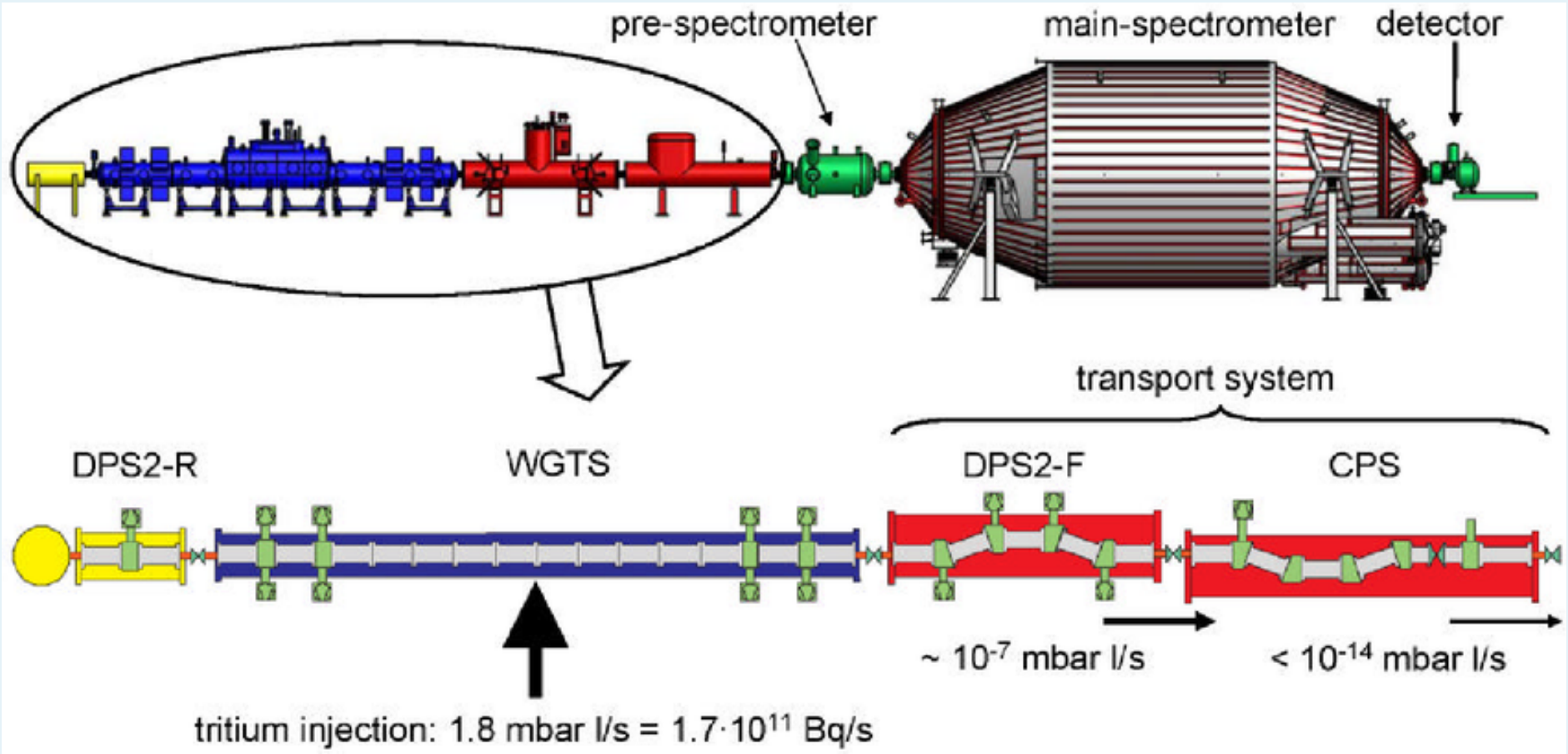

Scheme of flow

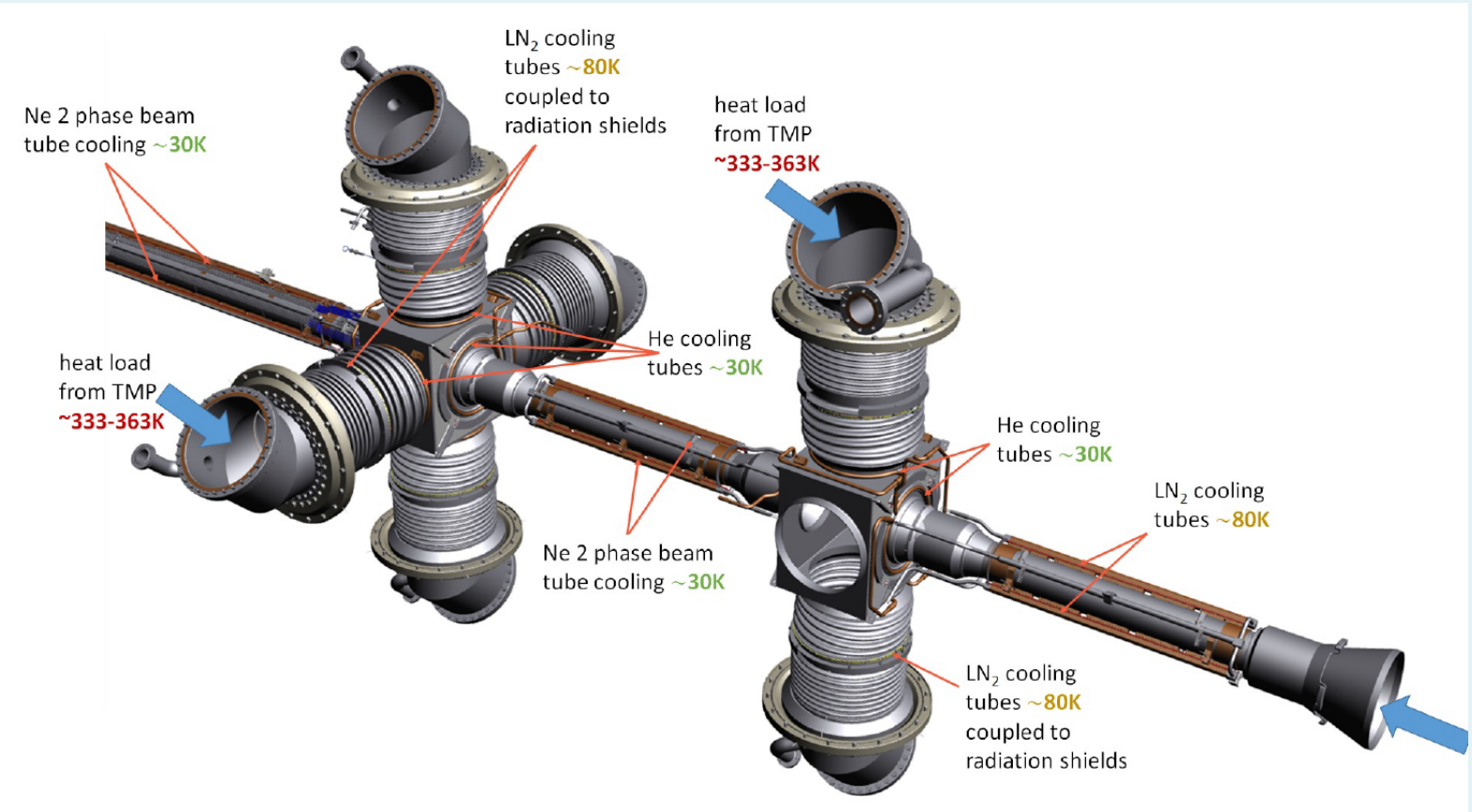

Scheme of flow

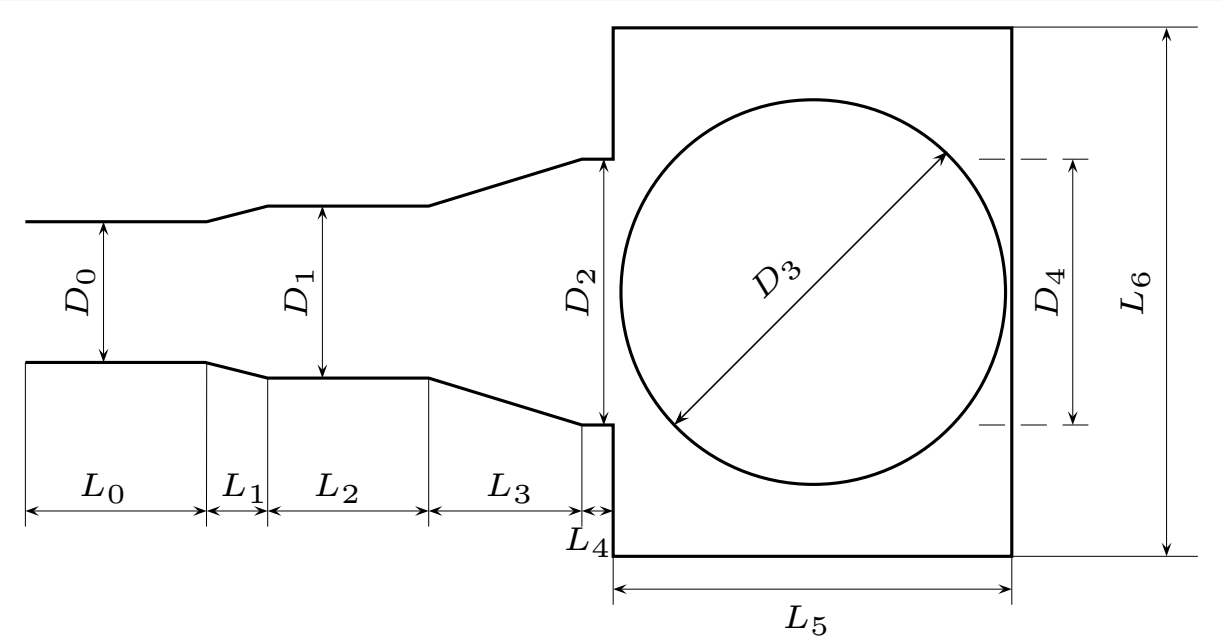

Flow-field. All pumps work

bulk velocity (m/s)

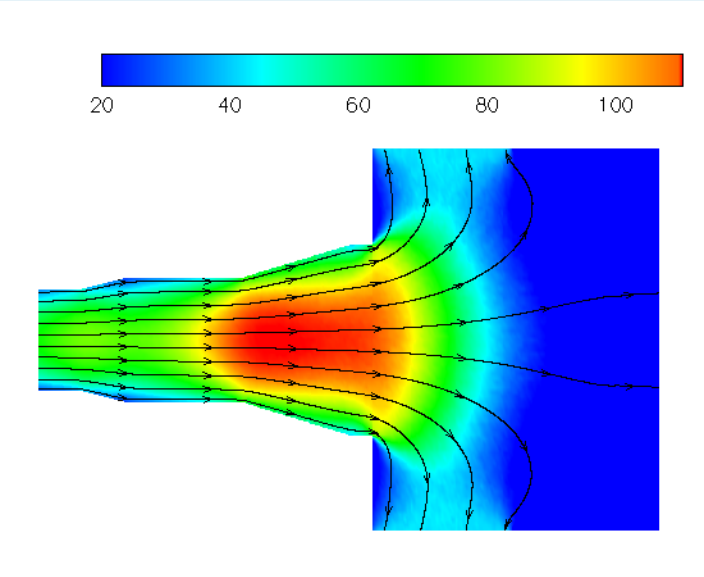

temperature (K)

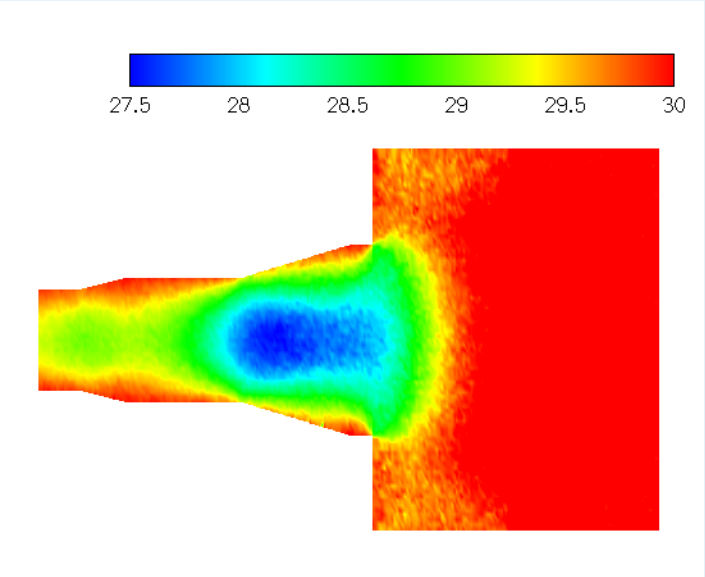

Flow-field. One pump fails

bulk velocity (m/s)

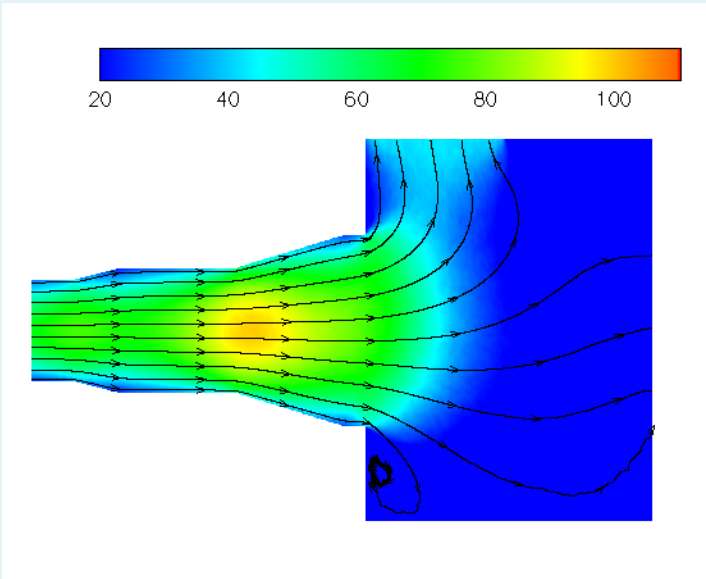

temperature (K)

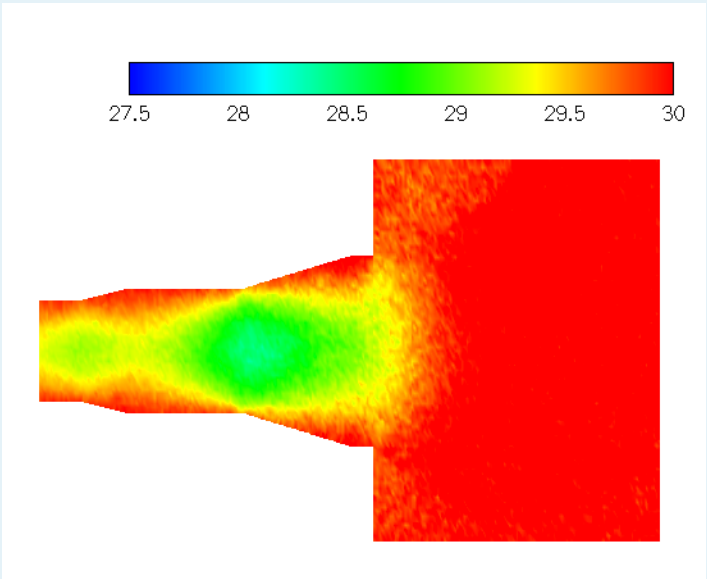

Transient flows through short tube

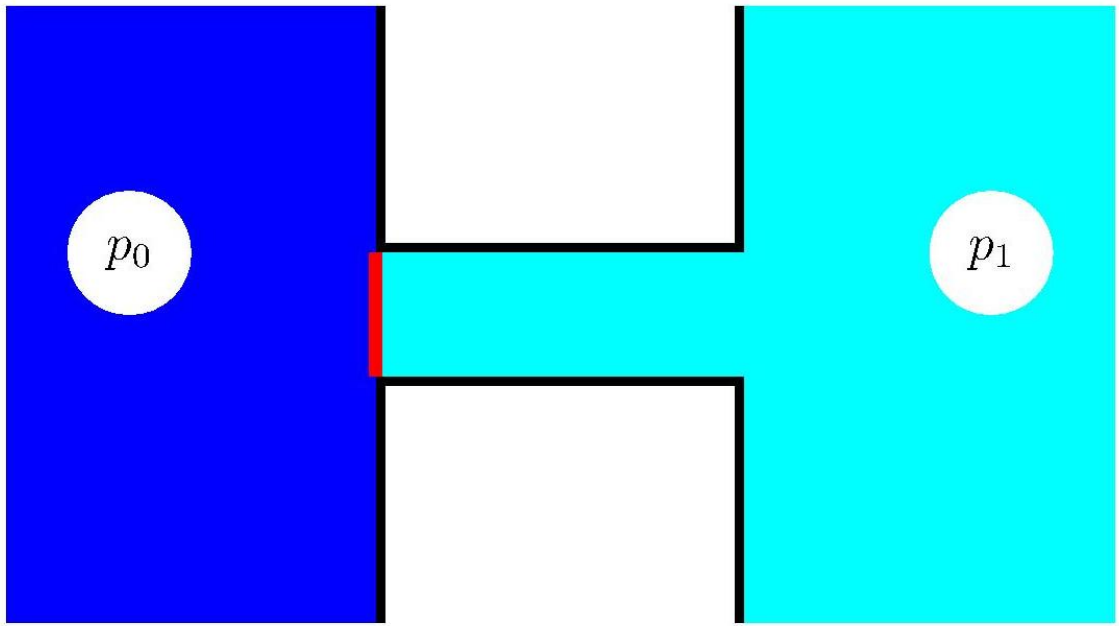

Transient flows through short tube

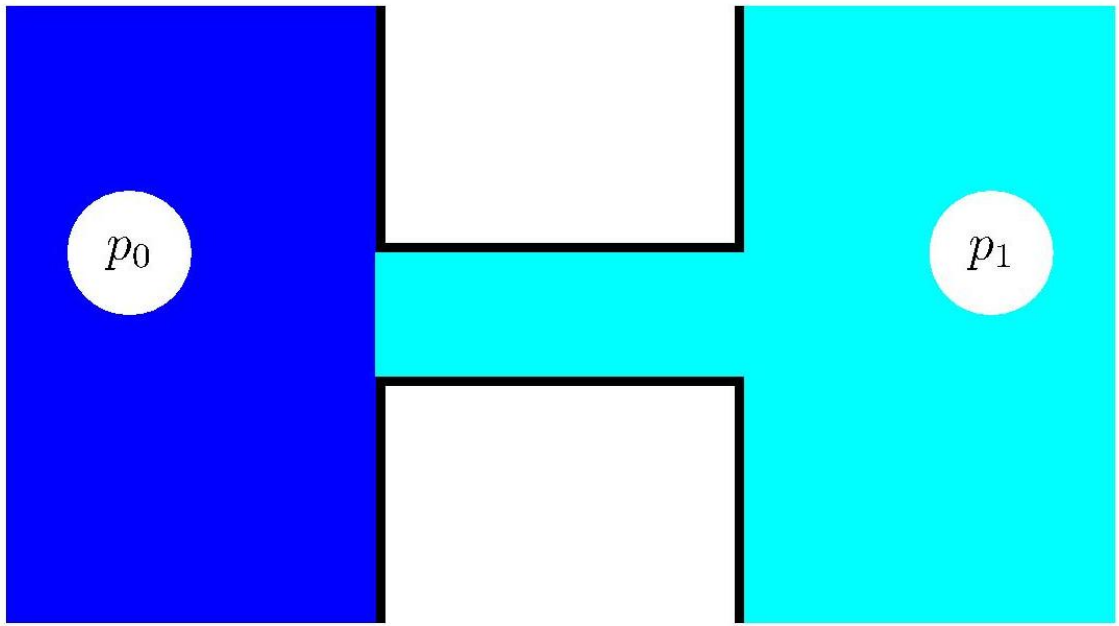

Transient flows through short tube

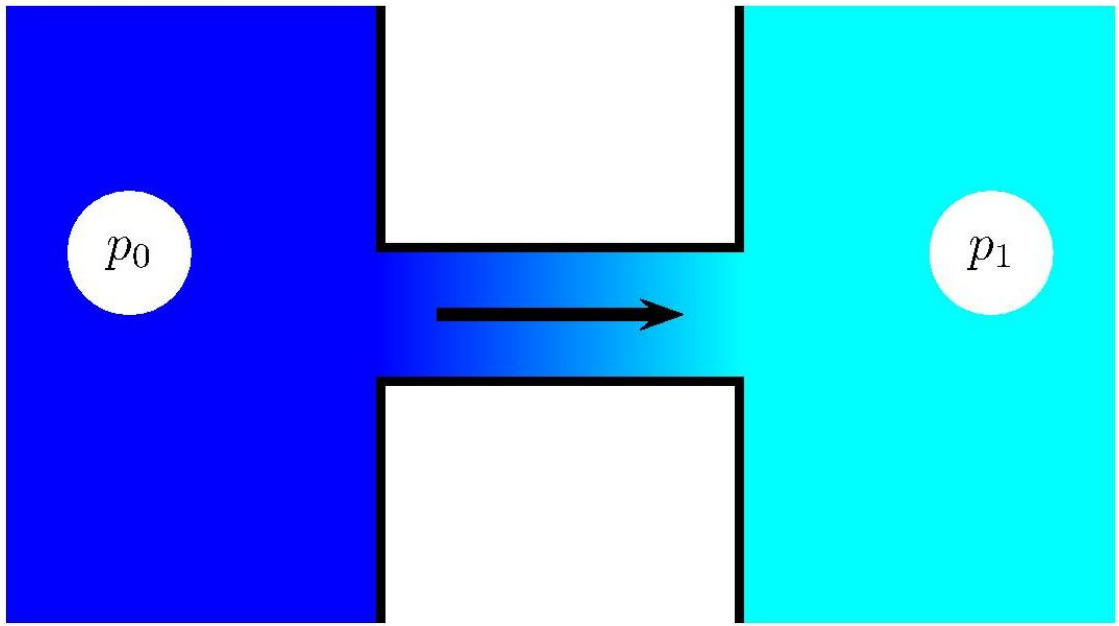

Flow rate vs time t ($\tau = a/v_m$) at $L/a = 1$ and $p_2/p_1 = 0.1$ solid - inlet, dashed - outlet

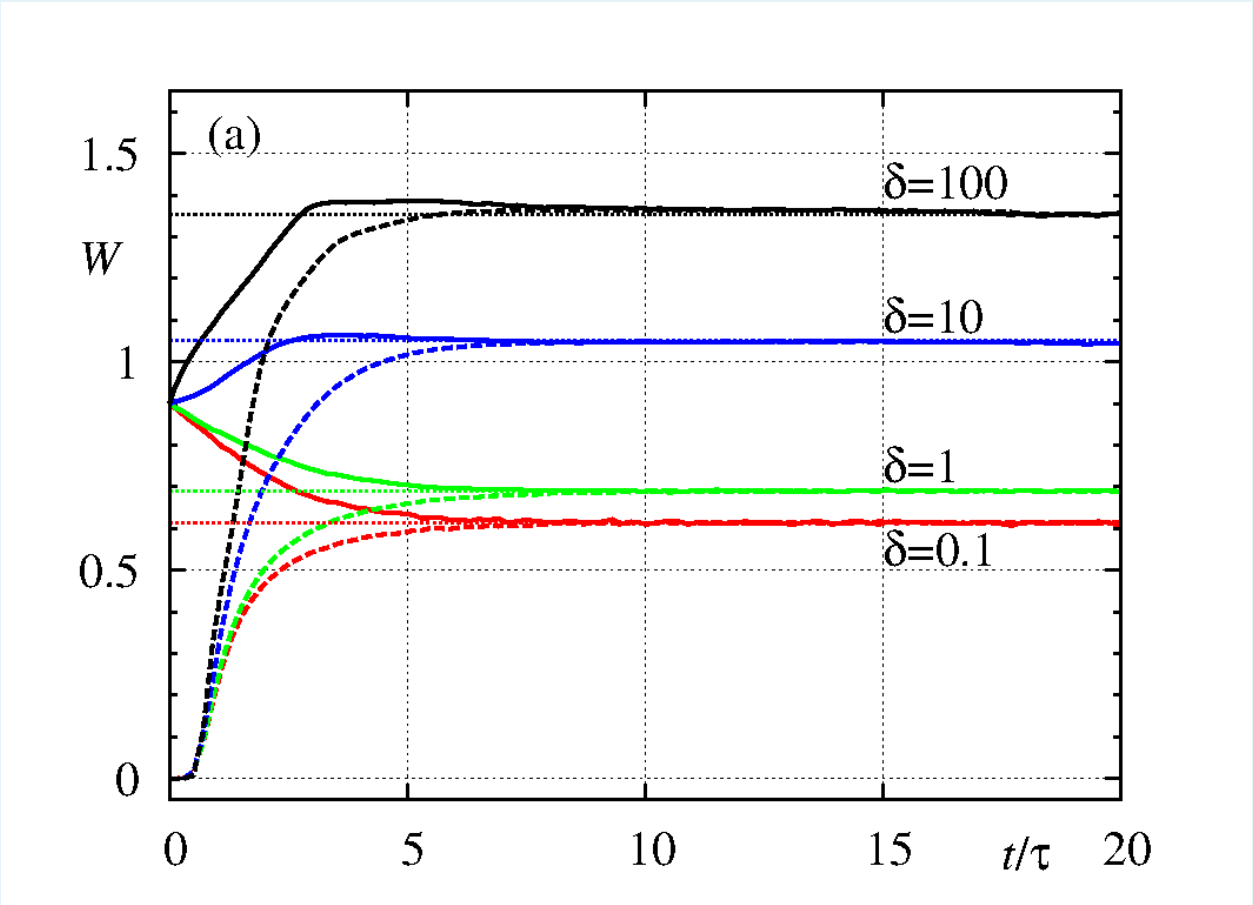

Sharipov, *Vacuum* **90**, P.25 (2013)

Flow rate vs time t ($\tau = a/v_m$) at $L/a = 1$ and $p_2/p_1 = 0.5$ solid - inlet, dashed - outlet

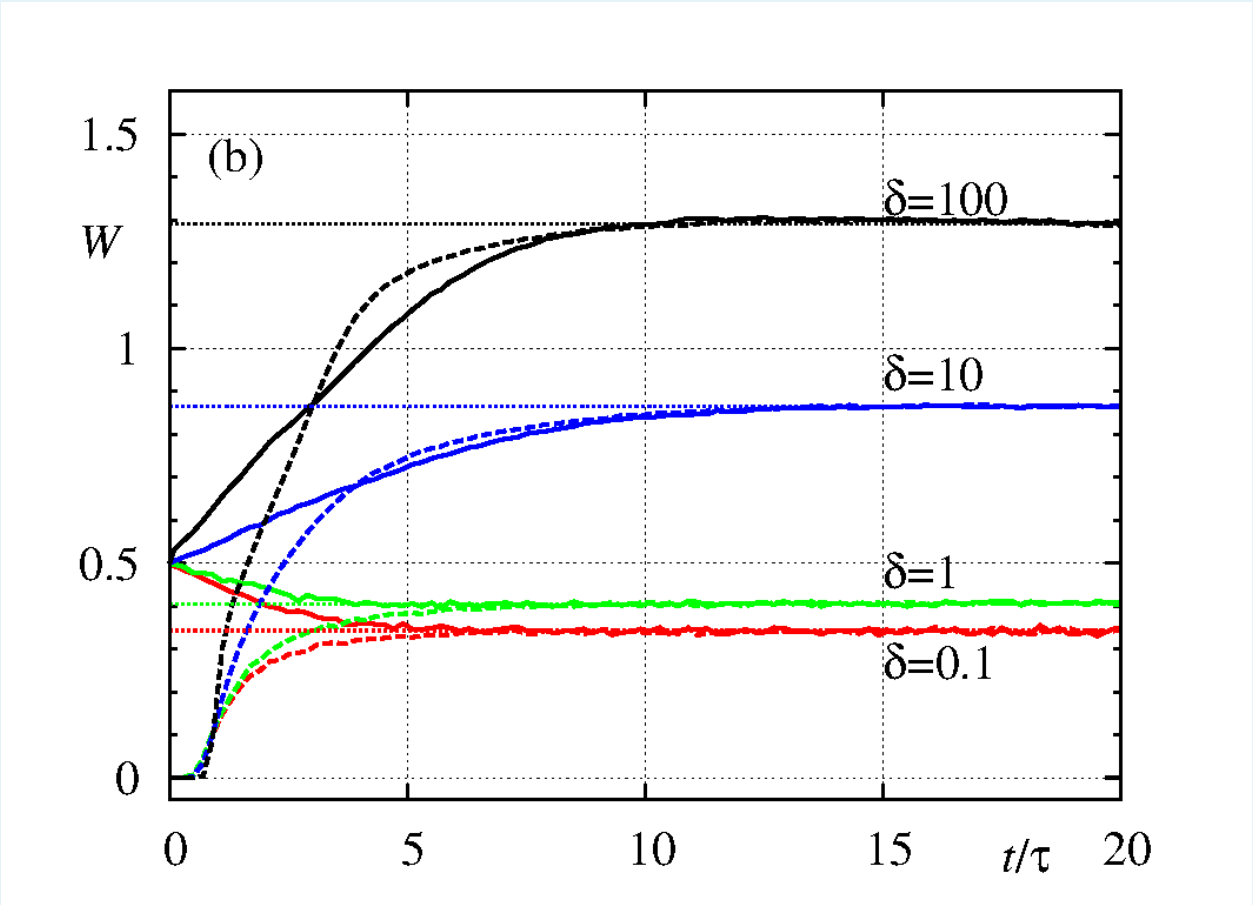

Sharipov, *Vacuum* **90**, P.25 (2013)

Flow rate vs time t ($\tau = a/v_m$) at $L/a = 5$ and $p_2/p_1 = 0.1$ solid - inlet, dashed - outlet

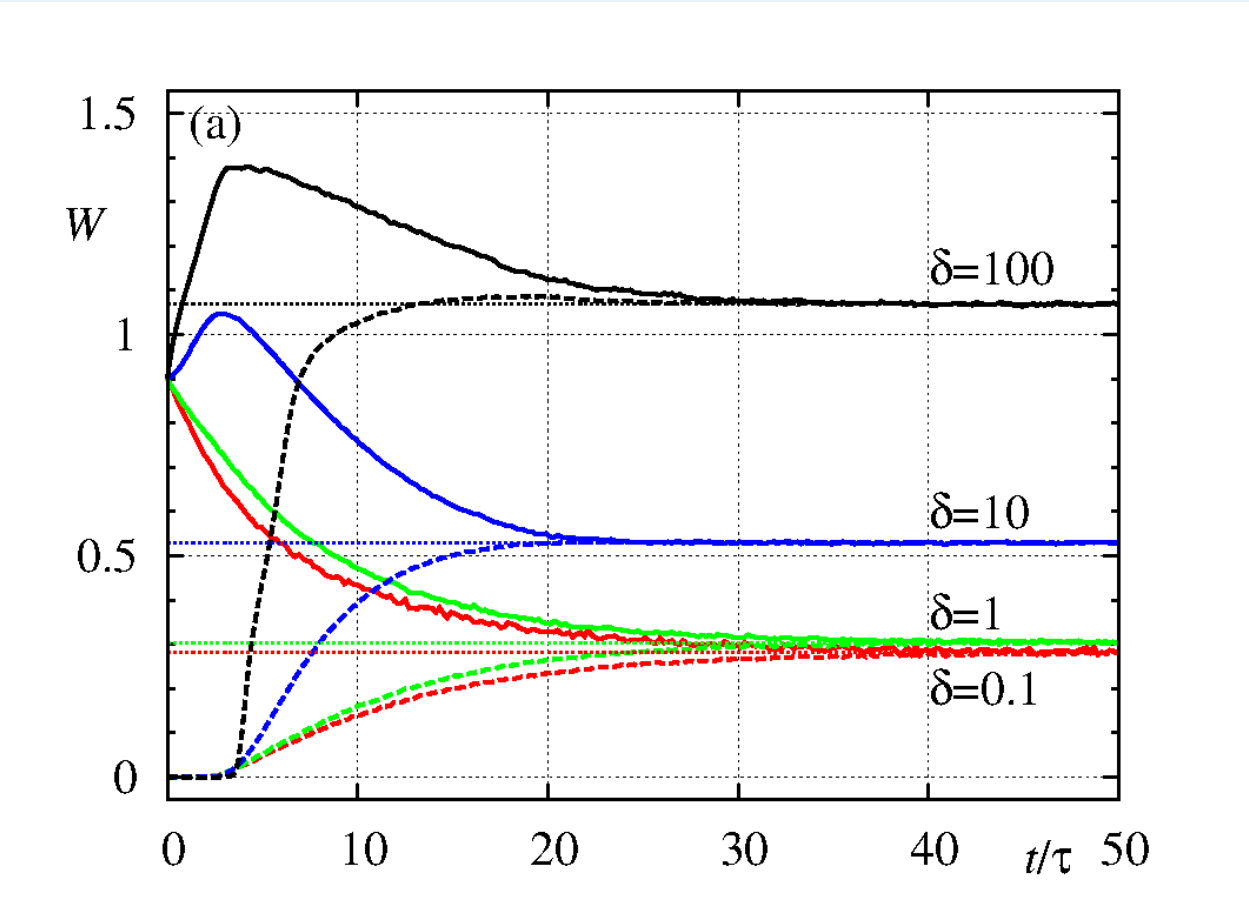

Sharipov, *Vacuum* **90**, P.25 (2013)

Flow rate vs time t ($\tau = a/v_m$) at $L/a = 5$ and $p_2/p_1 = 0.5$ solid - inlet, dashed - outlet

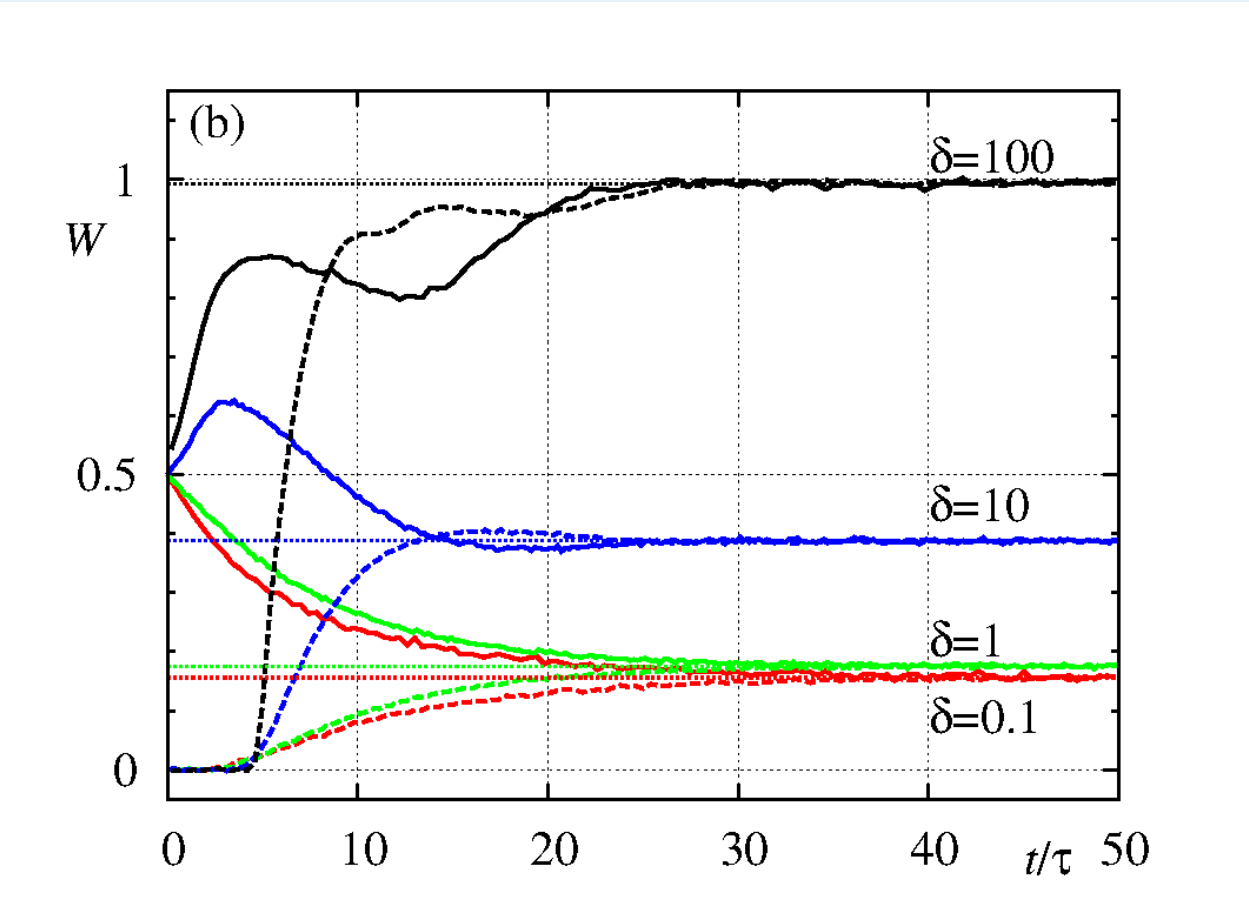

Sharipov, *Vacuum* **90**, P.25 (2013)

Flowfield $p_1/p_0 = 0.1,\ L/a = 5,\ \delta = 100$

$t = 1 \times \tau, \quad \tau = a/v_m$

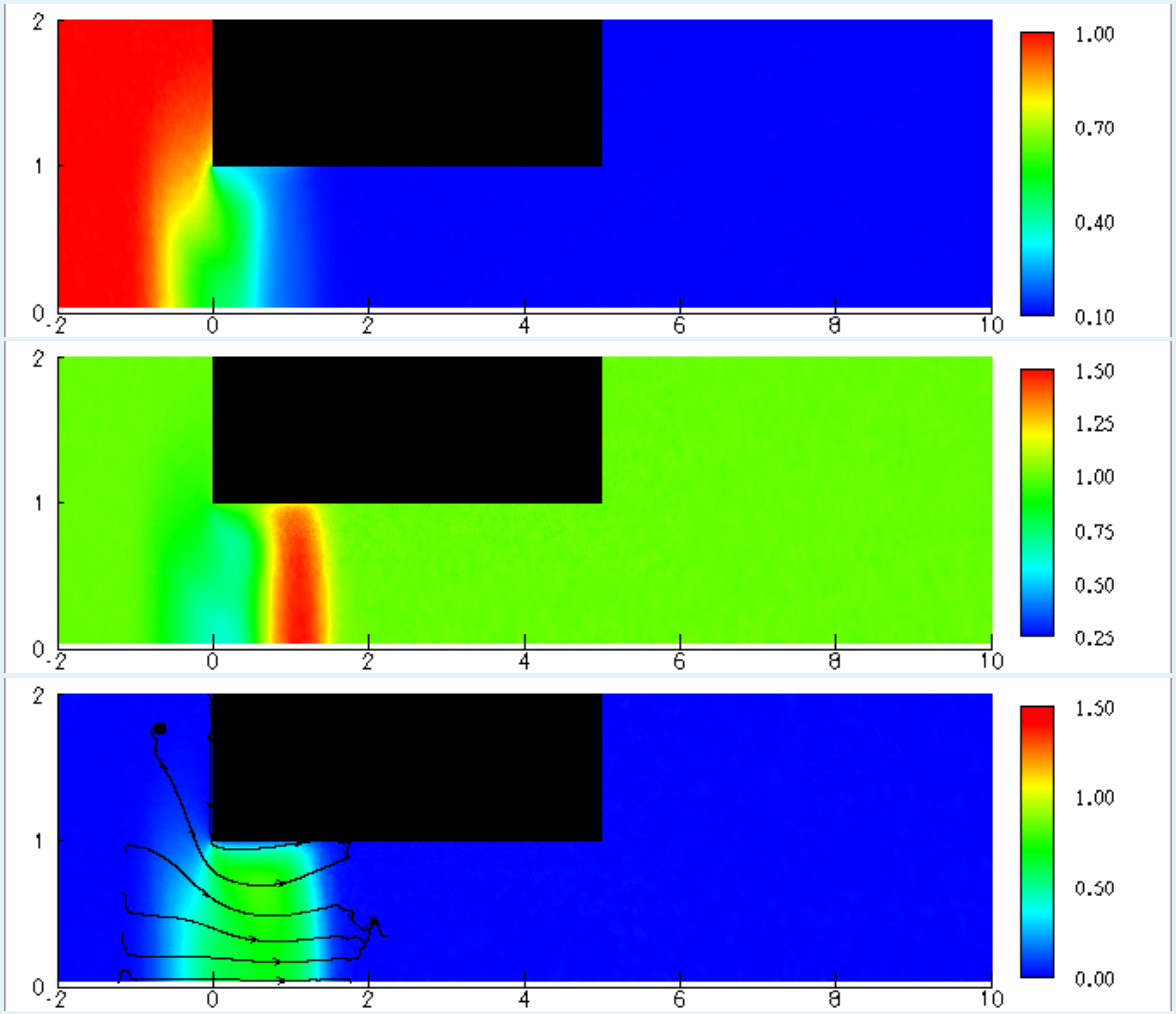

Density

ρ/ρ_0

Temperature

T/T_0

Bulk velocity

u_x/v_m

.

Flowfield $p_1/p_0 = 0.1,\ L/a = 5,\ \delta = 100$

$t = 2 \times \tau, \quad \tau = a/v_m$

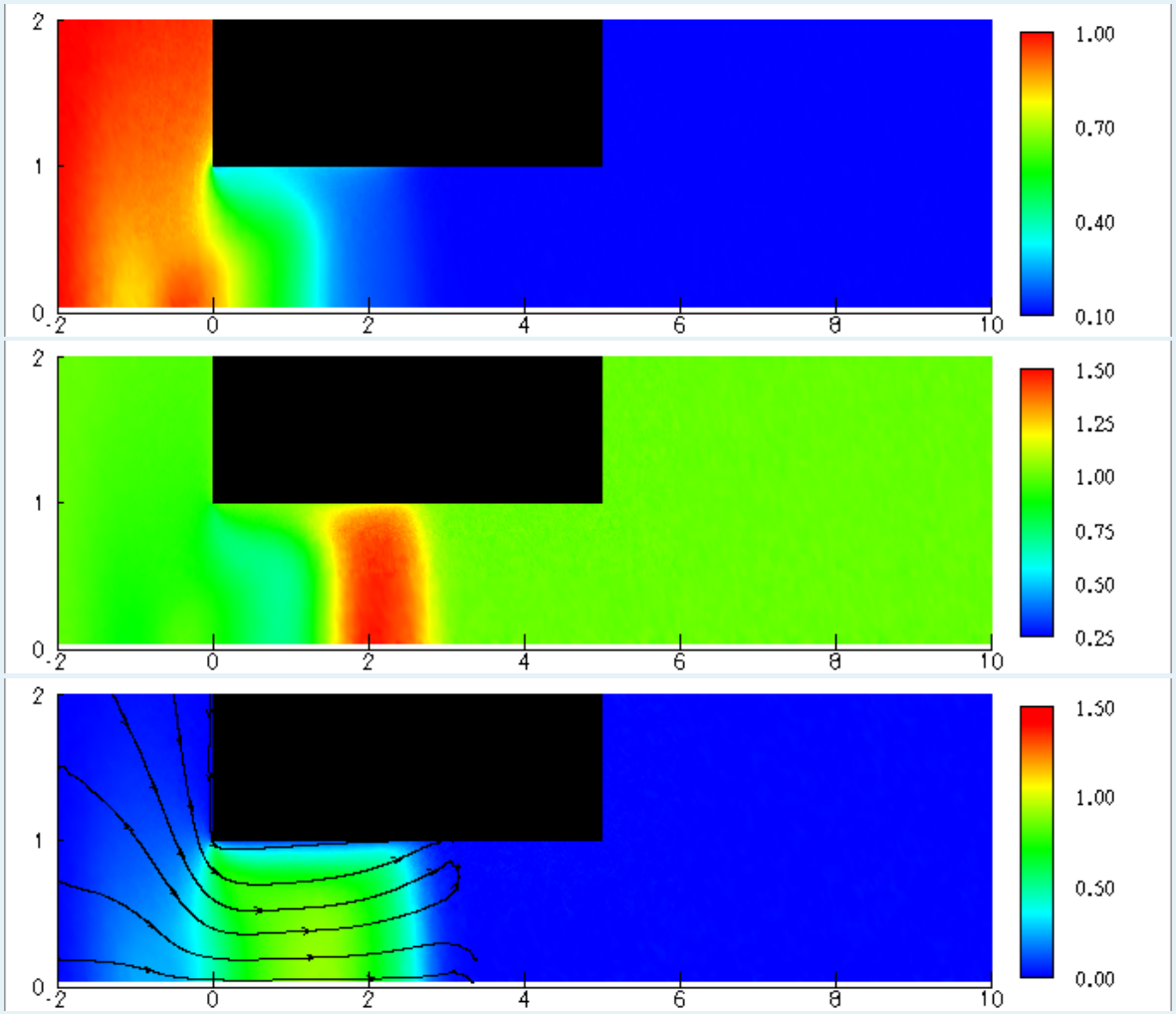

Density

ρ/ρ_0

Temperature

T/T_0

Bulk velocity

u_x/v_m

.

Flowfield $p_1/p_0 = 0.1,\ L/a = 5,\ \delta = 100$

$t = 4 \times \tau, \quad \tau = a/v_m$

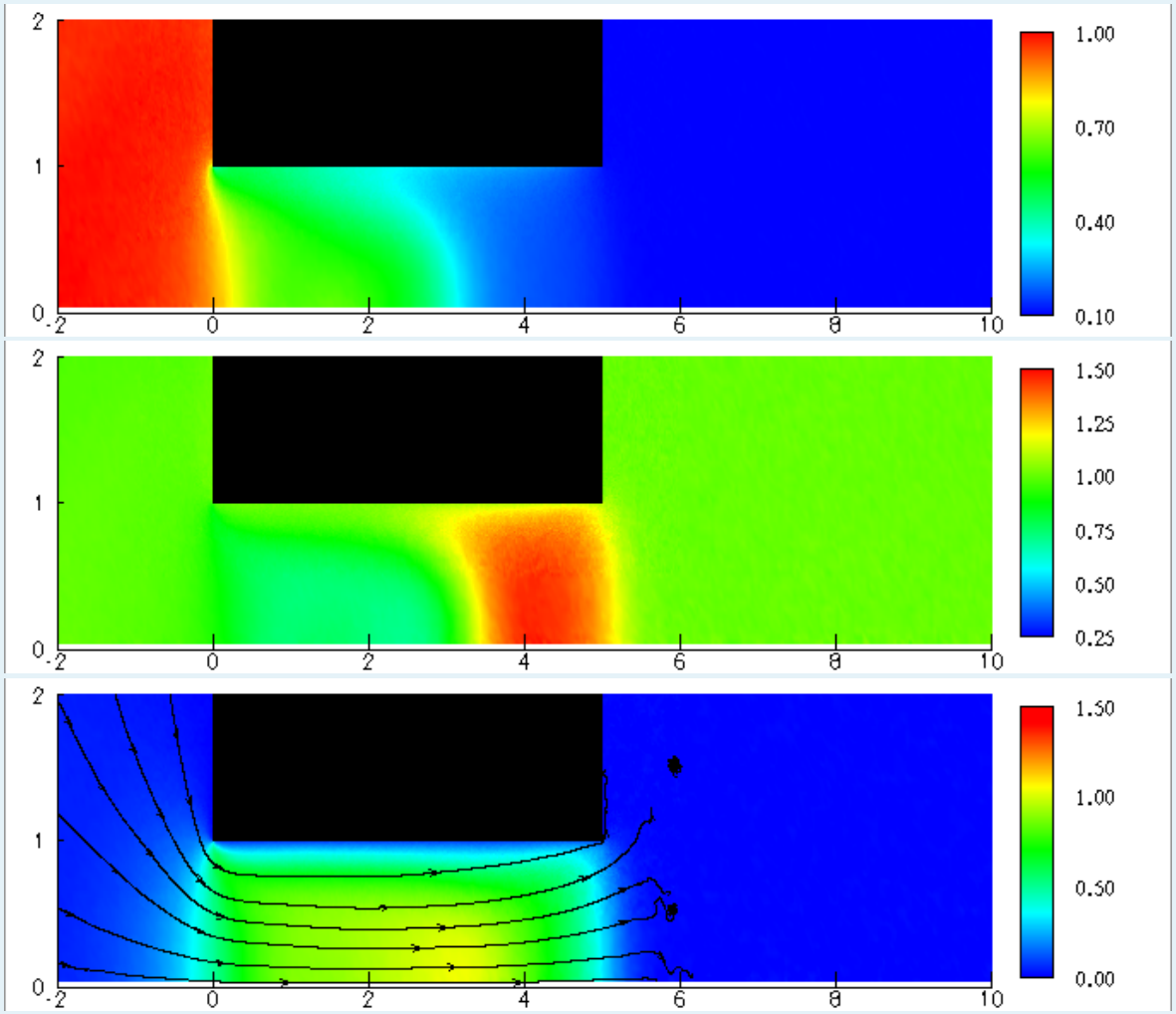

Density
ρ/ρ_0

Temperature
T/T_0

Bulk velocity
u_x/v_m

.

Flowfield $p_1/p_0 = 0.1,\ L/a = 5,\ \delta = 100$

$t = 8 \times \tau, \quad \tau = a/v_m$

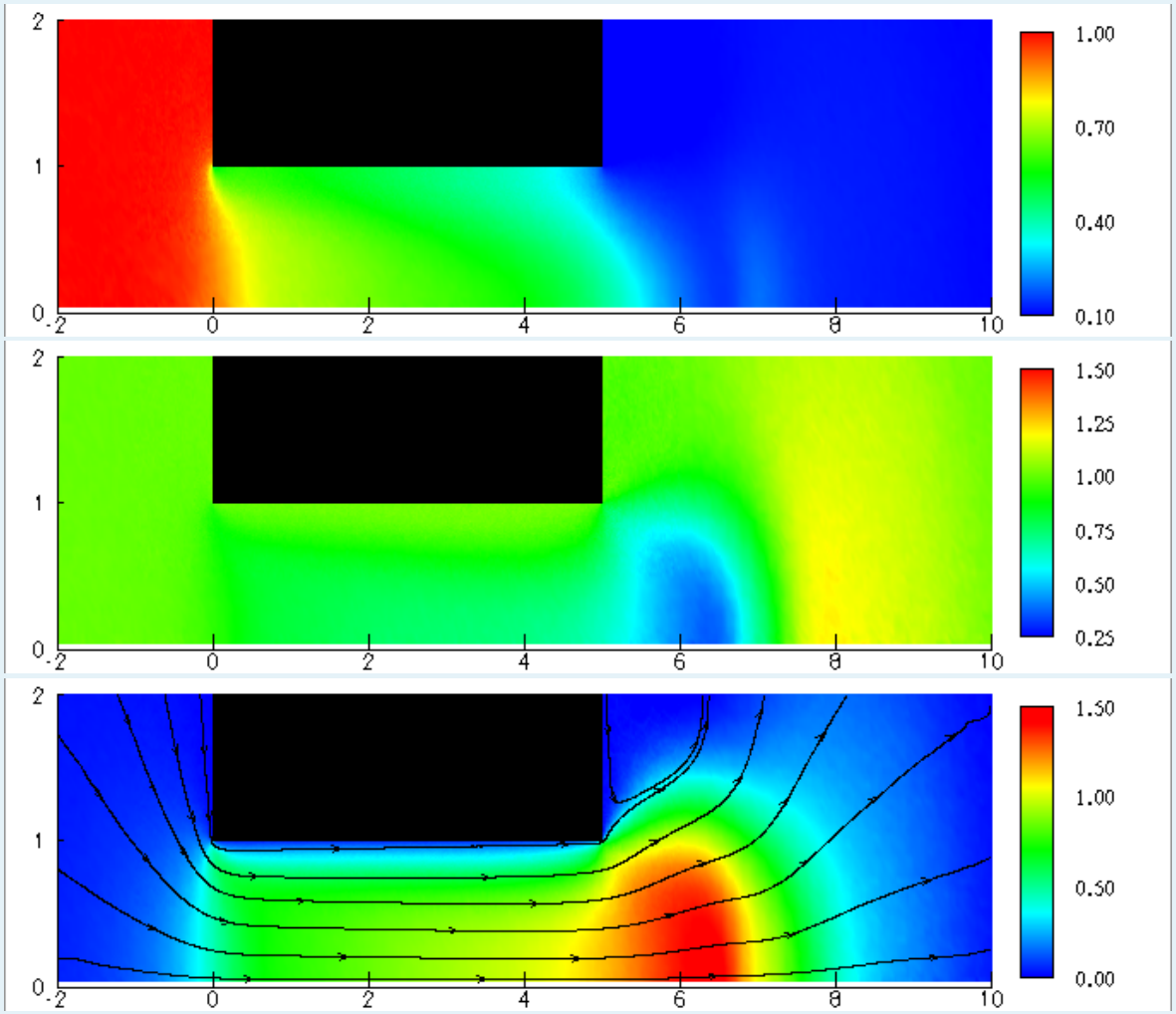

Density
ρ/ρ_0

Temperature
T/T_0

Bulk velocity
u_x/v_m

.

Flowfield $p_1/p_0 = 0.1,\ L/a = 5,\ \delta = 100$

$t = 15 \times \tau, \quad \tau = a/v_m$

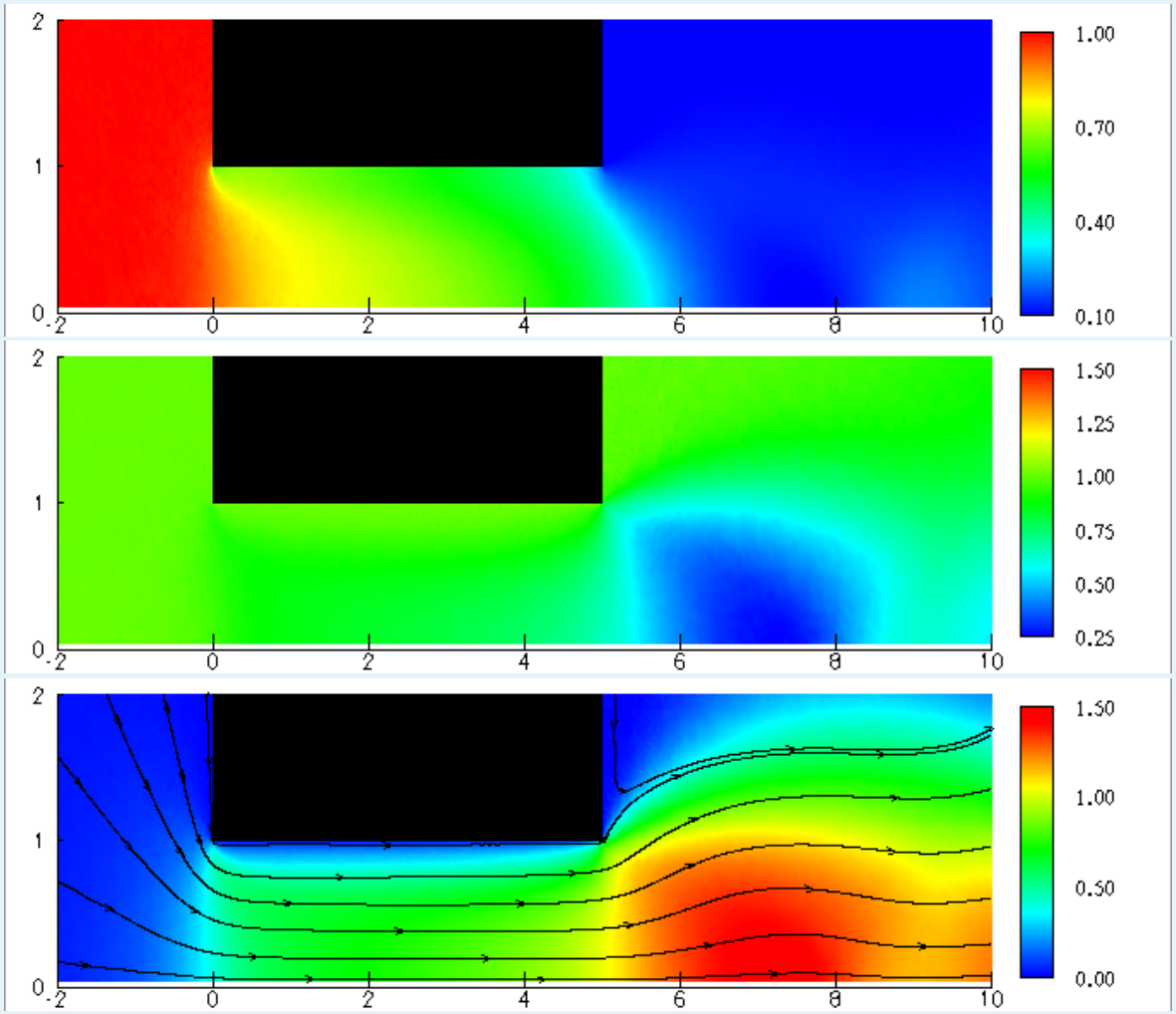

Density
ρ/ρ_0

Temperature
T/T_0

Bulk velocity
u_x/v_m

.

Flowfield $p_1/p_0 = 0.1,\ L/a = 5,\ \delta = 100$

$t = 30 \times \tau, \quad \tau = a/v_m$

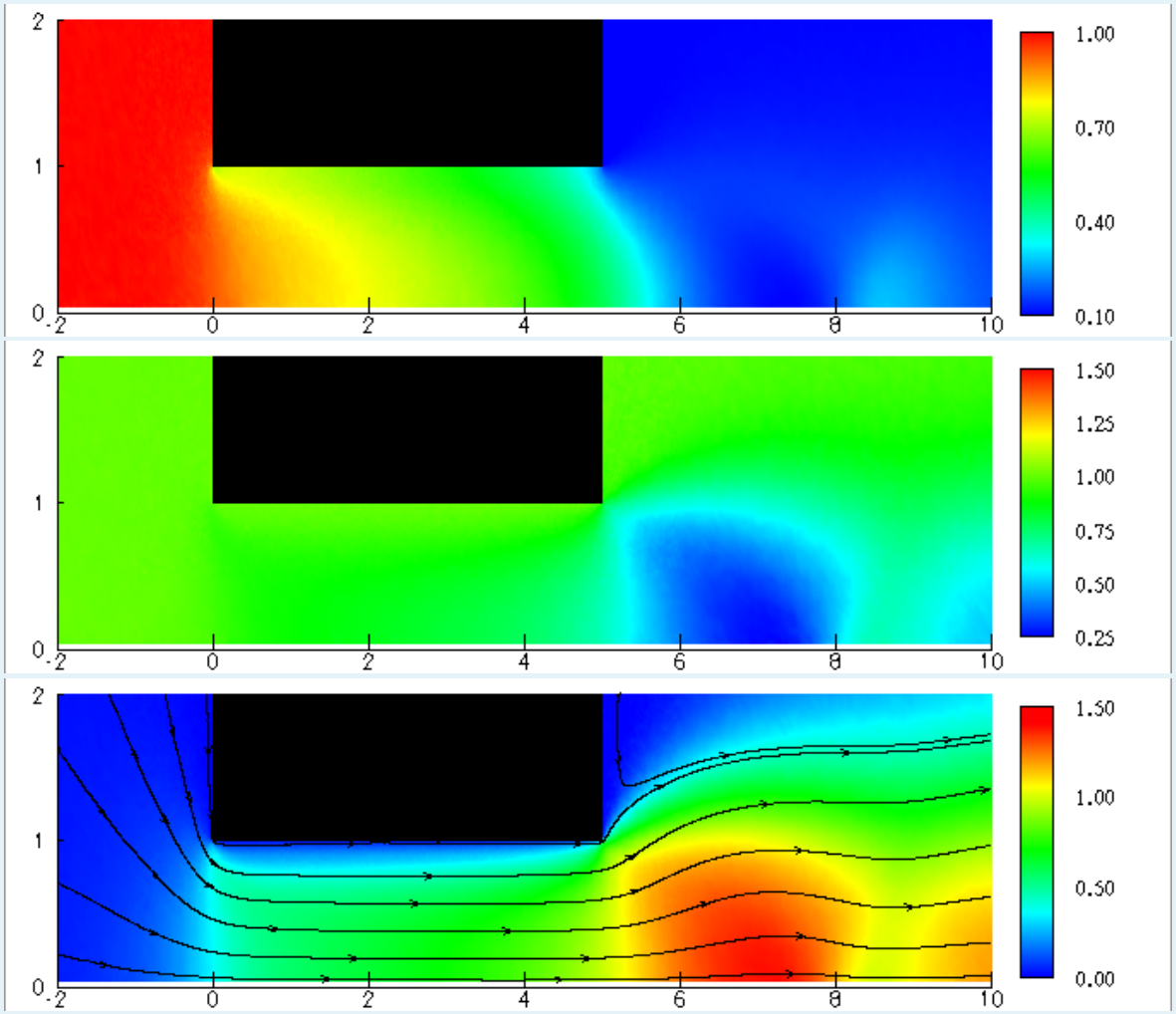

Density
ρ/ρ_0

Temperature
T/T_0

Bulk velocity
u_x/v_m

.

Flowfield $p_1/p_0 = 0.5,\ L/a = 5,\ \delta = 100$

$t = 1 \times \tau, \quad \tau = a/v_m$

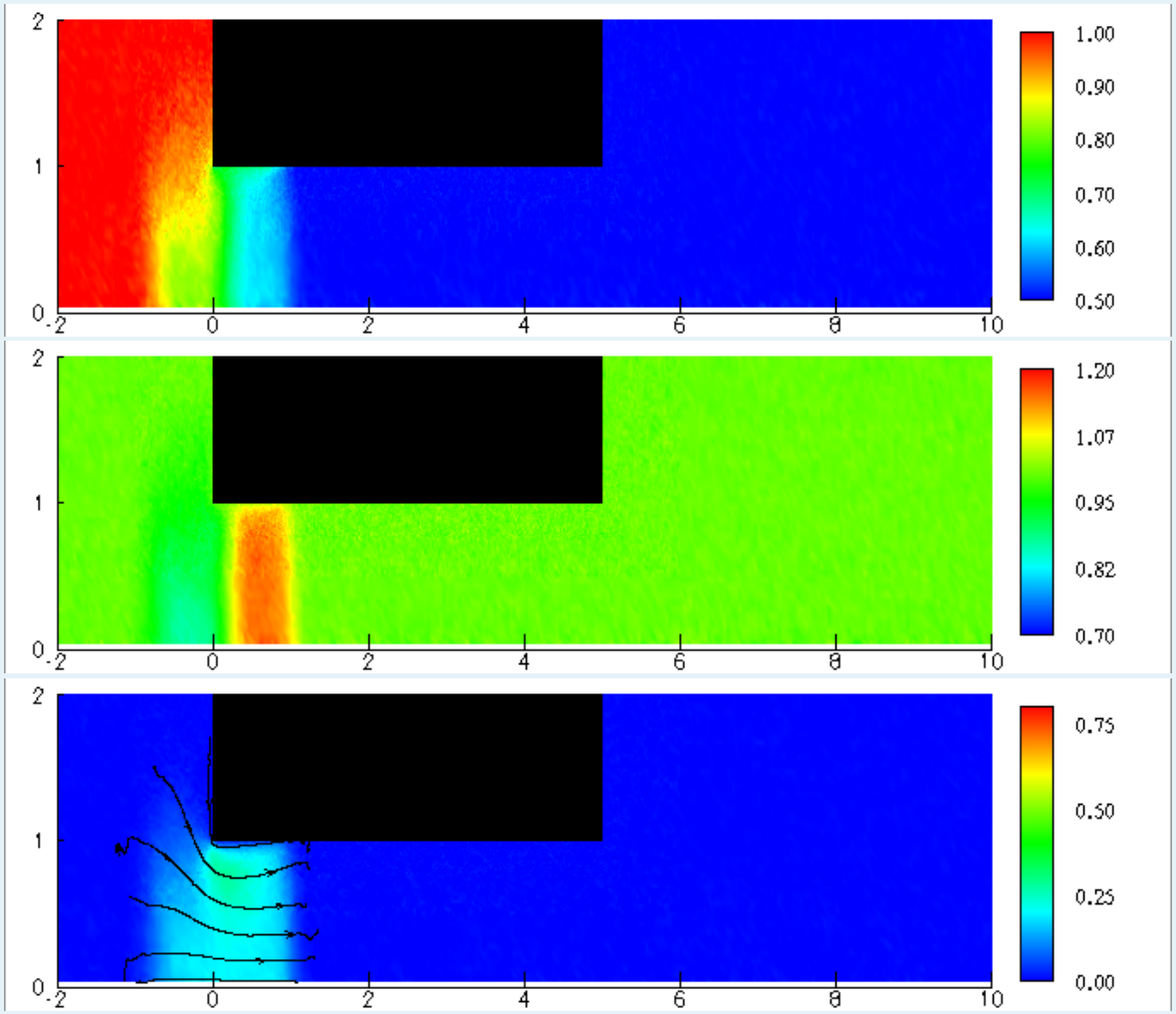

Density
ρ/ρ_0

Temperature
T/T_0

Bulk velocity
u_x/v_m

.

Flowfield $p_1/p_0 = 0.5,\ L/a = 5,\ \delta = 100$

$t = 2 \times \tau, \quad \tau = a/v_m$

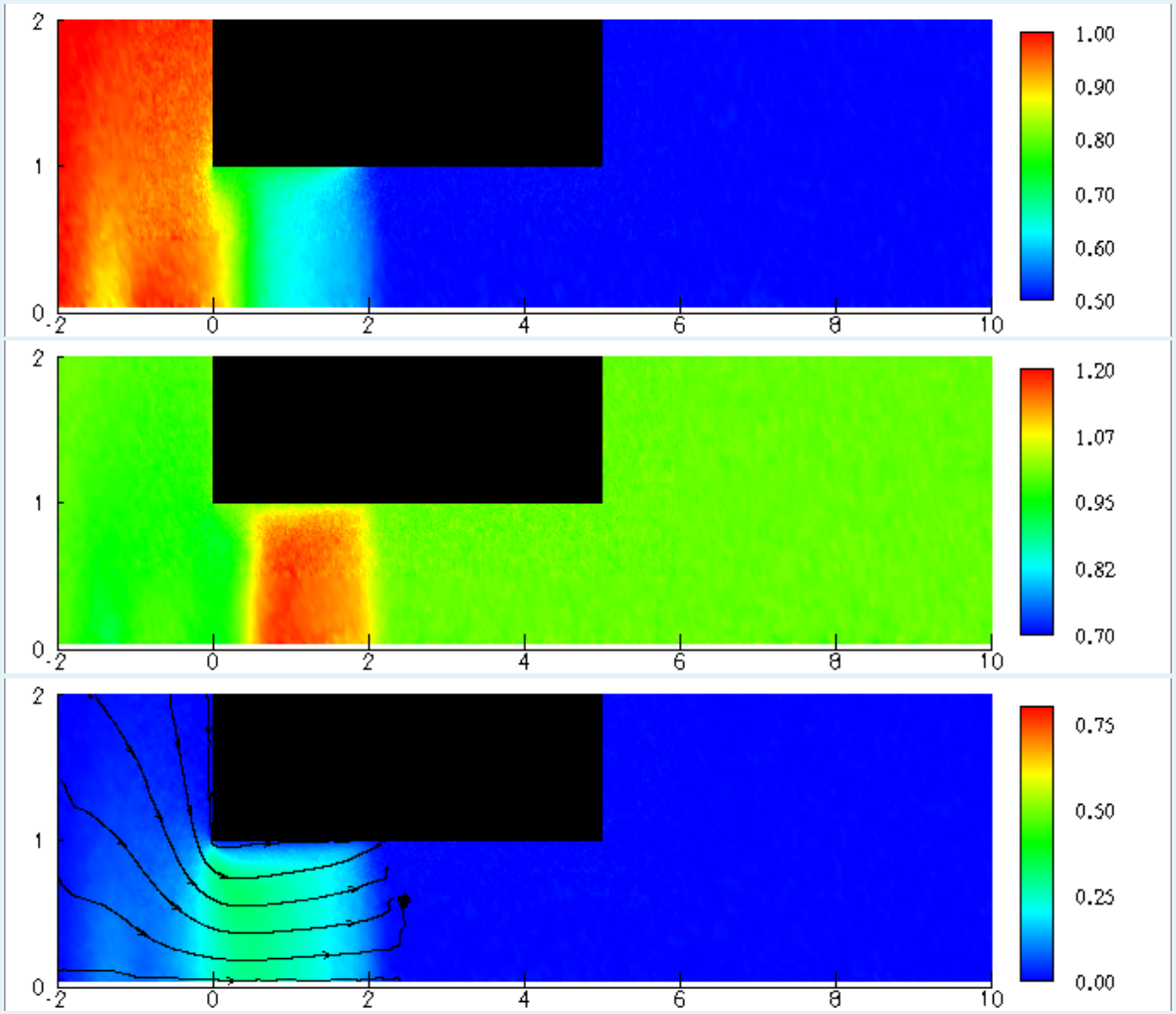

Density
ρ/ρ_0

Temperature
T/T_0

Bulk velocity
u_x/v_m

.

Flowfield $p_1/p_0 = 0.5,\ L/a = 5,\ \delta = 100$

$t = 4 \times \tau, \quad \tau = a/v_m$

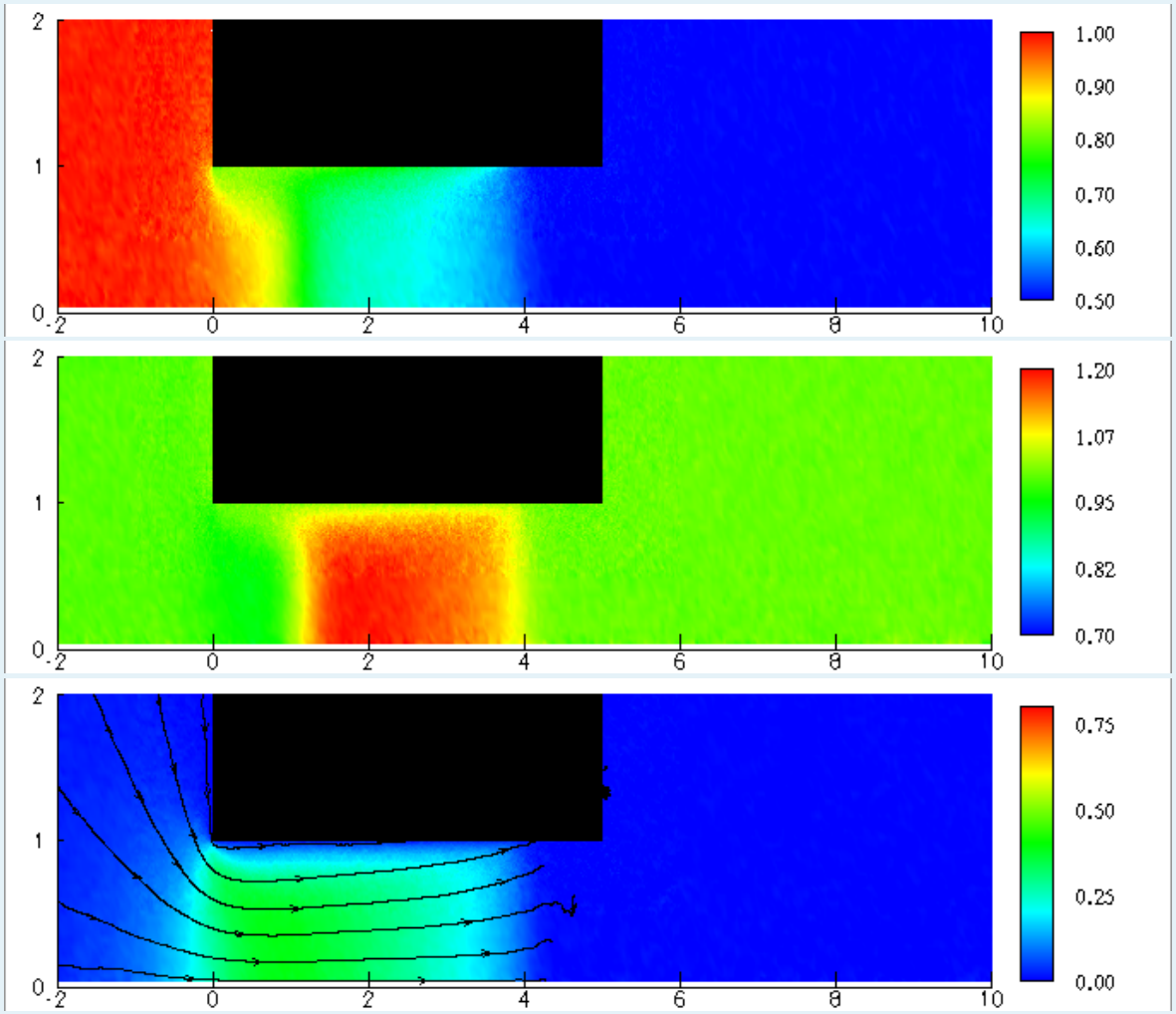

Density
ρ/ρ_0

Temperature
T/T_0

Bulk velocity
u_x/v_m

.

Flowfield $p_1/p_0 = 0.5,\ L/a = 5,\ \delta = 100$

$t = 8 \times \tau, \quad \tau = a/v_m$

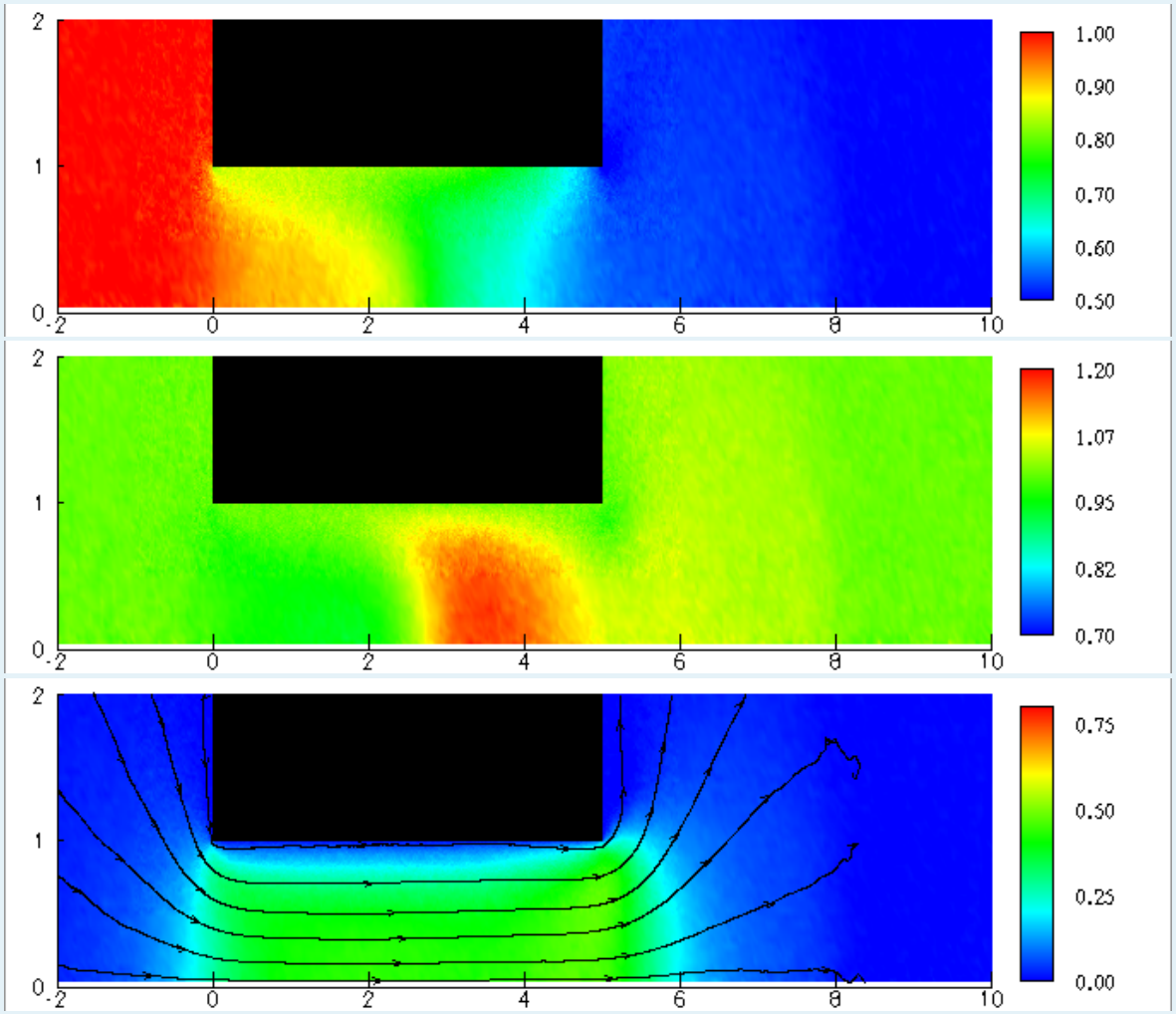

Density
ρ/ρ_0

Temperature
T/T_0

Bulk velocity
u_x/v_m

.

Flowfield $p_1/p_0 = 0.5,\ L/a = 5,\ \delta = 100$

$t = 15 \times \tau, \quad \tau = a/v_m$

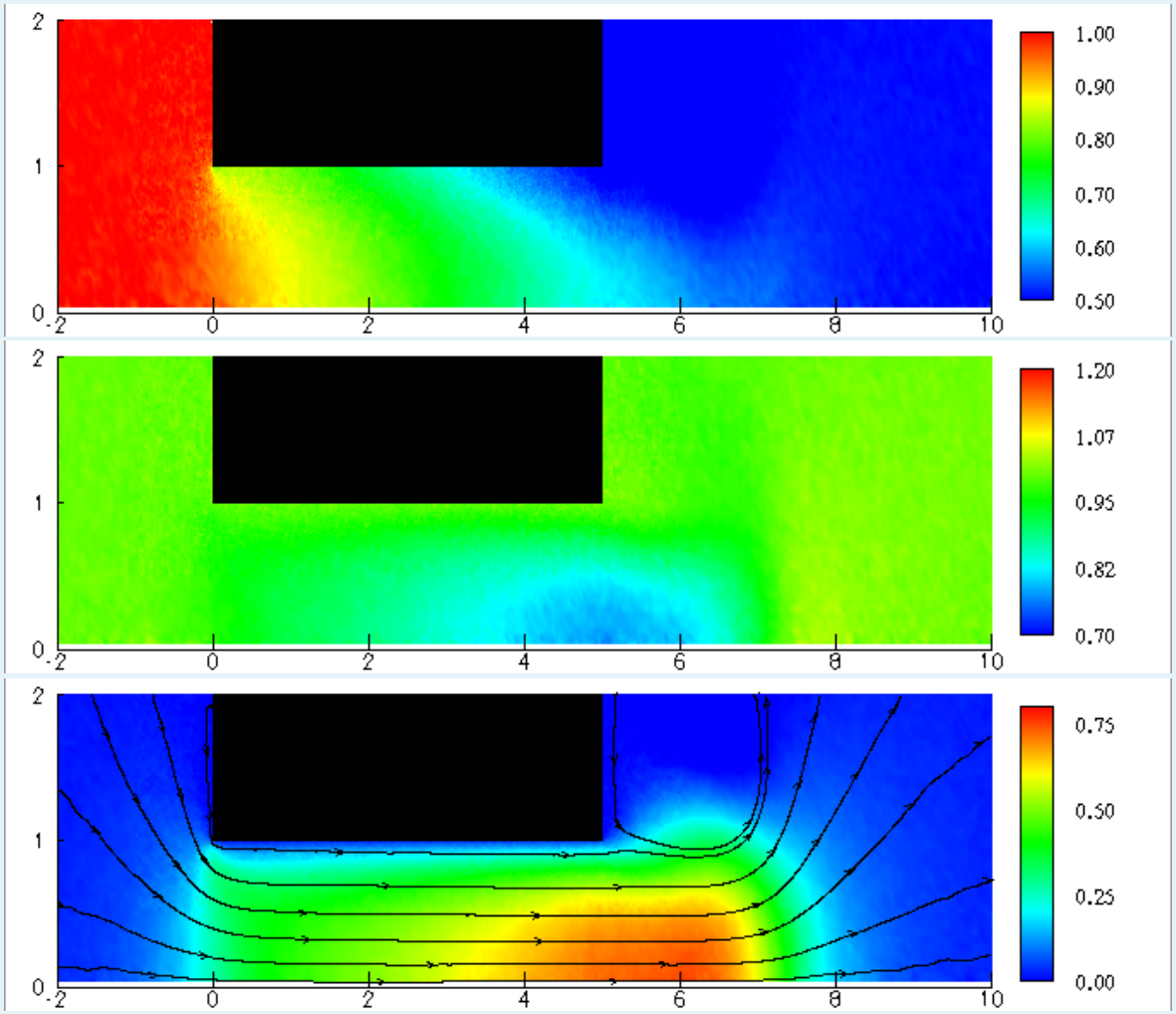

Density
ρ/ρ_0

Temperature
T/T_0

Bulk velocity
u_x/v_m

.

Flowfield $p_1/p_0 = 0.5,\ L/a = 5,\ \delta = 100$

$t = 30 \times \tau, \quad \tau = a/v_m$

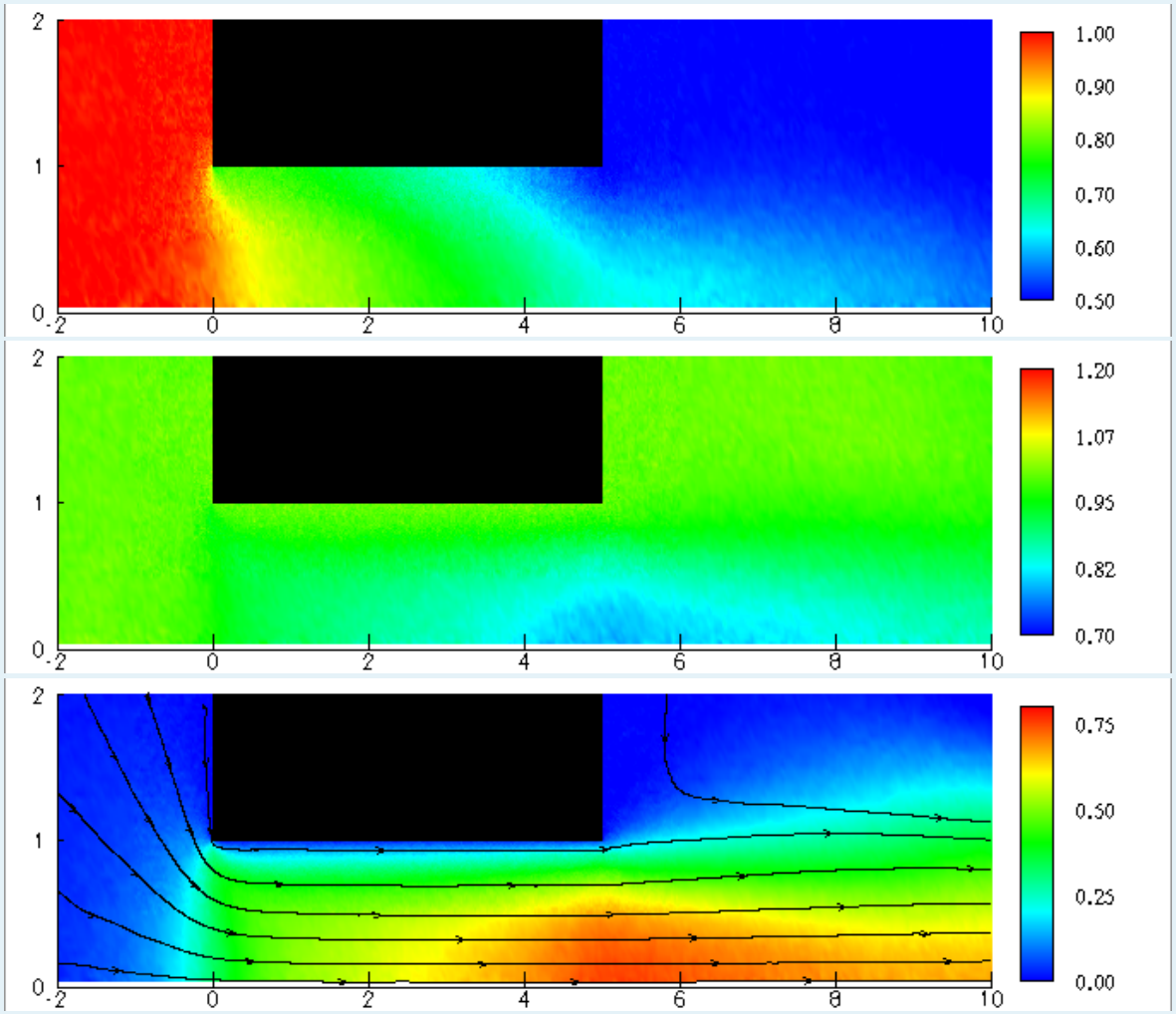

Density
ρ/ρ_0

Temperature
T/T_0

Bulk velocity
u_x/v_m

.

TPMC, DSMC. Numerical codes

- G. A. Bird, *Molecular Gas Dynamics and the Direct Simulation of Gas Flows* (Oxford University Press, 1994)
- G. A. Bird, *The DSMC method* (2013)

Lookup tables of χ

F. Sharipov, Direct simulation Monte Carlo method based on ab initio potential: Recovery of transport coefficients of multi-component mixtures of noble gases. *Phys. Fluids* **34**, 097114 (2022).

THE END
of Lecture 2

Thank you
for your attention
http://fisica.ufpr.br/sharipov